The influence of RGD peptide surface modification on the fixation of orthopaedic implants

PhD thesis

Brian Elmengaard, MD

Faculty of Health Sciences
University of Aarhus
Denmark
2004

From
The Orthopaedic Research Laboratory
Department of Orthopaedic Surgery, Aarhus University Hospital
Interdisciplinary Research Group at the
Interdisciplinary Nanoscience Center (iNANO)
Institute of Experimental Clinical Research, University of Aarhus

&

The Orthopaedic Biomechanics Laboratory
Midwest Orthopaedic and Minneapolis Medical Research Foundations
University of Minnesota, Minneapolis, MN, USA

The influence of RGD peptide surface modification on the fixation of orthopaedic implants

PhD thesis

Brian Elmengaard

Faculty of Health Sciences
University of Aarhus
Denmark
2004

Correspondence:
Brian Elmengaaard,MD
Orthopaedic Research Laboratory
Department of Orthopaedic Surgery
Aarhus University Hospital
Nørrebrogade 44, building 1A
DK-8000 Aarhus C
Denmark
Phone: +45 8949 4162
Fax: +45 8949 4150
Email: brianelm@dadlnet.dk

LIST OF PAPERS

The thesis is based upon the following papers:

I. The *in vivo* effect of RGD coating on orthopedic implants in two bone gap models. Elmengaard B, Bechtold JE, Søballe K. Accepted Journal of Biomedical Materials and Research: A. In Press

II. *In vivo* study of the effect of RGD-treatment on bone ongrowth on press-fit titanium alloy. Elmengaard B, Bechtold JE, Søballe K., Biomaterials. In Press

III. RGD coating stimulates bone ongrowth to weight-bearing press-fit orthopaedic implants. Elmengaard B, Bechtold JE, Foss M, Duch, M, Pedersen FS, Besenbacher F, Søballe K. Manuscript submitted to Journal of Orthopaedic Research 2004

The papers will be referred to in the text by their Roman Numeral (I-III)

Study II was presented in part at the Annual meeting of the Society of Biomaterials, June 2003, Reno, NV, USA and at the annual meeting of The Danish Orthopaedic Society 2002. This study was given the best poster award by the Danish Orthopaedic Society.
Study III will be presented in part at the Joint Meeting of Orthopaedic Research Societies of North America, Europe and Japan, October 2004, Banff, Canada. The author has been selected as a finalist in the New Young Investigator Award competition.

Mentors

Professor, DrSc
Kjeld Søballe, Department of Orthopaedic Surgery, Aarhus University Hospital, Denmark

Director & Assistant Professor, PhD
Joan E. Bechtold, Orthopaedic Biomechanics Laboratory, University of Minnesota

Chairman of the assessment committee

Professor, DrSc
Ivan Hvid, Department of Orthopaedic Surgery, Aarhus University Hospital, Denmark

Opponents

Professor, PhD
Carina B. Johansson, Department of Technology, Örebro University, Sweden

Chief Surgeon, DrSc
Søren Solgaard, Department of Orthopaedic Surgery, Hillerød Sygehus, Denmark

Public defense

Aarhus University Hospital, Tage-Hansens Gade
Auditorium A, December 3rd 2004, 15:00

PREFACE

This PhD thesis is based on scientific work and animal experiments performed at Orthopaedic Research Laboratory, Department of Orthopaedic Surgery, Aarhus University Hospital, Department of Physics and Astronomy, University of Aarhus and Orthopaedic Biomechanics Laboratory, Hennepin County Medical Center, Minneapolis, MN, USA. All animal experiments were carried out at the Animal Care Facilities, Hennepin County Medical Center in Minneapolis.

I am grateful to be part of the Interdisciplinary Research Group: Nanoscience and Biocompatibility, where work with co-researchers from the Interdisciplinary Nanoscience Center (iNANO) Departments of Physics/Astronomy and Molecular Biology have been a fantastic inspiration.

I am thankful to all the persons that assisted with practical work and valuable discussions:

- Laboratory technicians Jane Pauli, Anette Milton and Anette Baatrup
- all the PhD students and medical students in the implant research group at the Orthopaedic Research Laboratory
- Morten Foss, Mogens Duch and Jeanette Justesen at the Interdisciplinary Nanoscience Center (iNANO).
- The staff at the Orthopedic Biomechanics Laboratory in Minneapolis.
- Peter, Barb and Tony for assistance during surgery and for taking good care of the dogs.

I especially would like to thank my mentors Kjeld Søballe and Joan E. Bechtold who have made it all possible.
Last but not least I would like to thank Luise and Ida Marie for all the patience.

ACKNOWLEDGEMENTS

I am thankful for financial and materials support given by:

- The Interdisciplinary Research Group: Nanoscience and biocompatibility, grant no: 2052-01-0049; Danish Research Agency
- The Danish Rheumatism Association
- National Institute of Health grant no:AR4205
- Danish Medical Associations Foundation
- Biomet Inc. Warsaw, IN, USA provided implants
- Biomet Merck BioMaterials GmbH, Darmstadt, Germany provided peptide coating

CONTENTS

DEFINITIONS

Biological modification
The alteration of a material's performance by covalently coupling, to the material's surface, a biological relevant molecule that the tissue surrounding the material recognizes through a cellular or biomolecular pathway[108].

Gap
Circumferential and concentric defect between bone and implant.

Histomorphometry
Quantitative evaluation of tissue dimensions.

Press-fit
Insertion of an implant into an undersized cavity.

Osseointegration
The direct anchorage of implants by bone without fibrous tissue ongrowth at the interface.

Osteoconductive surface
A surface that permits bone growth on its surface or down into pores, channels or pipes[4].

Osteoinduction
The stimulation of primitive, undifferentiated and pluripotent cells into the bone-forming cell lineage[4].

Stereology
A method to obtain quantitative information about a three dimensional structure by analyzing two dimensional sections.

Tissue ongrowth
Direct contact between a tissue and the surface of the implant at the light microscope level.

ABBREVIATIONS

HA	Hydroxyapatite
RGD	Arginine-Glycine-Aspartic acid
Ti-6Al-4V	Titanium-6Aluminum-4Vanadium
PE	Polyethylene
RSA	Roentgen Stereo-photogrammetric Analysis
THA	Total Hip Arthroplasty
XPS	X-ray Photoelectron Spectroscopy

ABSTRACT

Early osseointegration of cementless implants is fundamental for the longevity of the implant.
The discovery of the RGD peptide, as an important mediator of osteoblast adhesion to implants, has lead to a new approach in designing biomaterials for use in orthopedic surgery. Implants can be biologically modified by covalent immobilization of RGD peptide on the surface of the implant. Immobilized RGD peptides facilitate osteoblast adhesion, spreading and differentiation *in vitro*. Only few *in vivo* studies have investigated the effect of RGD peptide in bone.

This thesis includes three papers based on four experimental animal studies and one *in vitro* study. All *in vivo* studies involved titanium alloy implants inserted in cancellous bone sites. The study design was paired, so that identical implants with and without immobilized RGD peptide were compared in the same animal. Implants were evaluated by push-out test and histomorphometry after four weeks of observation.

In study I, implants were inserted without load in the proximal tibia, and with load in the medial femoral condyle. A critical gap surrounded the implants in both cases. Push-out test showed that RGD coated implants with load had 2 to 3 fold higher median values for all mechanical parameters compared to the controls. A significant difference was only seen for total energy absorption.
For unloaded RGD coated implants, apparent shear stiffness was significantly higher compared to the controls. No difference was found in energy absorption and shear strength for unloaded implants.
Only half of the loaded and unloaded RGD coated implants had bone ongrowth. Fibrous tissue dominated the interface for both RGD coated and control implants.
Unloaded RGD coated implants had significantly more bone in the inner half of the gap while no difference of bone in the inner gap was observed for loaded implants. RGD coated implants had significantly less fibrous tissue in the inner half of the gap in both models. Loaded RGD coated implants also had significantly more bone marrow in the inner half of the gap. No difference in bone, bone marrow or fibrous tissue volume was observed in the outer half of the gap.

In study II, the implants were unloaded and inserted as press-fit in the proximal tibia. All parameters of mechanical fixation were higher in the RGD coated group compared with the control implants, with significantly higher apparent shear stiffness for RGD coated implants.
A significant increase in bone ongrowth and bone volume in a 0-100 μm circumferential zone was found for RGD coated implants. A significant decrease in fibrous tissue ongrowth was also found for the RGD coated implants.

In study III, an *in vitro* analysis of RGD coated titanium alloy discs with X-ray Photoelectron Spectroscopy verified that the RGD molecules were not organized randomly and that they did have the preferred orientation for cell adhesion as the phosphonate anchor was closer to the titanium surface than the RGD peptide.
The *in vivo* study included loaded, press-fit implants inserted in the medial femoral condyle.
No difference was seen in mechanical fixation. This was a predictable result because the implants were inserted with a tight press-fit. A significant increase in bone ongrowth and bone volume in a 0-100 μm circumferential zone was observed for RGD coated implants. Fibrous tissue ongrowth was not seen on any of the implants.

In conclusion, these studies demonstrated that biological modification of implants with RGD

peptide stimulates bone ongrowth to titanium alloy implants in a press-fit setting.
A similar bone stimulating effect is not seen when RGD coated implants are surrounded by a gap. However, a reduction in fibrous tissue in the inner half of the gap is a positive finding.
The results are encouraging and warrant further investigation in human implants.

INTRODUCTION

It is estimated that more than one million artificial joint prostheses are inserted each year worldwide.
Revision procedures constitute approximately10-20% of all total hip replacement performed in Scandinavia[74,99].
Revision rates are higher for younger patients with long life expectancy and higher level of physical activity[109]. Prostheses inserted after revision surgery have poorer fixation and shorter longevity[30,70]. This results in longer rehabilitation times, poorer functional outcome and reduction in quality of life for the patient [31,110]. Revision arthroplasty is also costly for the health system[40,67].
Approximately two-thirds of revision surgeries are due to aseptic loosening of the implants, while dislocations and infections account for about 10% each[73]. Other reasons for revision surgery can be femoral fractures, implant failure or unexplainable pain.
It is apparent that there is a need to improve the long term survival rate of the primary implants.

Two general fixation principles are currently used in joint replacement therapy. Implants can be fixated with or without cement. Cement fixation of implants is the current Gold Standard for older patients with a relative short life expectancy and low level of physical activity. For younger patients, cement fixation has its limitations. Younger patients typically have a higher level of physical activity. This high level of activity increases the forces applied on the components of the prosthesis, cement and surrounding bone. This may result in cracking of the cement and production of wear debris from the articulation surfaces (i.e. polyethylene and metal). The combination of wear debris and lack of implant stability is associated with osteolysis and implant loosening[50,81].

Cementless implants have higher survival rates than cemented implants in younger patients[52,73,74] and are the first choice for younger patients in most clinics.

Cementless implants are inserted with press-fit technique and rely on osseointegration and interference fit between implant and bone to obtain a good fixation.
Many factors influence the osseointegration of the implant. Surgical skill, choice of technique, implant design, and implant surface properties are major factors.

Early ossointegration is believed to influence the short term, as well as, the long term survival rate of implants[135]. Mjöberg presented a theory speculating that loosening of an implant begins at an early stage due to either insufficient initial fixation or early loss of fixation. The resulting micro-motion of the unstable implant will contribute to the long term generation of wear debris depending on factors such as the patients' weight and level of physical activity[81].

Current research in orthopaedic surgery and biomaterials is focusing on developing orthopaedic implants which can enhance the early osseointegration and stability, thereby potentially increasing the longevity of the implants.

The discoveries of biological structures, which influence osteoblast adhesion, proliferation and differentiation on surfaces, have led to the idea of using these structures to biologically modify the implant surface. By biological modification, an otherwise inert implant surface may obtain osteoconductive or inductive properties.

The extracellular matrix proteins can function as mediators of osteoblast and pre-osteoblast adhesion to surfaces. The proteins contain domains which interact with adhesion receptors on cells. The peptide sequence RGD (Arginine-Glycine-Aspartic acid) is now

recognized as a key domain in this interaction.

Synthetic RGD peptides can be chemically immobilized on the surface of orthopedic implants. The immobilized RGD peptides are believed to serve as direct adhesion sites for bone forming cells and their precursors. Several *in vitro* studies have demonstrated that immobilized RGD peptides can facilitate osteoblast adhesion on varies surfaces[27,37,62,77,106]. Only few *In vivo* studies have investigated the effect of RGD in bone [37,119].

PURPOSE OF EXPERIMENTAL STUDIES

The purpose of the presented experimental studies was to evaluate whether the early osseointegration and mechanical fixation of titanium alloy implants could be improved by immobilizing cyclic RGD peptide on the implant surface.
The implants were examined in four different experimental models, each exposing the implant to clinically relevant conditions. The four configurations varied the interface (press-fit or critical gap insertion) and loading condition (loaded or unloaded).
The implants were evaluated by histomorphometry and push-out test.

In addition to the *in vivo* trials, implants with immobilized cyclic RGD peptides were evaluated *in vitro* by X-ray Photoelectron Spectroscopy (XPS). The XPS analysis evaluated whether the immobilized RGD molecules had the preferred orientation for cell adhesion.

Hypotheses

Implants surrounded by a gap
Immobilized cyclic RGD peptide on titanium alloy implants will increase bone ongrowth and mechanical fixation compared to identical implants without cyclic RGD peptide.

Implants inserted as press-fit
Immobilized cyclic RGD peptide on titanium alloy implants will increase bone ongrowth compared to identical implants without cyclic RGD peptide. Only minor differences in mechanical fixation are expected as the implants are well fixed initially.

XPS analysis
The immobilized RGD peptide will have the preferred orientation for cell adhesion. The phosphonate anchor will be closer to the titanium surface than the RGD pentapeptide.

BACKGROUND

Factors influencing cementless implant fixation

Many factors influence the long term survival of a cementless joint prosthesis.
Factors which relate to the patient include presence of pathological bone disease (arthritis, osteoporosis, rheumatoid arthritis etc.) or systemic disease, infections, pharmacological treatment, level of physical activity, compliance with instructions and smoking.
Factors which do not relate to the patient include the skill of the surgeon, method of implant site preparation, implant design, implant surface characteristic and osteoconductive coatings.
All these factors must be taken into consideration when a suitable implant is chosen.

Cementless implants. Clinical and experimental background

Cementless implants are widely used in hip arthroplasty while the use of cementless implants in knee arthroplasty is still limited, because of the unpredictability of the individual outcome[52,109]. This section will focus primarily on total hip arthoplasty (THA).

The cementless THA consists of a femoral component, an acetabular cup and typically a liner of polyethylene, metal or ceramics.
The implants are usually made of titanium alloy (Ti-6Al-4V) or Crome-Cobolt. The surfaces of cementless implants are porous coated, gritblasted, smooth or a combination. Many femoral components have a proximal porous coating while the distal portion of the implant is gritblasted or smooth while others are fully coated.
The porous surface can be plasma sprayed (closed porous structure), or be made of beads or fiber mesh (open porous structure).

Some implants are coated with commercially pure (c.p.) titanium others with titanium alloy or Co-Cr. The metallic surface of the implant can also be coated with calcium phosphates (e.g. hydroxyapatite or tricalcium-phosphate).

The components are situated in different bone beds. The femoral stem is primarily fixated in the proximal femur which is rich in cancellous bone. The acetabular cup is predominantly placed in the subchondral cortical bone of the acetabulum.

As mentioned earlier the combination of good implant design and implant preparation method is essential to ensure long term survival of the cementless prosthesis. First and second generation of cementless implants preformed poorly, while the latest generations of implants with porous coating have short and mid-term survival rates equal to or better than cemented implants in younger patients[54,53,52,35,99]. The problems of early implant designs included too large femoral heads, poor liners and locking mechanisms, and too thin polyethylene [8,16,53,135].

Some of the first generation cementless implants had smooth surfaces on the entire stem and cup. The implants had unacceptable failure rates and their use was abandoned in the early 1990s [33,53].

The femoral components generally have high mid-term survival rates. Bourne et al. reported excellent survival rates of porous coated stems (100%) at 10 year follow-up[17]. Several other follow-up studies have reported close to 100% survival rates of porous coated stems at up to 10 years[11,35,46,58].

Several authors have reported higher failure rates of the cementless acetabular cup compared to the femoral stem[11,17,35,46].
Mid-term reports on the new porous coated hemispherical press-fit cups are however promising[53,75,52,132,138].

Hydroxyapatite coated implants was introduced in the late 80s and early 90s.
The advantage of hydroxyapatite is that it provides the implant osteoconductive properties.
Experimental studies have documented this osteoconductive effect of hydroxyapatite.
Søballe et al. demonstrated that hydroxyapatite coating of implants resulted in superior osseointegration and mechanical fixation compared to titanium implants in a 2 mm gap model. Superior osseointegration was also seen for hydroxyapatite coated implants inserted as press-fit[128,127].
The HA coating also enhances the fixation of implants exposed to intermittent loading and micromotion [129,125,126]
Rahbek et al. reported that hydroxyapatite had a sealing effect on the peri-implant migration of polyethylene particles[101,102].

The experimental results are supported by clinical studies. HA-coated prostheses generally have high short and mid- term survival rates and the patients have a significant reduction in thigh pain [17,20,24,66,120].
Havelin et al reported from the Norwegian hip register that HA coated stems had lower failure rates than porous coated femoral stems[52].
Radiostereometric analyses (RSA) of clinical implants have shown that hydroxyapatite coated femoral stems migrate less than uncoated control implants[130] and that hydroxyapatite coated acetabular cups obtain superior fixation[135].
Long term results beyond ten years are still needed before we make the final conclusion.

Some authors have reported unacceptable failure rates of 10-30% after ten years using hydroxyapatite coated acetabular cups[14, 21,22,76,104,80,82,111].

There may be several reasons for these high failure rates. Some relates to the design of the prosthesis. The longevity of poorly designed prostheses will not be increased by an osteoconductive coating. For example, the screw cups used in some of the mentioned studies are known to cause osteonecrosis and early migration[38,56,122].

Other reasons for failure relates to the coating and the substrate of coating.
Coating thickness is an important issue in relation to hydroxyapatite. The coating is to some extent resorbed, which has been reported in both experimental and retrieval studies[89,1].
Studies have reported that the resorbed hydroxyapatite is replaced by bone[91,88].
However, if the coating is too thick, an undermining delamination may occur. This can destabilize the implant. Although not documented by randomized studies, the optimal thickness is considered to be in the range of 50-100 microns[115] or less.

The substrate of coating is of great importance. Overgaard et al. reported delamination of the HA coating on gritblasted implants, and recommended porous surfaces for HA coatings[87]. Many of the follow-up studies reporting high failure rates for HA coated implants implicate the use of gritblasted or smooth cups[104,66,22].
Although gritblasted cups with HA performs poorly, some studies have reported excellent results with HA coated grit-blasted stems [105,121,141].
As Morscher et al. reported, HA coating is clearly unsuitable on all polyethylene cups[82].

In conclusion, the porous coated surface is superior to smooth or gritblasted surfaces. Calcium phosphate coatings in recommended thickness and on porous coated surfaces have improved the mid-term survival rates of cementless hip implants. The increased longevity of implants is most likely due to the osteoconductive properties of the calcium phosphates. The improved osteoconductive properties enhance early osseointegration and reduce migration of the implants.

Despite the good results with calcium phosphate coatings there is still room for improvement.
If the immobilized RGD peptide can provide the metallic implants with osteoconductive properties comparable to that of calcium-phosphates, it may useful in the future joint replacement therapy.

Bone-implant biology

The biological response after implantation is a complex and highly dynamic process and not fully understood. The process of bone ingrowth into porous implant surfaces has been compared to fracture healing [134].
It seems reasonable that there are similarities between fracture healing and the healing response after insertion of an implant as the surgical preparation of the implantation site involves traumatizing the bone by reaming or rasping. Detailed description of the phases of fracture healing and molecular biology involved are described elsewhere[34,79].

Immediately after implantation, a haematoma will form at the interface and inflammatory response will be initiated as signaling molecules will be released. Activated platelets and inflammatory cells (for example macrophages) as well as the traumatized bone[19] may be the source of signaling molecules. Signaling molecules include several cytokines for example Tumor Necrosis Factor (TNF-α), Interleukins (IL-1,IL-6) and the growth factors: Transforming Growth Factor (TGF-β), platelet derived growth factor (PDGF), insulin-like growth factor (IGF) and bone morphogenetic proteins (BMPs)[12,34,79].
The signaling molecules regulate a repair response which includes angiogenesis, removal of necrotic bone, and recruitment and differentiation of stem cells to osteoblasts[39].

Some of the initial events occurring at the implant interface after implantation are becoming better known. Early cell adhesion is one of the important events.
The adhesion process is a basic cellular process for most cells. The adhesion influences cell migration and differentiation[5].
It is now widely recognized that extracellular matrix proteins play an important role in the regulation of cell adhesion to substrates.
One current theory is that the surface of the implants will be saturated by proteins immediately after implantation[103]. The proteins come from the blood or tissue fluid. The first proteins may remain on the implant and mediate interactions between implant and cells. Alternatively, these proteins desorb and are replaced by more specialized extracellular bone matrix proteins such as osteopontin, bone sialoprotein, vitronectin or fibronectin[98].

The proteins are suggested to form an interposing layer between the implant and the tissue. Some investigators have described such an interposing layer between titanium implants and bone[3,10,59,71,84]. The layers have been reported to have a thickness between 20-200 nm. Albrektsson and Hansson reported that the layer was rich in glycosaminoglycans[3]. Later studies using immunoelectron microscopy and immunocytochemical techniques have shown that the interfacial layer is rich in noncollagenous extracellular proteins[10,98].

The extracellular bone matrix proteins contain domains of specific peptide sequences which function as mediators of cell adhesion. The RGD sequence is the best described sequence involved in the adhesion process and will be discussed in details below.
Transmembrane proteins on the cell surface, known as integrins, interact with the peptide sequences and trigger intracellular mechanisms which may lead to cell proliferation and differentiation.

Once the cells adhere to the surface, adhesion of more cells can be facilitated by another group of adhesion receptors. While integrins

mediate cell-substrate adhesion cadherins mediate cell-cell adhesion[5].
Once the cells adhere to each other, gap junctions will form. Gap junctions are transcellular channels which mediate cell-cell communication. The establishment of gap junctions is necessary for function of differentiated cells and thereby the organization of tissue[23,69].

The differentiated osteoblasts will then begin the mineralization process and immature woven bone will form. The immature bone is characterized by randomly oriented collagen fibers. The woven bone will be replaced by lamellar bone at a later stage by the process of bone remodeling.

Other peptide sequences can function as mediators of osteoblast cell adhesion. Some of these include the heparin-binding domain FHRRIKA[106] and KGD sequence[96,116].
Collagen I have been shown to promote osteoblast adhesion[43], but it was not capable to stimulate osteoblast differentiation alone[13].

RGD peptide

RGD peptide is the sequence of three amino acids: Arginine, glycine and aspartic acid. The RGD domain is found in many proteins throughout the body. In bone matrix RGD peptide have been isolated in the extracellular proteins: Osteopontin[131], bone sialoprotein[41], vitronectin[113], trombospondin[68], fibronectin[93] and some collagens.
The function of the RGD sequence was first discovered by Piesenbacher et al.[93]. They discovered that RGD played an important role in the communication between the extracellular matrix proteins and cells. The RGD peptide serves as an adhesion molecule for cell receptors. The adhesion process triggers intracellular events and leads to cell spreading and differentiation.
The regulatory mechanism of this process is complex and still not fully understood.

The receptors on the cells which interact with RGD are known as integrins. The integrins are a large family of transmembrane protein heterodimers which contain one α subunit and one β subunit[57,113]. The specificity of the integrin for a ligand is determined by the pairing of subunits[6]. The integrin receptor can be in a low- or high-affinity state, which influences its recognition of certain ligands[18]. More than 20 subunits are now recognized and less than half of the integrins recognize the RGD sequence[112].

Different cells express different integrins. The expression of specific integrin receptors and the pattern of expression vary depending on the stage of cell differentiation. Osteoprogenitor cell and osteoblasts express several integrins but typically a few specific integrins dominate these cell lines[48]. The integrins containing the $\alpha_v\beta_3$ and $\alpha_v\beta_5$ subunits commonly associated with vitronectin have been identified as playing an important role in the adhesion and proliferation of these cells[137,108,117]. Thomas et al. observed a significant reduction in osteoblast adhesion to the surface of a material when the added serum was depleted of vitronectin. Rezania et al. reported that only the vitronectin receptors governed long term cell adhesion[107].

Other integrin subunits have been suggested to play a role in the adhesion process of osteoblasts[37].
Growth factors have been suggested to enhance mineralization on RGD coated surfaces[7,28].

As several integrins on different cells recognizes the RGD sequence, another mechanism of control is required to ensure that selective cell adhesion takes place.

This control mechanism lies within the RGD containing protein itself. It is suggested that when the protein is inactive the RGD sequence is hidden within the structure of the

protein[113]. This means that the RGD sequence is inaccessible to the integrins.
Proteins are dynamic molecules and if stimulated they can undergo structural or conformational changes and thereby expose the RGD sequence[95,100,139].
Events that could stimulate conformational changes in extracellular matrix proteins could be the process of adsorption on a surface or pH changes.
The conformation of the presented RGD sequence and the side chain amino acids are important[61]. The conformation and side chains regulate which specific integrin can interact with the RGD peptide.
The conformation also plays an important role in the resulting cellular activity induced by the interaction between the integrin and the RGD peptide[9,72].
Studies of synthetic RGD with a constrained conformation have shown that small changes in the conformation can increase cellular activity dramatically[47,94].

It is possible that a biomaterials' ability to promote osseointegration can be predicted by how the surface binds extracellular bone matrix proteins.
RGD containing proteins adsorb more easily on certain surfaces. Kilpadi et al. showed that hydroxyapatite surfaces adsorb more fibronectin and vitronectin from serum than commercially pure titanium or stainless steel[64]. This resulted in an improved binding of osteoblast precursor cells. Specific domains in, the RGD containing, bone sialoprotein and osteopontin specifically interact with hydroxyapatite[41,131].
Matsuura and Okamoto et al. reported that RGD peptide regulates the cell adhesion on hydroxyapatite but not on titanium[78,86].

This might explain why hydroxyapatite is such a potent stimulator of bone ongrowth. Experimental studies have demonstrated that HA coated implants surrounded by a critical gap achieve 40 % bone ongrowth after only 4 weeks. A pattern of bidirectional bone growth was described for hydroxyapatite coated implants as bone density was higher at the implant interface than in the central section of the gap. Bone ongrowth on titanium implants was very limited[128,124]. It is possible that the osteoconductive effect of hydroxyapatite may be related to improved binding of RGD containing proteins on the surface.

Synthetic RGD

Several synthetic RGD peptides have been analyzed for the purpose of creating surfaces that stimulate bone ongrowth[27,37,62,77,106].
Soluble synthetic RGD peptides can also inhibit bone formation[45].The synthetic RGD peptides can be produced as either linear or cyclic peptides. The incorporation of RGD into a cyclic molecule has several advantages. The molecule is better protected from enzymatic cleavage than the linear peptide[15] and the conformation of the peptide can be more easily controlled[26,55]. The conformation of the cyclic peptide can then be changed by replacing the side-chain amino-acids. This has brought forward synthetic RGD peptides which are highly selective for certain integrins[72].

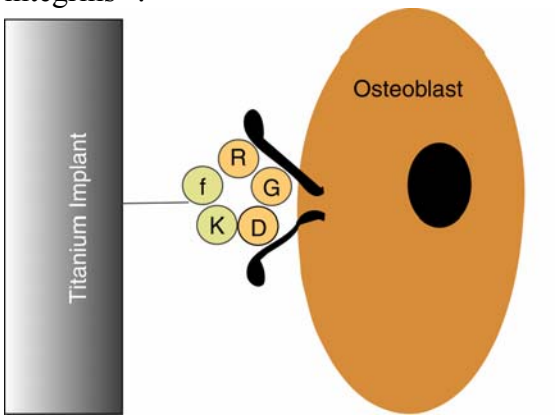

Fig. 1. Illustration of the interaction between the immobilized RGD peptide and the transmembrane integrin receptor on the osteoblast.

In this thesis we use titanium alloy implants with an immobilized cyclic-RGDfK peptide (Fig. 1) which binds to the $\alpha_v\beta_3$ and $\alpha_v\beta_5$ integrin subunits. *In vitro* studies have

demonstrated that this specific RGD peptide induce a high level of activity in osteoblasts and osteoprogenitor cells[9,62,92,97,140] .

The cyclic RGD molecule cannot be directly immobilized on the metallic surface of an orthopedic implant. A chemical linker and anchor molecule must exist in order to covalently couple the RGD peptide to the metal surface. Several anchor molecules can be used. In studies I and II a thiol anchor was used and in study III a phosphonate was used. Parallel *in vitro* studies had demonstrated that phosphonate anchored RGD molecules increased cellular activity[36].

As reported by Kantlehner et al. a spacer molecule of approximately 3.5 nm must be placed between the RGD and anchor molecule[62]. This allows the larger integrin protein structure to interact with the RGD molecule. The entire RGD, spacer and anchor molecule complex is seen in Fig. 2. The coating procedure will be described later.

According to the manufacturer, the RGD coating will remain active after one year of storage. No special packaging is necessary. It is unknown whether the RGD peptide coating is resistant to mechanical stimuli exerted on the surface during press-fit insertion. It is not believed to be a problem for two reasons. The RGD peptide complexes form individual covalent bonds with the surface and do not represent a layer that can delaminate. Considering that the individual molecules are only 4 nm of height the majority of the RGD coating will be protected by the macrostructure of the rough plasma sprayed surface.

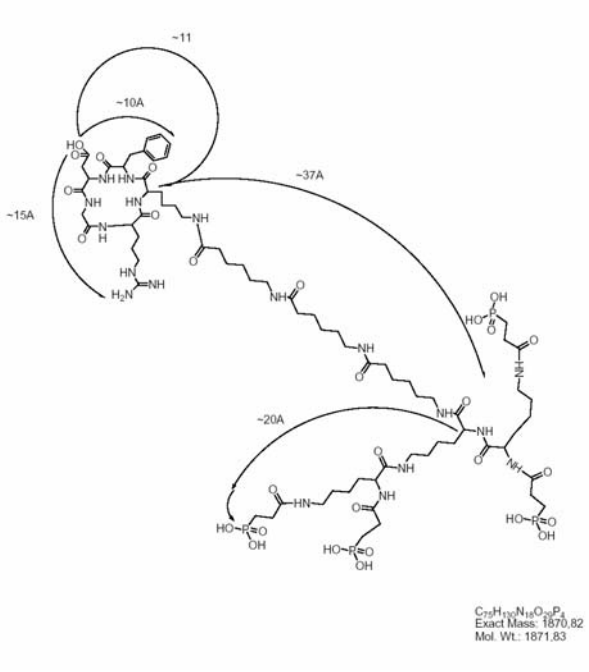

Fig. 2. The RGD molecule complex with a phosphonate anchor. The four phosphonate groups are coupled covalently to the oxide layer of the titanium alloy implant.
(The figure was kindly provided by Biomet-Merck BioMaterials, Darmstadt, Germany)

METHODS

In vitro study

X-ray Photoelectron Spectroscopy

Cyclic RGD with a phosphonate anchor was immobilized, as described below, on titanium alloy discs with a diameter of 10 mm.

The X-ray Photoelectron Spectroscopy (XPS) experiments were carried out on beamline 5 at the ASTRID synchrotron-radiation storage ring (University of Aarhus, Denmark), equipped with a Zeiss SX700 plane grating monochromator to select the desired photon energy (Fig. 3). P-polarized photons hit the sample surface with an angle of 45^{o} and the data presented were collected with a VG CLAM analyzer at 30 eV pass energy and 2 mm slit. The polar angles (the acquisition angle measured with respect to the surface) were either normal emission or 60^{o} off normal. The base pressure in the chamber was around 10^{-10} Torr.

To examine the orientation of the cyclic RGD peptide with phosphonate anchor molecules bound on the titanium alloy surface the intensity ratio of the 2p phosphor (P2p) and the 1s carbon (C1s) peak was measured for the two different polar angles. The change of emission angle changes the mean path of penetration of the emitted photoelectrons. The primary photon energies were 190 eV and 350 eV for the P2p and the C1s, respectively.

In vivo studies

Study design

The study design is paired. RGD coated implants were compared to control implants inserted in the contralateral extremity of the same dog. Only identical implantation sites and models were compared. Bilateral symmetry is assumed. The symmetry of the canine femurs have been described elsewhere[133]. The paired design reduces the risk of making conclusions that are based on biological variance rather than effect of a treatment.

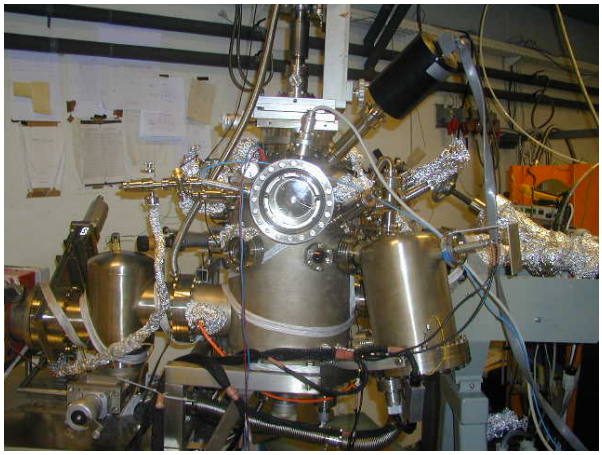

Fig. 3. XPS setup. The discs were placed in the Ultra High Vacuum chamber with a base pressure of approximately 10^{-10} torr.

Sample size

The sample size calculation was based on the following:

$$n1 = n2 = 2(t2\alpha + t\beta)^2 \times SD^2/D^2$$

Error of the first kind (2α) was selected to 5%. Based on previous studies, a SD of 50% for both mechanical and histological data is justified. The minimal clinically relevant difference (D=MIREDIF) not to be overlooked between groups was selected to 70%. Error of the second kind (β), the risk of concluding that two effects are identical if in fact the difference is below the MIREDIF (False negative result), was chosen to be 20% which means a power of 80%.

Based on these assumptions at least 7 experimental subjects had to be included. In the studies we included 8 subjects, to allow for the loss of one individual.

Animal model

The canine is a preferred large experimental animal for experimental studies of implants focusing on fixation and integration of implants used in joint replacement therapy. The proximal and distal sections of the long bones are rich in cancellous bone, which combined with cortical bone in humans represents the fixation areas of hip prosthesis in the proximal femur and acetabulum. The quality of the canine bone is in many ways similar to human bone. The dog is the large experimental animal which lies closest to humans[2]. The implantation sites are easily accessible, which reduces the surgical trauma on supporting tissue and skin.

The canine has 2-3 times faster bone healing and remodeling than humans[65]. This may present a disadvantage in extrapolating results from the canine to the human. On the other hand it is an advantage as observation time may be reduced.

The observation period used in this study is four weeks. This observation period has been suitable to detect differences in tissue response and mechanical fixation in earlier studies of hydroxyapatite coatings and other adjuvant therapies[124,83,129]. The studies presented in this thesis focus on the early biological response to a potential osteoconductive coating. As the bone remodeling rate is increasing, it may be difficult to differentiate between the early tissue response and the remodeling phase.

Ethical considerations

The animal experiments were approved by the Animal Care and Use Committee of the Minneapolis Medical Research Foundation, Minnesota, USA. The surgery and observation was carried out at the approved Animal Care Facilities, Hennepin County Medical Center in Minneapolis following the regulations of the National Institute of Health, USA.

Implants

Geometry

The implants used in the studies are cylindrical in shape. This shape presents several advantages. The implantation site is easily prepared by drilling a hole. Conditions for all implants are therefore standardized. The cylindrical shape also allows serial vertical sectioning of the central portions of the implant which makes unbiased stereological sampling possible[90]. Furthermore the shape is suitable for mechanical push-out testing.

Metal and surface

The implants used in this study are made of titanium alloy (Ti-6Al-4V). The surface structure is a closed porous coating obtained by plasma spraying a titanium alloy core with melted titanium alloy (Biomet® Inc., Warsaw, IN, USA). The plasma spraying of the implants is performed by a manufacturer of human implants. The surface structure is therefore comparable to that seen on commercially available hip implants.
The surface pore size and roughness was not measured for implants used in this study. In earlier studies performed at our institution the plasma spray process identical to the one used in this study resulted in a pore size of 200-1000 μm at the substrate and the surface of the coating, respectively. The gross surface roughness of the plasma spray process (Ra) was 47 μm, with a profile depth of 496 μm (determined using a roughness meter (Perthen, Hannover, Germany) with a stylus tip radius of 3 μm) [123].

Dimensions

The dimension of the cylindrical implant in study I and II is 6 mm in diameter and 10 mm in length. In study III the diameter is 5.8 mm. The core is threaded allowing attachment to an anchor screw or end plates.

RGD coating

The RGD coating was performed by a third party (Biomet-Merck BioMaterials GmbH, Darmstadt, Germany). The coating procedure involves the following steps: The cyclic RGD peptide (-RGDfK[-beta-mercaptopropionyl]) with thiol (study I and II) and phosphonate (study III) anchor was synthesized as described elsewhere[51 60]. The implants were first sterilized by autoclave and then suspended in a sterile filtrated 100 µM solution of the RGDfK peptide in PBS-Buffer at pH 8.3. This concentration has been shown to be optimal for cell adhesion[62]. The implants were left in the suspension for 24 hours and subsequently washed 3 times in PBS-Buffer followed by air drying in a laminar airflow chamber. Following this coating procedure, all implants were sterilized using irradiation (35 kGy of Co-60 for 14 h, Risø National Laboratory, Roskilde, Denmark).
Biomet-Merck Biomaterials GmbH performed quality control of the coating by cell adhesion studies. Further quality control of the plasma sprayed implants used in the studies was not performed by the author. In study III, titanium alloy disc Ø10 mm was coated in the same batch as the implants used in the *in vivo* study. These discs were subjected to analysis by X-ray Photoelectron Spectroscopy (XPS) as described earlier.

Experimental models

The implants were inserted in four different experimental models:

- Unloaded implants with a 1.5 mm gap
- Unloaded implants inserted as press-fit
- Loaded implants with a 0.75 mm gap
- Loaded implants inserted as press-fit

The experimental models used in study I an II are based on earlier models developed by Dr. Kjeld Søballe[124]. Based on the results of study I and II, a new modification of the previous experimental models was developed for study III.
For gap models the gap size is based on earlier studies performed at our institution. Although most orthopedic implants are inserted as press-fit in the clinical setting, as little as 10-20% of the implant may be in direct contact with bone early after implantation[42]. This is mainly due to the anatomical variations at the implantation site [85,118]. The interface between bone and implant can be described as series of gaps with variable gap sizes intersected by focal bone-implant contact points.

The gaps will result in poor osseointegration of porous coated titanium implants as bone ongrowth will be absent or very limited. The implants will typically be fixated by a dense membrane of fibrous tissue. Previous studies at our institution have shown that the gaps must be at least 1 mm in an unloaded model and 0.75 mm in a loaded model to be a critical defects[83,124].

Unloaded 1.5 mm gap (Fig. 4)
The implant was inserted into the proximal tibia. The gaps in this study are regarded as critical size defects at the 4 week observation period. The gap was obtained by attaching a bottom and top washer with a diameter of 9 mm, creating a 1.5 mm circumferential gap between the implant and the surrounding bone. This model provides the implant with stable and unloaded mechanical conditions.

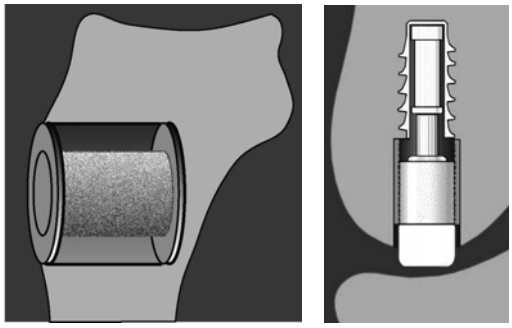

Fig. 4. Experimental gap models without load (left) and with load (right). The load is generated via a polyethylene plug which extends into the

knee. The PE plug pushes against the tibial plateau during each gait cycle.

Loaded 0.75 mm gap (Fig. 4)
The implant was inserted into the medial femoral condyle aligned with the weight-bearing axis. To stabilize the implant, the model required an anchor screw with a centralized threaded pin and insertion of a distal centralizing ring. The implant was situated in a cavity with a diameter of 7.5 mm creating a 0.75 mm circumferential gap. A polyethylene (PE) plug was screwed on the pin distally extending into the joint cavity. Through contact between the PE plug and the tibial plateau, the implants were loaded during each gait cycle. The PE plug allowed full range of motion in the knee joint. The intraarticular placement allowed flow of joint fluid at the gap-implant interface.

Unloaded press-fit (Fig. 5)
The implant was inserted into the proximal tibia. The implantation cavity was created by drilling an undersized (0.1 mm) hole. The implant was then inserted by repeated hammer blows.

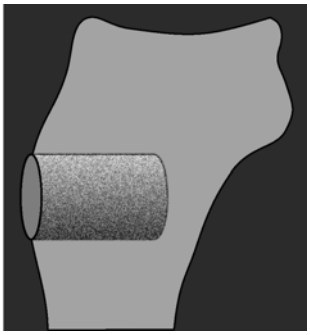

Fig. 5. Press-fit implant inserted in the cancellous region of the proximal tibia.

Loaded press-fit (Fig. 6)
The implant was inserted into the medial femoral condyle. The implant system consisted of proximal threaded tail with a diameter of 3.8 mm fixed to the plasma spray section of the implant with a diameter of 5.8 mm. The tail prevented tilting of the implant during insertion. A distal thread allowed attachment of a PE plug. The drill hole was 0.3 mm undersized. The placement and loading conditions was similar to the loaded gap model as described above.

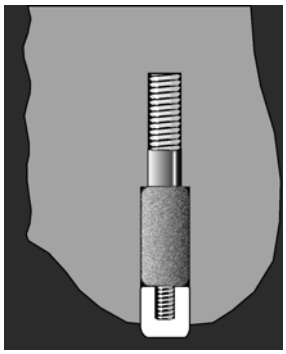

Fig. 6. Press-fit implant in the medial femoral condyle. A stabilizing tail prevents side motion. The implant is loaded via the PE plug.

Anesthesia

Surgery was done under general anesthesia. Premedication was given consisting of IV 4 ml Atrophine Sulphate 0.4 mg/ml, 0.4 ml Azepromazine Maleate 10/mg/ml and 1 g Rocephin (ceftriaxone sodium).
Anesthesia was induced with Thiopental 5% 8 ml prior to intubation and additional milliliters was given as needed. A tracheal tube (size 8) was placed and anesthesia was maintained with Isoflurane 1.5%. The animals maintained their own respiration and a veterinarian nurse assisted breathing as needed. A pulse oxymeter was used to monitor vital functions.

Surgical Technique

All surgery was performed under sterile conditions. All implantation sites were exposed through a medial approach, leaving the medial collateral ligament intact. All drilling was performed at two rotations per second to prevent thermal trauma and osteonecrosis. The implantation site was cleaned using isotonic saline with polymyxin B. After carefully ensuring haemostasis, the

capsule and fascia were closed in layers using an absorbable vicryl suture. The skin was closed with staples. Postoperative x-rays were taken to control implant placement.

Study I

Unloaded model
The implant was inserted in the proximal tibia 10 mm distal to the joint line. The periost was removed in the area of drilling. A guide wire was inserted followed by a 9.0 mm cannulated drill. Bottom and top washers of 9.0 mm diameter were attached to create the 1.5 mm circumferential gap, stabilize the implants, and prevent soft tissue ingrowth from the outer surface. The implant was inserted with light hammer blows.

Loaded model
The knee joint was accessed through an incision just medially to the patella. The weight-bearing area of the medial femoral condyle was identified during flexion through a range of motion. A 2.1 mm Φ guide wire was inserted through the weight-bearing articulating surface and remained within the central portion of the condyle. A 7.5 mm cannulated drill was used. An anchor screw and distal centralizing ring were inserted. The implants were then inserted, leaving a 0.75 mm circumferential gap. The polyethylene plug was screwed on. Before closure it was assured that the protruding PE plug did not interfere with the full range motion of the knee.

Study II

In the proximal tibia, 8 mm distal to the joint the periost was removed in the area of drilling. Initially a guide wire was inserted, followed by a 5.9 mm cannulated drill. Drilling was performed at 2 rotations per second to prevent thermal trauma to the bone. The implant was inserted press-fit with repeated incremental hammer blows.

Study III

Surgical access and insertion of a guide-wire was identical to that described for loaded implants in study I. Using a 3.5 mm cannulated drill, a hole 2.5 cm deep is created. This followed by a 5.5 mm cannulated drill to a depth of 1.5 cm. Then a 6.1 mm cannulated drill used for the proximal 0.5 cm portion. This created a press-fit with the proximal threaded tail, and with the plasma spray implant surface. The implant was inserted axially with tight press-fit by repeated hammer blows. The PE plug was then screwed onto the threaded distal portion of the implant. Before closure it was assured that the protruding PE plug did not interfere with the full range motion of the knee.

Post operative observation

Prophylactic antibiotics were administered for a minimum of 3 days, or until the dogs were no longer febrile (Rocephin 1 gram IM per day). Pain treatment consisted of IM 0.0075 mg/kg/daily Bupronex (buprenophine hydrochloride) 0.3 mg/ml and as needed.
The animals were assessed daily with regards to hind limb function, signs pain and discomfort and diet intake by a veterinarian experienced with research animals.
The dogs were housed two in each cage two days postoperatively and were allowed free daily exercise.
The animals were euthanized after four weeks of observation. The animals were premedicated and anaesthetized as described above. Then a saturated thiobarbital solution was given to induce immediate heart failure. Cultures were taken from all implantation sites and articular fluid.

Specimen preparation

The distal femur and proximal tibiae were harvested and stored at –20 ° C approximately two weeks prior to preparation. Two transverse bone-implant specimens were cut

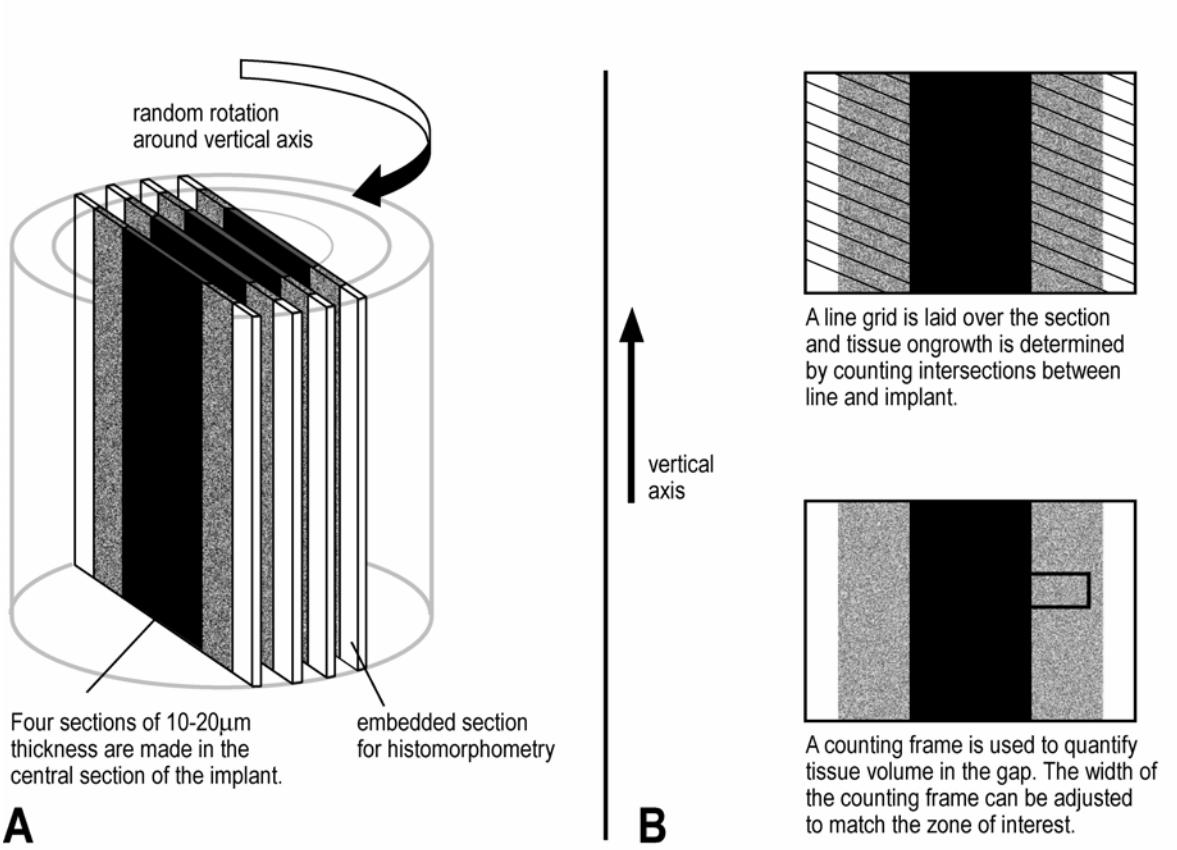

Fig. 7. (A) The embedded transverse cut specimens were randomly rotated around the vertical axis and four central sections were cut. (B) Tissue ongrowth was determined using a line grid. The tissue at line-surface intersections was counted. To quantify tissue volume in the concentric zones a counting frame and point counting was used.

on a water-cooled diamond band saw (Exact Appartebau, Germany). The outermost specimen of 3 mm was used for mechanical testing. The remaining specimen was fixed in 70% ethanol for histological evaluation.

Histological evaluation

The specimens were dehydrated in graded ethanol (70-100%) containing 0.4% basic fuchsine and embedded in methylmethacrylate. According to stereological principles, the vertical section technique was applied to obtain unbiased histomorphometric estimates[49,90].The embedded specimens with the implant *in situ* were randomly rotated around the vertical axis and serially sectioned to 10-20 µm using a Leiden microtome (Leiden, Holland) (Fig.7). The application of stereological sampling on four serial sections of the central portion of the implant allows three-dimensionally structured tissue to be quantified with a three-dimensional measure (tissue volume). During sectioning the specimens was counterstained with 2% light green[44]. The light green stains mineralized bone only in the cutting surface and thereby provides a reliable plane of focus in the light microscope regardless of minor differences in thickness of the sections.

For quantification, the focus plane of the green colored mineralized tissue was obtained. The method of sectioning and staining allows differentiation between three groups of tissue. Bone tissue was defined as tissue stained green with the characteristic structure of bone. Bone is categorized as either lamellar bone or irregular structured woven bone.

Fibrous tissue is colored red and included: 1) dense fibrous tissue completely dominated by fibers. The fibers are regular (orientated parallel to each other) or irregular without a clear orientation but forming a three dimensional network. 2) loose fibrous tissue with less fibers and appearance of more cells. A differentiation between the two types of

fibrous tissue was attempted. However, the distinction between the two fibrous tissue forms was made difficult by transitional tissue which could be categorized as either type. This resulted in too low reproducibility. Bone marrow was tissue showing the typical cellular masses of blood cells lying between the round empty fat cells.

Histomorphometry was performed on specimens blinded to the examiner using an image-analysis system (C.A.S.T-Grid; Olympus, Denmark). Tissue ongrowth was defined as tissue in direct contact with the implant surface at the light microscope level and was determined using a line intercepting technique. The tissue at intersections between line and implant surface was counted in successive adjacent fields at the bone-implant interface. The percentage of tissue ongrowth was calculated by dividing the number of tissue intersections by the total number of intersections.
Tissue surrounding the implants was quantified in selected zones. For implants surrounded by a gap, the gap was divided in an inner and outer zone each covering half of the gap. For press-fitted implants the zones were 0-100 µm and 0-500 µm or 0-750 µm. The tissue volume was determined by point-counting technique.
As a rule of thumb the amount of intersections or hits on the tissue of interest should be 100-200[90].

Mechanical testing

Implants were tested to failure by a push-out test on an Instron Universal Test Machine (Model 4302, Instron, UK). The test was blinded to the examiner. The specimens were placed on a metal support jig with a 7.4 mm circular opening. This left a clearance of the hole in the support jig of 0.7 mm as recommended by Dhert et al.[29]. A preload of 2 N was applied to define contact position. Displacement rate was 5.0 mm/minute. Ultimate shear strength (MPa), apparent shear strength (MPa/mm), and energy absorption (J/m^2) were calculated from load-displacement curves (Fig. 8).

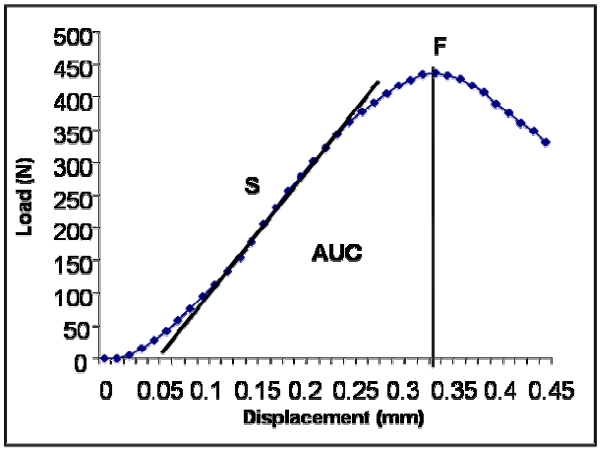

Fig. 8. Load-displacement curve obtained from push-out testing. Ultimate shear strength (MPa) was calculated from the maximum force (F) applied before failure was complete in the interface. Apparent shear stiffness (MPa/mm) was calculated from the slope (S) of the curve. The area under the curve (AUC) represents the total energy absorption (J/m^2).

The transverse sections used for push-out testing varied in length (range 2.7-3.4 mm). Therefore all push-out parameters were normalized by the area of the cylindrical implant (Area = π x diameter x length). As the true area of the porous coated implant is unknown we used the area of the smooth cylinder. This means that the push-out results are overestimated compared to the true value.

Reproducibility

Double measurements were carried out to calculate the intra-observer variation. The measurements were carried out by the same person using identical equipment and setup. The coefficient of error CE was calculated as described by Therkelsen[136]:

$$s^2 = (1/(2k)) \sum d^2$$

where k is the number of double measurements and d is the difference between first and second assessment. Then CE is calculated as:

$$CE = s / \bar{x}$$

where x is the mean value of first and second assessment.

Push-out test
Double measurements were performed on eight randomly selected load-displacement curves. The CE for ultimate shear strength (USS), apparent shear stiffness (ASS) and total energy absorption (TEA) were 0%, 9%, and 0% respectively. The low coefficient of error for USS and TEA is due to the computerized identification of ultimate shear strength and calculation of the area of the curve, while the stiffness is calculated by individual judgment of the slope of the curve (Fig. 8).

Histomorphometry
Double measurements were carried out for ongrowth and bone volume in the gap for eight randomly selected implants. The CE for bone, fibrous tissue and bone marrow was for ongrowth 8 %, 13%, 2% respectively and for bone, fibrous tissue and bone marrow volume in the gap 17 %, 6 % and 6 % respectively.

Statistics

The statistical software STATA Intercooled 8.0 (STATA Inc., USA) was used. The difference between pairs was evaluated with regards to normal distribution by graphical plotting. As normality could not be assumed, the data was subjected to a non-parametric analysis (Wilcoxon Signed Ranks Test). Data is presented as median and interquartile ranges unless otherwise noted.

Exclusions

Study I
The push-out testing of two implants, in the group of loaded gap implants, produced values more than ten times the median of the remaining implants. One implant was from the control group and the other from the RGD coated group. Histological examination of the implants did not show any bony integration which could explain such a relative large increase in mechanical fixation. The only plausible explanation was malalignment during push-out testing. The push-out sections were therefore excluded from the study. After consulting a statistician, we decided to regard the push-out results as independent data and accordingly use an unpaired statistical test (Mann-Whitney).
The histological sections from these dogs were included in the study.

Study II
Implants from two dogs were excluded at the time of specimen preparation. One dog was excluded since 3 mm of the implant on one side was protruding from the drill hole, because a piece of bone broke off during surgery. Following specimen removal, it was determined that the absent bone accounted for too much of the implant surface to enable unbiased sectioning. In another dog, the macroscopic examination of one section intended for histological examination suggested that it was placed in cortical bone. This was confirmed by histological examination and the dog was excluded.

Study III
The thread used to attach the polyethylene plug broke off one implant during implantation. The implant could not be replaced without compromising the controlled conditions. To keep the study paired, the animal was excluded from the study at the time of surgery.

RESULTS

In vitro study

X-ray Photoelectron Spectroscopy

X-ray Photoelectron Spectroscopy (XPS) shows that a distinct phosphor signal is detected from the titanium surface coated with the cyclic RGD peptide (Fig. 9). Since this signal is absent in the case of the non-coated titanium samples (data not shown), it is concluded that the phosphor signal arises from the phosphonate anchor in the coating.

The peak area ratio between normal and 60^{o} off normal emission for the P2p and the C1s differs by a factor of two (0.19 vs. 0.37, respectively) even though the kinetic energy of the emitted photoelectrons are nearly the same leading to approximately the same mean free path[142]. This indicates that the carbon- and phosphor atom distributions in the coated layer is not the same and that the mean distance from the titanium surface to the phosphor atoms is smaller, than the mean distance from the titanium to the carbon atoms.

A rough estimate using an electron mean free path of 6 Angstrom, which corresponds to a dense layer of carbon as e.g. graphite, gives a mean layer of 0.4 nm material on top of the phosphor atoms.
Due to the spatially large anchor molecule consisting of four phosphonate molecules and only one spacer, the electron density in the adsorbed layer is expected to be low as compared to a dense carbon layer.
Therefore, the real value of the electron mean free path, and thereby the resulting estimate of the layer thickness, is probably significantly larger.

It can be concluded, that the cyclic RGD peptide with phosphonate anchor molecules were not randomly ordered and that on average the phosphonate anchor was situated closer to the titanium surface than the average carbon atom.

The length of the entire RGD-phosphonate anchor molecule was approximate 4 nm as indicated in Fig.2, while the average thickness of the layer on top of the phosphor atoms was measured to 0.4 nm.
Several reasons are possible: Some areas may not be ordered or the atomic density of the self assembled layer is low as mentioned above. Furthermore, although the cyclic RGD structure is rigid, the linker unit is rather flexible and there is no reason to assume that all linkers will take maximum distance. Molecules could therefore be lying down exposing the phosphonate anchor.

Overall, the result supports that there is an average preferred orientation of the cyclic RGD molecules with the phosphonate anchor directed towards the titanium surface. A more quantitative XPS study has not been carried out.

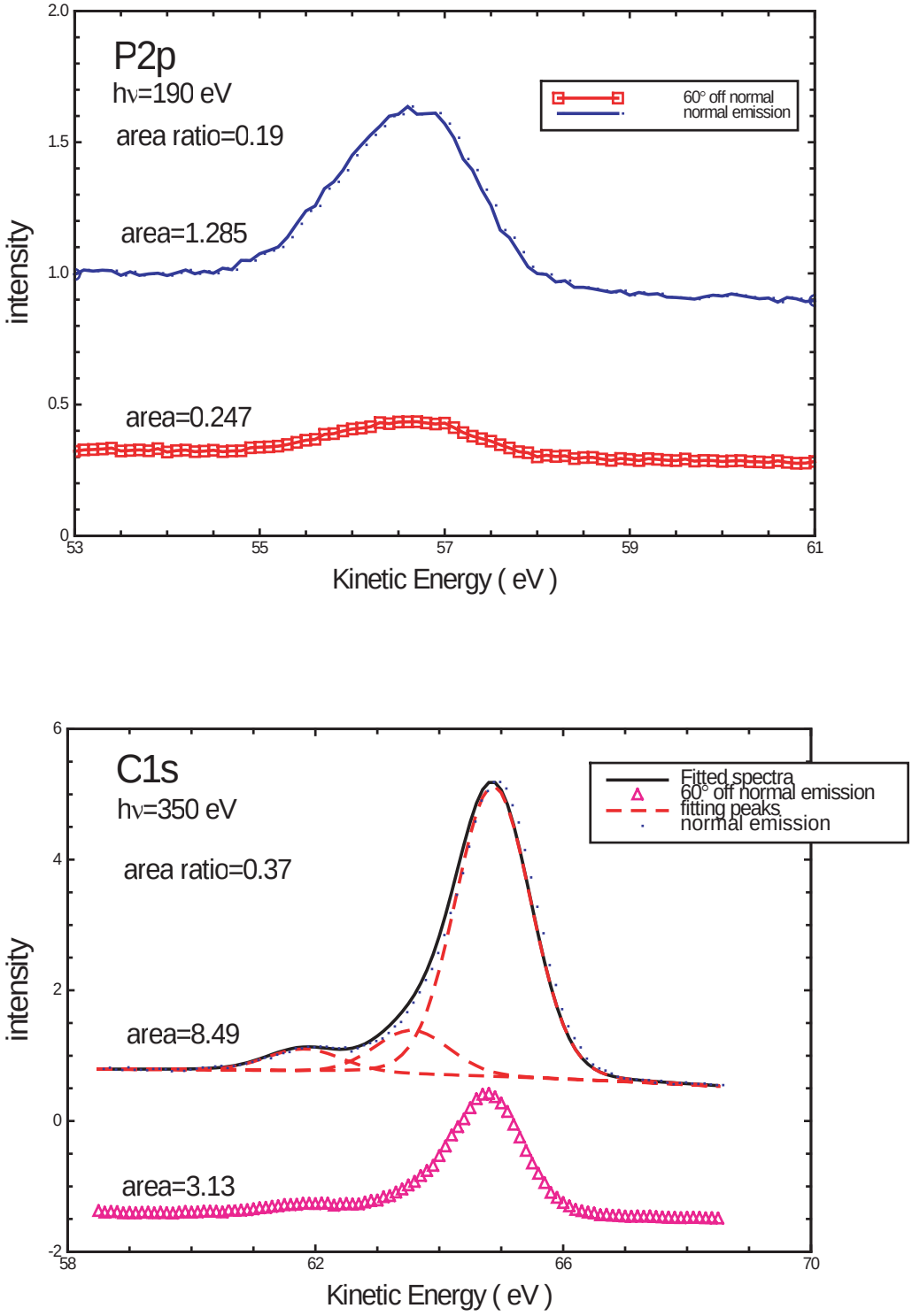

Fig. 9. Results from Xray Photoelectron Spectroscopy. The 2p phosphor (P2p) peak (top) and the 1s carbon (C1s) peaks (bottom) measured for normal emission and 60o off normal emission.
The photon energy was h_v=190 eV and 350 eV, respectively.

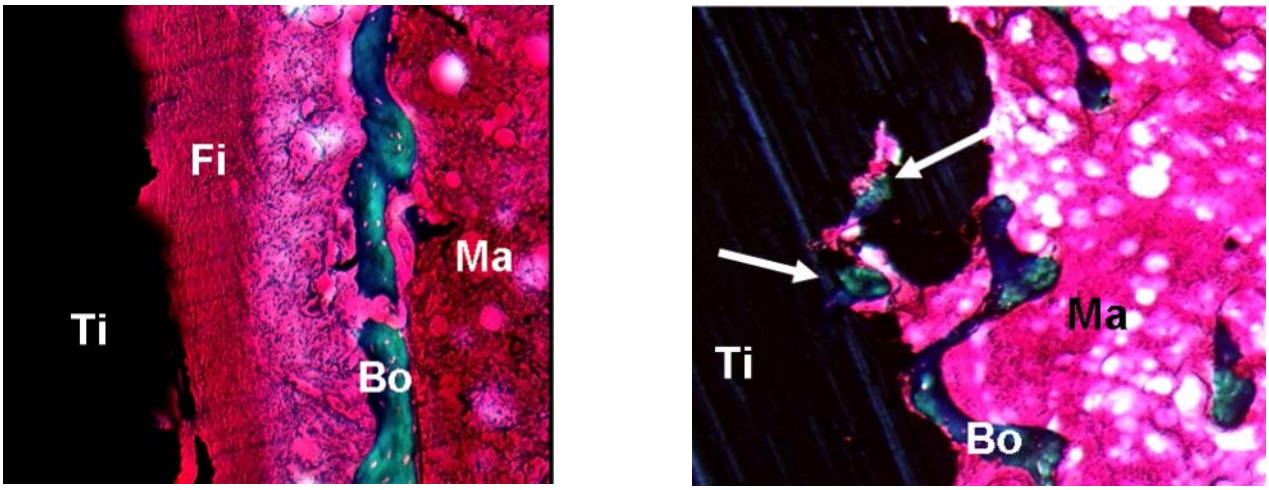

Fig. 10. Histological slides of unloaded implants surrounded by a gap (Study I). On the left a control implant. A dense fibrous membrane (Fi) is surrounding the implant (Ti). The bone tended to form a shell like structure around the fibrous membrane. On the right a RGD coated implant. Only small fraction of bone ongrowth (arrows) was seen. The presence of bone ongrowth disrupted the fibrous membrane formation as the bone ongrowth was always supported by bone marrow (Ma) as seen.

Fig. 11. Histological slides of loaded implants surrounded by a gap. Two RGD coated implants had signs of bidirectional bone growth, as illustrated by arrows (left). Most implants were covered by a fibrous membrane (right). Less fibrous tissue was seen for RGD coated implants in the inner half of the gap.

In vivo studies

For all studies the animals completed the observation time. No complications were seen. There were no signs of infections or fever. All cultures were without growth of pathogens. Within 48 hours postoperatively, the dogs were fully weight-bearing on their hind-limbs and had a normal diet intake

Histology

Study I
Fibrous tissue dominated the implant-tissue interface. A general observation was that the fibrous tissue on the control implants was more undisrupted and appeared to form a thicker and denser fibrous membrane (Fig. 10).
A small amount of bone ongrowth was seen on half (4/8) of the RGD coated implants for both loaded and unloaded implants. Two of

the loaded RGD coated implants had areas with bidirectional bone growth (Fig.11). Only 1/8 of the loaded control implants and 2/8 of the unloaded control implants had areas with small amounts of bone ongrowth. Bone marrow dominated the gap.

Study II
Only woven bone ongrowth was seen for both RGD coated and control implants.
Fibrous tissue ongrowth was seen on 2/6 of the RGD coated implants, while all control implants had some degree of fibrous tissue ongrowth. A dense fibrous membrane occupied the majority of the interface of two control implants. No dense fibrous tissue formation was observed on any of the RGD coated implants.

Study III
No fibrous tissue was seen for the RGD coated or control implants.
The majority of bone ongrowth consisted of woven bone.

Mechanical fixation

The results from all push-out tests can be seen in Table 1.

Study I
The effect of RGD coating was moderate as significant difference was not found in all parameters. Unloaded implants had significantly higher apparent shear stiffness compared to the control group (p=0.01). Moderately higher ultimate shear strength (p=0.1) and lower total energy absorption (p=1.0) was observed.
Loaded implants with RGD showed a significant three-fold increase in total energy absorption (p=0.04), a 2- fold median increase in ultimate shear strength (p=0.08) and a 3-fold median increase in shear stiffness (p=0.1).

Study II
Apparent shear stiffness was significantly higher for RGD coated implants (p=0.04). Only moderate increases were observed for shear strength (p=0.23) and total energy absorption (p=0.12).

Study III
Only a small, non-significant, median increase was observed for RGD coated implants in all parameters.

Model		Ultimate Shear Strength (MPa)	Apparent shear stiffness (MPa/mm)	Total Energy Absorption(J/m^2)
Unloaded 1.5 mm gap Study I	**RGD**	0.19(0.10-0.20)	0.91***** (0.40-1.49))	15(7-36)
	Control	0.15(0.08-0.19)	0.47(0.24-0.64)	23(9-31)
Loaded 0.75 mm gap Study I	**RGD**	0.38 (0.14-0.55)	1.51 (0.47-2.04)	64***** (47-81)
	Control	0.14(0.09-0.30)	0.54 (0.32-0.86)	19 (16-50)
Unloaded Press-fit Study II	**RGD**	4.47(2.48-8.34)	16.44***** (12.56-23.64)	1490(640-2660)
	Control	3.23(2.92-3.97)	9.06(7.92-13.40)	1250(940-1460)
Loaded Press-fit Study III	**RGD**	6.9(4.9-8.4)	29(23-37)	1300(800-1600)
	Control	6.7(5.7-7.9)	25(21-33)	1200(1000-1400)

Table 1. Results from push-out test. Values presented as median and interquartile ranges *p<0.05

	Unloaded 1.5 mm gap			Loaded 0.75 mm gap		
n=8	**ongrowth**	**0-750 µm**	**750-1500µm**	**ongrowth**	**0-375µm**	**375-750µm**
Bone						
RGD	0.3(0-1.7)	8.9*(7.3-11.5)	8.0(5.9-11.8)	0.3(0-5.8)	7.3(5.6-13.9)	7.2(4.4-13.7)
Control	0(0-1.0)	7.3(6.1-9.5)	5.9(4.5-9.8)	0(0-0)	6.7(4.1-10.4)	10(7.5-16.7)
Fibrous tissue						
RGD	90(77.2-99.7)	13(7.6-35.5)	0(0-0)	98(94.2-100)	34(27.2-47.1)	0.7(0-4.5)
Control	95(75.2-100)	21*(13.3-44.1)	0(0-0.3)	100(100-100)	59*(32.3-92.0)	0.5(0-19.2)
Bone marrow						
RGD	8.1(0-22.0)	70(77.8-52.6)	90(85.7-93.4)	0(0-0)	51*(46.6-60.2)	89(81.9-94.1)
Control	4.6(0-22.8)	68(46.3-78.4)	92(89.9-94.9)	0(0-0)	28(19.3-59.2)	87(60.0-91.0)

Table 2. Results from histomorphometry (study I, implants with gap). Values are given as percentage tissue ongrowth and tissue volume in the two zones (median and interquartile ranges). *p <0.05.

Histomorphometry

Study I
Results can be seen in Table 2.

Unloaded implants
A significantly higher bone volume percentage (p=0.04) was seen for RGD coated implants in the inner half of the gap (0-750 µm) while the fibrous tissue volume percentage was significantly reduced (p=0.02) for RGD coated implants (Fig. 12). No significant difference was seen in bone marrow volumes (p=0.7). No differences were seen in any tissues in the outer half of the gap

Loaded implants
Only minor differences were seen in terms of tissue ongrowth. Fibrous tissue volume was significantly lower for RGD coated implants in the inner half of the gap (p=0.03). In this zone bone marrow volume was significantly higher for RGD coated implants (p=0.03), while no difference was seen in bone volume (p=0.21) No significant differences were seen in any tissues in the outer half of the gap. Line scatter plot for fibrous tissue and bone marrow are seen in Fig. 13.

Study II
Results can be seen in Table 3 and Fig. 14. Significantly higher bone ongrowth (p=0.03) and bone volume in a 0-100 µm zone (p=0.047) was seen for RGD coated implants. Fibrous tissue ongrowth was significantly

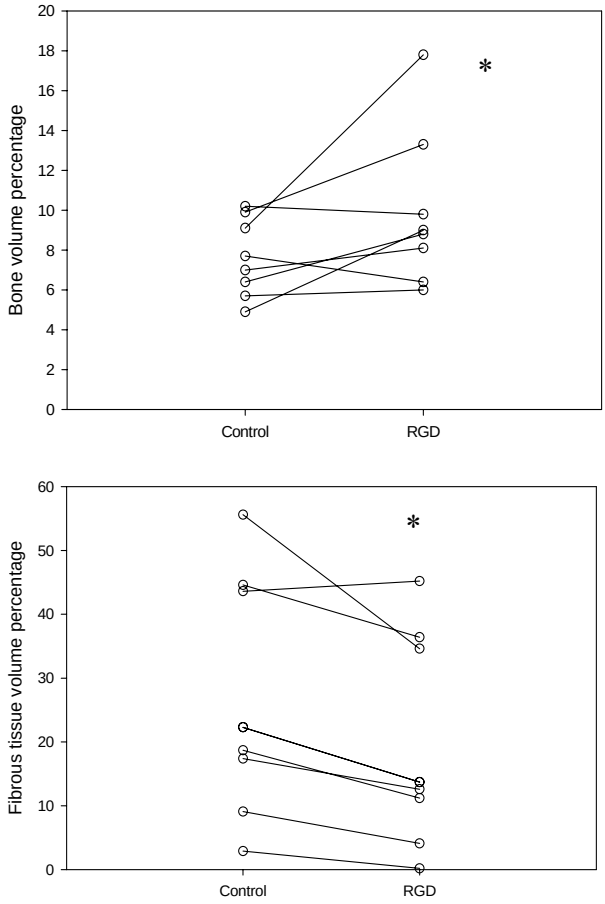

Fig. 12. Percentage of bone volume (above) and fibrous tissue volume (below) in the inner half of the gap of unloaded implants. The paired values are connected with a line. *p<0.05.

lower for RGD coated implants (p=0.04). Fibrous tissue was seen only at the interface. Significantly more bone marrow was seen for control implants in the 0-100 µm zone (p=0.03). No differences were observed in the 0-500 µm zone.

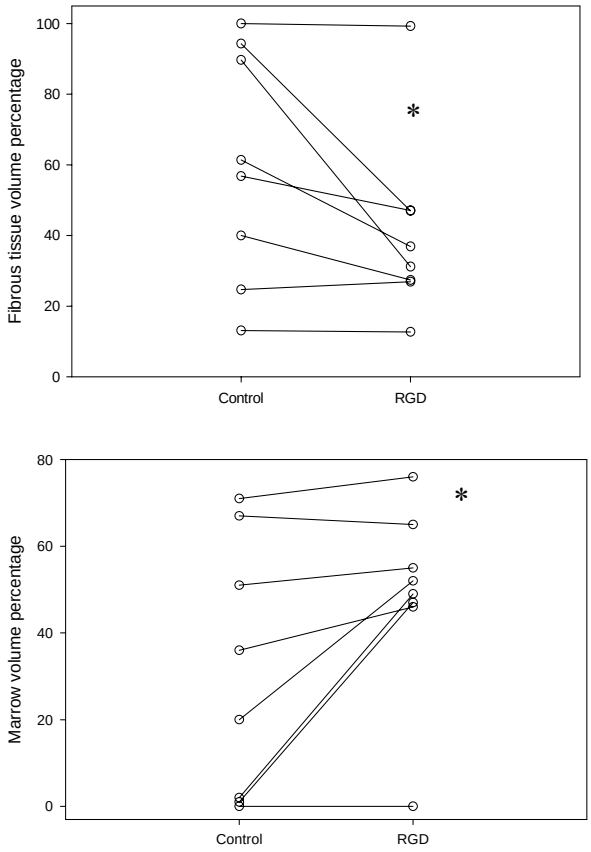

Fig. 13. Percentage of fibrous tissue volume (above) and bone marrow volume (below) in the inner half of the gap of loaded implants (study I). The paired values are connected by a line.*p<0.05.

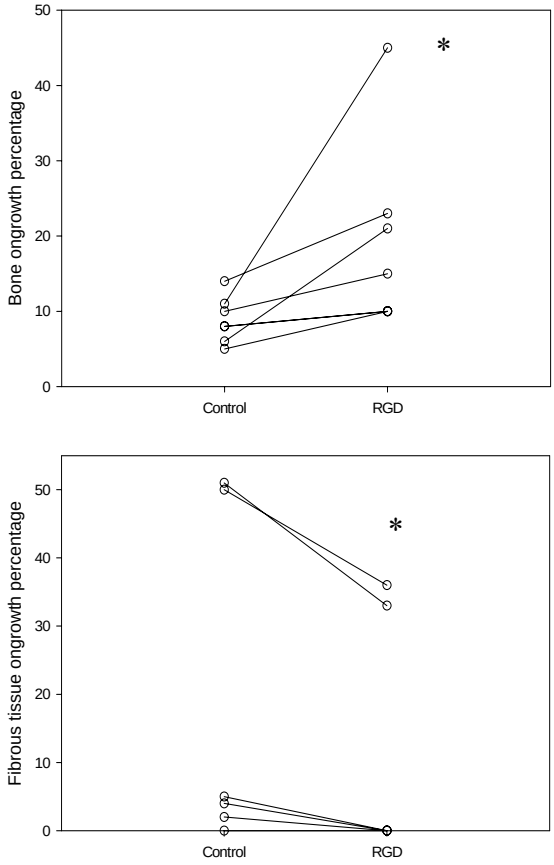

Fig. 14. Percentage of bone ongrowth (above) and fibrous tissue (below) for unloaded press-fit implants. Paired values are connected by a line. *p<0.05.

n=6	**Ongrowth**	**0-100 µm**	**0-750 µm**
	Bone (%)		
RGD	18* (10-23)	26*(23-32)	17(11-21)
Control	9(6-11)	19(18-24)	16(14-20)
	Fibrous tissue (%)		
RGD	0* (0-33)	0(0-1)	0(0-0)
Control	5 (2-50)	0(0-0)	0(0-0)
	Bone marrow (%)		
RGD	67(54-85)	71(68-76)	83(77-89)
Control	88(45-89)	81*(76-82)	83(80-86)

Table 3. Results from histomorphometry (study II, unloaded, press-fit). Values are given as percentage tissue ongrowth and tissue volume in the two zones (median and interquartile ranges). *p<0.05.

Study III

Results for bone are shown in table 4. Significantly more bone ongrowth (Fig.15) and bone volume in a 0-100 µm zone was observed for RGD coated implants. The main difference was seen for woven bone. No difference was found in lamellar bone volume or lamellar bone ongrowth. No fibrous tissue was seen on any implant. Bone marrow ongrowth and volume in the 0-100 µm zone was significantly higher for control implants than RGD coated implants (Fig. 16). No difference in bone marrow volume was seen between the two groups in the 0-500 µm zone. Bone marrow volume was in this zone 50%(49-54) and 49%(46-52) for control and RGD coated implants respectively.

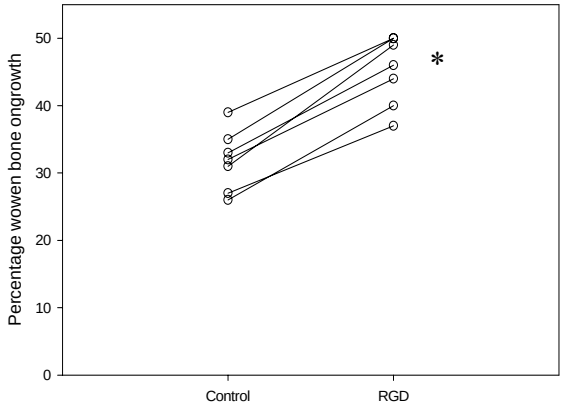

Fig. 15. Percentage of bone ongrowth for loaded press-fit implants. Paired values are connect by lines. *p<0.05.

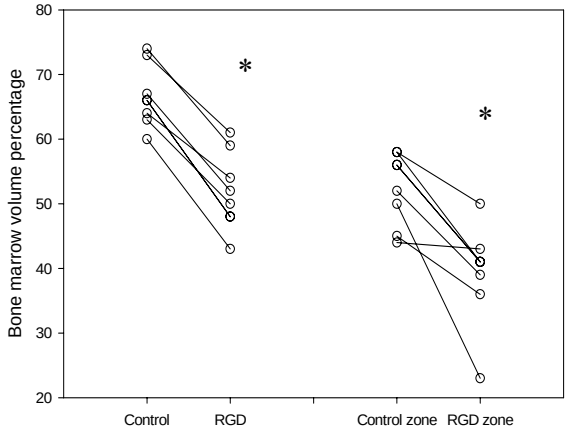

Fig. 16. Percentage of bone marrow ongrowth (left) and bone marrow volume (right) in the 0-100 µm zone surrounding the loaded press-fit implants. Paired values are connected by a line. *p<0.05.

n=7	**Total bone**		**Woven bone**		**Lamellar bone**	
	RGD	Control	RGD	Control	RGD	Control
Ongrowth	48* (41-52)	34(27-37)	46*(40-50)	32(27-35)	2(1-3)	1(0-3)
0-100 µm zone	59* (57-64)	48(42-55)	40*(37-46)	33(21-36)	19(13-21)	15(11-19)
0-500 µm zone	51(48-54)	50(46-51)	7(6-8)	6(5-7)	43(42-44)	44(40-49)

Table 4. Results from histomorphometry (Study III, loaded press-fit). The distribution of bone is shown (median and interquartile ranges). *p<0.05.

DISCUSSION

Controlling the biological response to a given biomaterial by modifying the surface with synthetic biomimetic peptides at the nanometer level is an intriguing idea.
Numerous factors are involved in regulation of biological events. Biological systems are dynamic and able to adapt to environmental changes. Due to the complexity of biological systems, the response may not always turn out as predicted.
Some of the current strategies of research on biomaterials include:

- Identification of suitable surface textures on the micro- and nanometer level
- Chemical alterations of the implants surfaces
- New metal compositions
- Local delivery of osteogenic growth factors
- Gene therapy via viral vectors

In most cases, *in vitro* cell assays are the first step to test the effect of biomaterials or adjuvant therapies. Those treatments that prove successful will be tested *in vivo* in small and larger laboratory animals.
There is a need for more efficient *in vitro* methods to predict the biological response to biomaterials *in vivo*.
Numerous new orthopedic biomaterials applications are being proposed based on *in vitro* cell assays.
It is a difficult task to select which applications should be tested further in experimental animal trails.
Cell assays are not always a good way to test biomaterials for several reasons. With few exceptions, most cell lines used in cell assays are derived from malignant tumor cells. Tumor cells may not express DNA/proteins in a manner which may be directly comparable to that of the normally differentiated cell *in vivo*. The cell media which is typically bovine serum may not reflect the conditions at the implantation site. Finally, it is reasonable to assume that a natural competition between cells *in vivo* is occurring. Most cell assays include only single cell lines and will therefore not address this issue.
There are also some limitations of experimental *in vivo* animal trials used in biomaterials research. The selection of an appropriate experimental animal is important as there may be great variations between species. The implant model must be carefully designed to mimic the clinical conditions as good as possible.
Besides being non toxic and safe, new applications in joint replacement therapy must fulfill some basic requirements. They must be rather resistant to mechanical stimuli, both during the implantation procedure but also to the continuous mechanical load exerted on the implant during daily living.
As most of today's innovations are more expensive than before, there is an increased need for prioritizing which innovations deserve a clinical trial.

In the current studies we have analyzed an immobilized cyclic RGD peptide on the surface of an orthopedic implant. The RGD peptide sequence is an important adhesion domain found in the non-collagenous extracellular matrix proteins (ECM).
Via the RGD peptide domain, ECM proteins can regulate a variety of cellular events. The RGD peptide domain in the ECM proteins has especially been associated with cell adhesion and proliferation on biomaterials.
Synthetic RGD peptides have been extensively studied *in vitro*. Immobilized RGD peptide can stimulate cell adhesion and activity in a cell assay.
Soluble RGD peptide can prevent cell adhesion and bone mineralization by blocking adhesion receptors on the cell surface.
Considering the promising results from *in vitro* testing we decided to test the immobilized RGD peptide *in vivo*.

Only three other published studies had reported *in vivo* results of RGD peptide coated implants in bone, at the beginning of

the trial. Ferris et al. inserted smooth K-wires coated with RGDC (H-Arg-Gly-Asp-Cys-OH) in the femur of the rat. The RGDC peptide is recognized by $\alpha_5\beta_1$ integrins The implants were evaluated by pull-out testing and histomorphometry [37]. The histomorphometry was done after pull-out testing, and not with the implant *in situ*. This is a limitation as the presence of a thin intersecting layer of fibrous tissue may not be detected. Generally the results were conditionally positive, as no difference in bone coverage was observed. A significantly higher bone thickness of the bone surrounding the implant was found in the RGD coated group. There was no difference in the mechanical fixation.
Schliephake et al. inserted square smooth implants in the mandibula of the canine[119]. A comparison was made between uncoated implants, collagen + cyclic RGD peptide coated implants and collagen coated implants in an unloaded setting. A significant increase in bone ongrowth was seen between one and three months in the group of RGD coated implants. They found no difference in bone ongrowth between the three implant types after one or three months. The authors concluded that the study only provided weak evidence of a positive effect of RGD.
Kantlehner et al. implanted cyclic RGD coated PMMA implants in the patellar groove of the rabbit [62]. They reported that RGD coated implants displayed bone ongrowth contact while uncoated control implants were covered in fibrous tissue. However, the paper lacks quantitative results and detailed descriptions of applied methods.

Here we examined the effect of the RGD coating in four different experimental implant models in cancellous bone beds in the canine. Specifically, we considered implant bone interfaces that were press-fit or having a gap, and implants that were loaded or unloaded.

Experimental studies of implants in both press-fit and gap settings are relevant and essential as the formation of gaps is unavoidable around press-fitted implants due to anatomical variation.
We selected a plasma sprayed titanium alloy implant, as this is a common combination of surface structure and metal in implants used in THA. The porous structure is comparable to that used on commercially available implants.
We analyzed the implants after 4 weeks, because earlier experimental studies have shown that differences in early osseointegration can be detected at this stage, and RSA studies have shown that early osseointegration can prevent the migration of implants[130]. Early migration may lead to accelerated loosening of the implant [63,114].

In vitro analysis

To mediate cell adhesion, it is a requirement that the RGD peptide is orientated correctly on the implant surface. One way to analyze the orientation of the molecule is by using the X-ray Photoelectron Spectroscopy technique. The XPS technique involves bombardment of the surface by X-rays with well defined energy and measuring the kinetic energy of the resulting emitted photoelectrons. The kinetic energies give a “fingerprint” of the chemical composition of the outermost atomic layers. By measuring at different exit angles, it is possible to estimate the relative position of different chemical components.
The XPS technique is not well suited for a porous coated surface since it will represent a range of different exit angles. We therefore had to carry out the XPS analysis on RGD peptide coated polished titanium alloy discs. These implants were coated in the same peptide solution as the porous coated implants used in study III. We found that the RGD peptide molecule had a preferred orientation. The anchor molecules were closer to the implant surface than the carbon molecules of the peptide. Currently available techniques cannot predict the orientation of the RGD peptide complex on a rough surface.

However, there is no reason to assume that the molecules would obtain a different orientation in relation to the surface on a porous coated implant.
The peptides did not obtain their theoretical maximum length. This is likely due to a large degree of flexibility in the chemical linker.
It should be noted that the behavior of the linker may be different *in vivo* than under the special conditions required for XPS analysis.

Implants inserted as press-fit

We analyzed implants inserted as press-fit during unloaded and loaded conditions in two different anatomic sites. The normal bone volume percentage (BVP) in the two different bone beds is different. The unloaded implants were placed in the proximal tibia where the host bone bed had a mean BVP of 22%. The loaded implants were placed in the distal femur where the mean BVP was measured to be 48%. Both models used undersized implantation sites, (0.1 and 0.3 mm, respectively). Earlier studies examining HA coated vs. titanium alloy implants in a press-fit model did not find any significant difference in mechanical fixation between the two groups[128]. For this reason we did not expect to find significant differences in mechanical fixation when the implants were press fit. However, we did expect to see differences in the histomorphometric description of bone and tissue distribution.

Unloaded press-fit implants
Push-out testing of the unloaded press-fit implants showed a significant, almost two-fold median increase in apparent shear stiffness for RGD coated implants. Ultimate shear strength and energy absorption were also increased with 40% and 20% median increase respectively ($p>0.05$).

The increase in mechanical fixation for unloaded RGD coated implants was supported by the histomorphometric findings. The unloaded RGD coated implants had significantly more bone ongrowth and significantly less fibrous tissue ongrowth. The bone volume percent in the 0-100 μm zone was also significantly higher for RGD coated implants. All bone ongrowth observed for all unloaded implants was exclusively woven bone.
No difference in tissue distribution was seen in a 0-750 μm concentric zone, indicating that the effect of RGD was localized to the interface.

Loaded press-fit implants
For loaded press-fit implants, however, no difference was found in the mechanical fixation.
We did find significantly more bone ongrowth on RGD peptide coated implants. The increase was rather consistent as seen in Fig. 15. A significantly higher bone volume percentage was also seen in the 0-100 μm zone for RGD peptide coated implants.
Only 4% of the total bone ongrowth was lamellar bone. This finding was seen for both RGD coated implants and control implants. The remaining bone ongrowth consisted of woven bone.
No fibrous tissue was seen for either group, and as a result the control group had significantly higher bone marrow ongrowth and bone marrow percentage in the 0-100 μm zone.
No difference in bone volume or bone marrow volume percent was seen in the 0-500 μm zone.

The results for both loaded and unloaded models clearly indicate that RGD coating have an osteoconductive effect on implants inserted as press-fit.

Implants with a gap

We analyzed the effect of RGD coated implants surrounded by a critical size defect under loaded and unloaded conditions.

Unloaded gap implants
For unloaded gap implants the median apparent shear stiffness was three fold higher than the control group ($p<0.05$). Minor differences were seen in ultimate shear strength and total energy absorption.
Generally the load-displacement curves for RGD coated implants showed a more rapid increase in force, and earlier failure than control implants (Fig. 17). The control implants were on average displaced almost twice the distance of RGD coated implants before failure in the interface between implant and bone.
The prolonged load-displacement curves of control implants increased the area under the curve (energy absorption).
This suggests higher elastic properties of the tissue surrounding the control implants as compared to the RGD coated implants.

The histomorphometric analysis provides a possible explanation for this, as control implants had significantly more fibrous tissue and significantly less bone in the inner half of the gap. The interface of all implants was dominated by fibrous tissue and bone marrow. No significant differences were found in ongrowth of any tissue between the two groups. Half of RGD coated implants had small percentages of bone ongrowth, while this was only the case for two of the control implants (n=8).
No difference in tissue distribution between the two groups was found in the outer half of the gap.

Loaded gap implants
For loaded gap implants, a significantly higher total energy absorption was seen for RGD coated implants. For RGD coated implants, the median ultimate shear strength and apparent shear stiffness were two and three fold higher than control implants. Although this was not a significant difference, the statistical test may have been compromised due to reduced sample sizes caused by necessary exclusions.

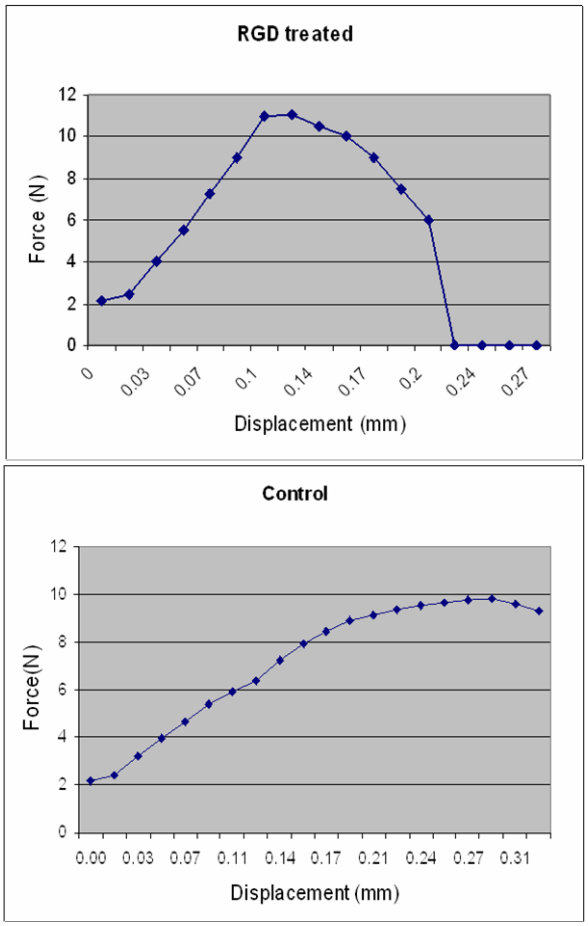

Fig. 17. Sample of load-displacement curves for unloaded paired implants surrounded by a gap. RGD coated implants reached maximum force more rapidly, while control implants had prolonged curves.

Significantly less fibrous tissue and significantly higher bone marrow volume percentage was seen in the inner half of the gap. Fibrous tissue dominated the interface of both the RGD coated and control implants. As for unloaded gap implants, half of the RGD coated implants had small percentages of bone ongrowth. Only one control implant had a small percentage of bone ongrowth (n=8).
In vertical sections from two of the loaded RGD coated implants bidirectional bone growth was seen (Fig. 11).
No difference in tissue distribution was seen in the outer half of the gap.

We had hypothesized that we would find significantly more bone ongrowth on both loaded and unloaded RGD coated implants. Although some RGD coated implants had bone ongrowth, this was far less than we had expected. We have observed bone ongrowth percentages of 20-50% after a 4 week observation period in other studies analyzing different types of HA coating in unloaded 1 mm gap models[25,128].

The finding of significantly less fibrous tissue (loaded and unloaded) in the inner half of the gap and significantly more bone (unloaded) and bone marrow (loaded) is interesting.
The reason for this difference can be explained by the differences in bone and bone marrow ongrowth between RGD coated and control implants. The presence of bone ongrowth and bone marrow disrupted the fibrous tissue membrane. Bone ongrowth was always supported by bone marrow (Fig. 10) and never separated from the gap by a fibrous tissue membrane.
The lack of bone and bone marrow ongrowth in control implants may have resulted in an accelerated formation of the fibrous membrane.
From a histological view point, the fibrous membrane surrounding the control implants appeared denser compared to the RGD coated implants in many sections.

Implants with RGD coating did not have an osteoconductive effect when surrounded by a gap. Although we found positive results such as improved mechanical fixation and a reduction in fibrous tissue in the inner half of the gap, the RGD coating does not provide the improvements in mechanical fixation and osseointegration which would be expected with a calcium-phosphate coated implant.

There may be many explanations why RGD exerts an osteoconductive effect in the press-fit setting and not in the gap setting.
Immediately after implantation, the gap implant is exposed to more bleeding and a larger hematoma will form as compared to the press-fit implant which is positioned close to vital bone. The gap setting obviously is a more challenging environment.
In contrast to the highly dynamic behavior of the extracellular proteins which are believed to mediate cell adhesion, the RGD peptide is a rather rigid structure. It requires a rather specific interaction with cell receptors and cannot adapt to environmental changes.

Limitations

It is important to emphasize that the presented studies describe the tissue response to the RGD peptide coated implants. No conclusions regarding the specific interaction between cell receptors and the RGD peptide can be drawn. We assume that the effect of RGD peptide is facilitation of the cell adhesion process; however it has not yet been demonstrated that this interaction between immobilized RGD peptide and cells occur *in vivo*.

The experimental models cannot address the complex setting of a total hip prosthesis.
For example, the controlled axial (shear) loading condition of these loaded implants does not include the more complex loading patterns of a femoral stem and acetabular components during activities of daily living. We have chosen shear loading because it is a difficult environment in which to establish secure bony fixation of the implant [32].

CONCLUSION

These studies demonstrated that immobilized cyclic RGD peptide has an osteoconductive effect on porous coated titanium alloy implants at 4 weeks of observation time. The osteoconductive effect is seen only when the implants are placed in close contact with bone. Fibrous tissue was reduced around RGD peptide coated implants surrounded by a critical gap; but the mechanism of this effect is unclear and demands further investigation.

The results indicate that immobilized RGD peptide has the potential to enhance the osseointegration of press-fitted clinical implants.

SUGGESTIONS FOR FUTURE RESEARCH

These results support the concept of biological modification of surfaces with biomimetic peptides as a mean to enhance the osseointegration of orthopedic implants. Other domains of the extracellular matrix proteins are known to facilitate cell adhesion. There have been some reports that combinations of these domains may have a synergetic effect of cell adhesion and activity. Therefore the immobilization of two or more of these domains may further enhance the osseointegration of implants.

The method of using immobilized peptide to enhance the integration of implants may also have great potential in other medical areas than orthopedic surgery.

Another interesting strategy in improving biomaterials is controlling the conformation of the extracellular proteins. Many of the biological signals transmitted in bone matrix are highly dependant on the conformation of the proteins. It is known that proteins bind differently to different surfaces. A better understanding of proteins' behavior on implant surfaces may lead to the development of better biomaterials. The proteins conformation may be influenced by the surface chemistry or surface topography at the nanometer level.

REFERENCE LIST

1. Aebli N, Krebs J, Schwenke D, Stich H, Schawalder P, Theis JC. Degradation of hydroxyapatite coating on a well-functioning femoral component. J Bone Joint Surg Br 2003;85:499-503.

2. Aerssens J, Boonen S, Lowet G, Dequeker J. Interspecies differences in bone composition, density, and quality: potential implications for in vivo bone research. Endocrinology 1998;139:663-670.

3. Albrektsson T, Hansson HA. An ultrastructural characterization of the interface between bone and sputtered titanium or stainless steel surfaces. Biomaterials 1986;7:201-205.

4. Albrektsson T, Johansson C. Osteoinduction, osteoconduction and osseointegration. Eur Spine J 2001;10 Suppl 2:S96-101.

5. Anselme K. Osteoblast adhesion on biomaterials. Biomaterials 2000;21:667-681.

6. Aplin AE, Howe A, Alahari SK, Juliano RL. Signal transduction and signal modulation by cell adhesion receptors: the role of integrins, cadherins, immunoglobulin-cell adhesion molecules, and selectins. Pharmacol Rev 1998;50:197-263.

7. Aplin AE, Short SM, Juliano RL. Anchorage-dependent regulation of the mitogen-activated protein kinase cascade by growth factors is supported by a variety of integrin alpha chains. J Biol Chem 1999;274:31223-31228.

8. Astion DJ, Saluan P, Stulberg BN, Rimnac CM, Li S. The porous-coated anatomic total hip prosthesis: failure of the metal-backed acetabular component. J Bone Joint Surg Am 1996;78:755-766.

9. Aumailley M, Gurrath M, Muller G, Calvete J, Timpl R, Kessler H. Arg-Gly-Asp constrained within cyclic pentapeptides. Strong and selective inhibitors of cell adhesion to vitronectin and laminin fragment P1. FEBS Lett 1991;291:50-54.

10. Ayukawa Y, Takeshita F, Inoue T, Yoshinari M, Shimono M, Suetsugu T, Tanaka T. An immunoelectron microscopic localization of noncollagenous bone proteins (osteocalcin and osteopontin) at the bone-titanium interface of rat tibiae. J Biomed Mater Res 1998;41:111-119.

11. Badhe NP, Quinnell RC, Howard PW. The uncemented Bi-Contact total hip arthroplasty. J Arthroplasty 2002;17:896-901.

12. Barnes GL, Kostenuik PJ, Gerstenfeld LC, Einhorn TA. Growth factor regulation of fracture repair. J Bone Miner Res 1999;14:1805-1815.

13. Becker D, Geissler U, Hempel U, Bierbaum S, Scharnweber D, Worch H, Wenzel KW. Proliferation and differentiation of rat calvarial osteoblasts on type I collagen-coated titanium alloy. J Biomed Mater Res 2002;59:516-527.

14. Blacha J. High osteolysis and revision rate with the hydroxyapatite-coated ABG hip prostheses: 65 hips in 56 young patients followed for 5-9 years. Acta Orthop Scand 2004;75:276-282.

15. Bogdanowich-Knipp SJ, Chakrabarti S, Williams TD, Dillman RK, Siahaan TJ. Solution stability of linear vs. cyclic RGD peptides. J Pept Res 1999;53:530-541.

16. Bojescul JA, Xenos JS, Callaghan JJ, Savory CG. Results of porous-coated anatomic total hip arthroplasty without cement at fifteen years: a concise follow-

up of a previous report. J Bone Joint Surg Am 2003;85-A:1079-1083.

17. Bourne RB, Rorabeck CH, Patterson JJ, Guerin J. Tapered titanium cementless total hip replacements: a 10- to 13-year followup study. Clin Orthop 2001;112-120.

18. Byzova TV, Kim W, Midura RJ, Plow EF. Activation of integrin alpha(V)beta(3) regulates cell adhesion and migration to bone sialoprotein. Exp Cell Res 2000;254:299-308.

19. Canalis E, McCarthy T, Centrella M. Growth factors and the regulation of bone remodeling. J Clin Invest 1988;81:277-281.

20. Capello WN, D'Antonio JA, Feinberg JR, Manley MT. Hydroxyapatite coated stems in younger and older patients with hip arthritis. Clin Orthop 2002;92-100.

21. Capello WN, D'Antonio JA, Feinberg JR, Manley MT. Ten-year results with hydroxyapatite-coated total hip femoral components in patients less than fifty years old. A concise follow-up of a previous report. J Bone Joint Surg Am 2003;85-A:885-889.

22. Chung YY, Kim HD, Kim KS. Bone ingrowth on a smooth-surfaced hydroxyapatite-coated acetabular cup. Int Orthop 2002;26:283-286.

23. Civitelli R. Cell-cell communication in bone. Calcif Tissue Int 1995;56 Suppl 1:S29-S31.

24. D'Antonio JA, Capello WN, Manley MT, Geesink R. Hydroxyapatite femoral stems for total hip arthroplasty: 10- to 13-year followup. Clin Orthop 2001;101-111.

25. Daugaard H, Elmengaard B, Bechtold JE, Jensen TB, Søballe K. Comparison of three different hydroxyapatite coatings in an unloaded implant model - experimental canine study. American Society of Biomechanics Annual Meeting, Portland, OR, USA 2004

26. Dechantsreiter MA, Planker E, Matha B, Lohof E, Holzemann G, Jonczyk A, Goodman SL, Kessler H. N-Methylated cyclic RGD peptides as highly active and selective alpha(V)beta(3) integrin antagonists. J Med Chem 1999;42:3033-3040.

27. Dee KC, Andersen TT, Bizios R. Design and function of novel osteoblast-adhesive peptides for chemical modification of biomaterials. J Biomed Mater Res 1998;40:371-377.

28. Dee KC, Rueger DC, Andersen TT, Bizios R. Conditions which promote mineralization at the bone-implant interface: a model in vitro study. Biomaterials 1996;17:209-215.

29. Dhert WJ, Verheyen CC, Braak LH, de Wijn JR, Klein CP, de Groot K, Rozing PM. A finite element analysis of the push-out test: influence of test conditions. J Biomed Mater Res 1992;26:119-130.

30. Dohmae Y, Bechtold JE, Sherman RE, Puno RM, Gustilo RB. Reduction in cement-bone interface shear strength between primary and revision arthroplasty. Clin Orthop 1988;214-220.

31. Dreghorn CR, Hamblen DL. Revision arthroplasty: a high price to pay. BMJ 1989;298:648-649.

32. Duda GN, Eckert-Hubner K, Sokiranski R, Kreutner A, Miller R, Claes L. Analysis of inter-fragmentary movement as a function of musculoskeletal loading conditions in sheep. J Biomech 1998;31:201-210.

33. Duparc JMassin P. Results of 203 total hip replacements using a smooth, cementless femoral component. J Bone Joint Surg Br 1992;74:251-256.

34. Einhorn TA. The cell and molecular biology of fracture healing. Clin Orthop 1998;S7-21.

35. Emerson RH, Jr., Head WC, Emerson CB, Rosenfeldt W, Higgins LL. A comparison of cemented and cementless titanium femoral components used for primary total hip arthroplasty: a radiographic and survivorship study. J Arthroplasty 2002;17:584-591.

36. Enderle A, Jeschke B, Pokinskyj P, Jonczyk A, Hersel U, Kanthlehner M, Kessler H, Nies B. Optimisation of the rgd-peptide coating on metallic surfaces or bone substitutes. 17th European Society for Biomaterials Conference, Barcelona, Spain 2002

37. Ferris DM, Moodie GD, Dimond PM, Gioranni CW, Ehrlich MG, Valentini RF. RGD-coated titanium implants stimulate increased bone formation in vivo. Biomaterials 1999;20:2323-2331.

38. Fink B, Protzen M, Hansen-Algenstaedt N, Berger J, Ruther W. High migration rate of two types of threaded acetabular cups. Arch Orthop Trauma Surg 2004;124:17-25.

39. Frost HM. The biology of fracture healing. An overview for clinicians. Part I. Clin Orthop 1989;283-293.

40. Furnes A, Lie SA, Havelin LI, Engesaeter LB, Vollset SE. The economic impact of failures in total hip replacement surgery: 28,997 cases from the Norwegian Arthroplasty Register, 1987-1993. Acta Orthop Scand 1996;67:115-121.

41. Ganss B, Kim RH, Sodek J. Bone sialoprotein. Crit Rev Oral Biol Med 1999;10:79-98.

42. Geesink RG. Osteoconductive coatings for total joint arthroplasty. Clin Orthop 2002;53-65.

43. Geissler U, Hempel U, Wolf C, Scharnweber D, Worch H, Wenzel K. Collagen type I-coating of Ti6Al4V promotes adhesion of osteoblasts. J Biomed Mater Res 2000;51:752-760.

44. Gotfredsen K, Budtz-Jorgensen E, Jensen LN. A method for preparing and staining histological sections containing titanium implants for light microscopy. Stain Technol 1989;64:121-127.

45. Gronowicz GA, Derome ME. Synthetic peptide containing Arg-Gly-Asp inhibits bone formation and resorption in a mineralizing organ culture system of fetal rat parietal bones. J Bone Miner Res 1994;9:193-201.

46. Grubl A, Chiari C, Gruber M, Kaider A, Gottsauner-Wolf F. Cementless total hip arthroplasty with a tapered, rectangular titanium stem and a threaded cup: a minimum ten-year follow-up. J Bone Joint Surg Am 2002;84-A:425-431.

47. Grzesik WJ, Ivanov B, Robey FA, Southerland J, Yamauchi M. Synthetic integrin-binding peptides promote adhesion and proliferation of human periodontal ligament cells in vitro. J Dent Res 1998;77:1606-1612.

48. Grzesik WJ, Robey PG. Bone matrix RGD glycoproteins: immunolocalization and interaction with human primary osteoblastic bone cells in vitro. J Bone Miner Res 1994;9:487-496.

49. Gundersen HJ, Bendtsen TF, Korbo L, Marcussen N, Moller A, Nielsen K, Nyengaard JR, Pakkenberg B, Sorensen FB, Vesterby A, . Some new, simple and efficient stereological methods and their use in pathological research and diagnosis. APMIS 1988;96:379-394.

50. Harris WH. Wear and periprosthetic osteolysis: the problem. Clin Orthop 2001;66-70.

51. Haubner R, Gratias R, Diefenbach B, Goodman SL, Jonczyk A, Kessler H. Structural and functional aspects of RGD-containing cyclic pentapeptides as highly

potent and selective integrin alpha(v)beta(3) antagonists. Journal of the American Chemical Society 1996;118:7461-7472.

52. Havelin LI, Engesaeter LB, Espehaug B, Furnes O, Lie SA, Vollset SE. The Norwegian Arthroplasty Register: 11 years and 73,000 arthroplasties. Acta Orthop Scand 2000;71:337-353.

53. Havelin LI, Vollset SE, Engesaeter LB. Revision for aseptic loosening of uncemented cups in 4,352 primary total hip prostheses. A report from the Norwegian Arthroplasty Register. Acta Orthop Scand 1995;66:494-500.

54. Herberts P, Malchau H. Long-term registration has improved the quality of hip replacement: a review of the Swedish THR Register comparing 160,000 cases. Acta Orthop Scand 2000;71:111-121.

55. Howe A, Aplin AE, Alahari SK, Juliano RL. Integrin signaling and cell growth control. Curr Opin Cell Biol 1998;10:220-231.

56. Huiskes R. Finite element analysis of acetabular reconstruction. Noncemented threaded cups. Acta Orthop Scand 1987;58:620-625.

57. Hynes RO. Integrins: a family of cell surface receptors. Cell 1987;48:549-554.

58. Jacobsen S, Jensen FK, Poulsen K, Sturup J, Retpen JB. Good performance of a titanium femoral component in cementless hip arthroplasty in younger patients: 97 arthroplasties followed for 5-11 years. Acta Orthop Scand 2003;74:375-379.

59. Johansson C, Lausmaa J, Ask M, Hansson HA, Albrektsson T. Ultrastructural differences of the interface zone between bone and Ti 6Al 4V or commercially pure titanium. J Biomed Eng 1989;11:3-8.

60. Jonczyk A, Goodman S, Diefenbach B, Sutter A, Kessler H. Patent DE 19538741. 1997

61. Kang YK, Jhon JS. Preferred conformations of a linear RGD tripeptide. J Pept Res 2000;56:360-372.

62. Kantlehner M, Schaffner P, Finsinger D, Meyer J, Jonczyk A, Diefenbach B, Nies B, Holzemann G, Goodman SL, Kessler H. Surface coating with cyclic RGD peptides stimulates osteoblast adhesion and proliferation as well as bone formation. Chembiochem 2000;1:107-114.

63. Karrholm J, Borssen B, Lowenhielm G, Snorrason F. Does early micromotion of femoral stem prostheses matter? 4-7-year stereoradiographic follow-up of 84 cemented prostheses. J Bone Joint Surg Br 1994;76:912-917.

64. Kilpadi KL, Chang PL, Bellis SL. Hydroxylapatite binds more serum proteins, purified integrins, and osteoblast precursor cells than titanium or steel. J Biomed Mater Res 2001;57:258-267.

65. Kimmel DB, Jee WS. A quantitative histologic study of bone turnover in young adult beagles. Anat Rec 1982;203:31-45.

66. Lai KA, Shen WJ, Chen CH, Yang CY, Hu WP, Chang GL. Failure of hydroxyapatite-coated acetabular cups. Ten-year follow-up of 85 Landos Atoll arthroplasties. J Bone Joint Surg Br 2002;84:641-646.

67. Lavernia CJ, Drakeford MK, Tsao AK, Gittelsohn A, Krackow KA, Hungerford DS. Revision and primary hip and knee arthroplasty. A cost analysis. Clin Orthop 1995;136-141.

68. Lawler J, Weinstein R, Hynes RO. Cell attachment to thrombospondin: the role of ARG-GLY-ASP, calcium, and integrin receptors. J Cell Biol 1988;107:2351-2361.

69. Lecanda F, Towler DA, Ziambaras K, Cheng SL, Koval M, Steinberg TH, Civitelli R. Gap junctional communication modulates gene expression in osteoblastic cells. Mol Biol Cell 1998;9:2249-2258.

70. Lie SA, Havelin LI, Furnes ON, Engesaeter LB, Vollset SE. Failure rates for 4762 revision total hip arthroplasties in the Norwegian Arthroplasty Register. J Bone Joint Surg Br 2004;86:504-509.

71. Linder L. High-resolution microscopy of the implant-tissue interface. Acta Orthop Scand 1985;56:269-272.

72. Locardi E, Mullen DG, Mattern RH, Goodman M. Conformations and pharmacophores of cyclic RGD containing peptides which selectively bind integrin alpha(v)beta3. J Pept Sci 1999;5:491-506.

73. Lucht U. The Danish Hip Arthroplasty Register. Acta Orthop Scand 2000;71:433-439.

74. Malchau H, Herberts P, Eisler T, Garellick G, Soderman P. The Swedish Total Hip Replacement Register. J Bone Joint Surg Am 2002;84-A Suppl 2:2-20.

75. Maloney WJ, Galante JO, Anderson M, Goldberg V, Harris WH, Jacobs J, Kraay M, Lachiewicz P, Rubash HE, Schutzer S, Woolson ST. Fixation, polyethylene wear, and pelvic osteolysis in primary total hip replacement. Clin Orthop 1999;157-164.

76. Manley MT, Capello WN, D'Antonio JA, Edidin AA, Geesink RG. Fixation of acetabular cups without cement in total hip arthroplasty. A comparison of three different implant surfaces at a minimum duration of follow-up of five years. J Bone Joint Surg Am 1998;80:1175-1185.

77. Massia SP, Stark J. Immobilized RGD peptides on surface-grafted dextran promote biospecific cell attachment. J Biomed Mater Res 2001;56:390-399.

78. Matsuura T, Hosokawa R, Okamoto K, Kimoto T, Akagawa Y. Diverse mechanisms of osteoblast spreading on hydroxyapatite and titanium. Biomaterials 2000;21:1121-1127.

79. McKibbin B. The biology of fracture healing in long bones. J Bone Joint Surg Br 1978;60-B:150-162.

80. Meijerink HJ, Gardeniers JW, Buma P, Lemmens JA, Schreurs BW. Hydroxyapatite does not improve the outcome of a bipolar hemiarthroplasty. Clin Orthop 2004;143-150.

81. Mjoberg B. The theory of early loosening of hip prostheses. Orthopedics 1997;20:1169-1175.

82. Morscher EW, Hefti A, Aebi U. Severe osteolysis after third-body wear due to hydroxyapatite particles from acetabular cup coating. J Bone Joint Surg Br 1998;80:267-272.

83. Mouzin O, Soballe K, Bechtold JE. Loading improves anchorage of hydroxyapatite implants more than titanium implants. J Biomed Mater Res 2001;58:61-68.

84. Murai K, Takeshita F, Ayukawa Y, Kiyoshima T, Suetsugu T, Tanaka T. Light and electron microscopic studies of bone-titanium interface in the tibiae of young and mature rats. J Biomed Mater Res 1996;30:523-533.

85. Noble PC, Alexander JW, Lindahl LJ, Yew DT, Granberry WM, Tullos HS. The anatomic basis of femoral component design. Clin Orthop 1988;148-165.

86. Okamoto K, Matsuura T, Hosokawa R, Akagawa Y. RGD peptides regulate the specific adhesion scheme of osteoblasts to hydroxyapatite but not to titanium. J Dent Res 1998;77:481-487.

87. Overgaard S, Lind M, Glerup H, Bunger C, Soballe K. Porous-coated versus grit-blasted surface texture of hydroxyapatite-

coated implants during controlled micromotion: mechanical and histomorphometric results. J Arthroplasty 1998;13:449-458.

88. Overgaard S, Lind M, Josephsen K, Maunsbach AB, Bunger C, Soballe K. Resorption of hydroxyapatite and fluorapatite ceramic coatings on weight-bearing implants: a quantitative and morphological study in dogs. J Biomed Mater Res 1998;39:141-152.

89. Overgaard S, Lind M, Rahbek O, Bunger C, Soballe K. Improved fixation of porous-coated versus grit-blasted surface texture of hydroxyapatite-coated implants in dogs. Acta Orthop Scand 1997;68:337-343.

90. Overgaard S, Soballe K, Gundersen HJ. Efficiency of systematic sampling in histomorphometric bone research illustrated by hydroxyapatite-coated implants: optimizing the stereological vertical-section design. J Orthop Res 2000;18:313-321.

91. Overgaard S, Soballe K, Lind M, Bunger C. Resorption of hydroxyapatite and fluorapatite coatings in man. An experimental study in trabecular bone. J Bone Joint Surg Br 1997;79:654-659.

92. Pallu S, Bareille R, Dard M, Kessler H, Jonczyk A, Vernizeau M, Amedee-Vilamitjana J. A cyclo peptide activates signaling events and promotes growth and the production of the bone matrix. Peptides 2003;24:1349-1357.

93. Pierschbacher MD, Ruoslahti E. Cell attachment activity of fibronectin can be duplicated by small synthetic fragments of the molecule. Nature 1984;309:30-33.

94. Pierschbacher MD, Ruoslahti E. Influence of stereochemistry of the sequence Arg-Gly-Asp-Xaa on binding specificity in cell adhesion. J Biol Chem 1987;262:17294-17298.

95. Plow EF, Haas TA, Zhang L, Loftus J, Smith JW. Ligand binding to integrins. J Biol Chem 2000;275:21785-21788.

96. Plow EF, Pierschbacher MD, Ruoslahti E, Marguerie GA, Ginsberg MH. The effect of Arg-Gly-Asp-containing peptides on fibrinogen and von Willebrand factor binding to platelets. Proc Natl Acad Sci U S A 1985;82:8057-8061.

97. Porte-Durrieu MC, Guillemot F, Pallu S, Labrugere C, Brouillaud B, Bareille R, Amedee J, Barthe N, Dard M, Baquey C. Cyclo-(DfKRG) peptide grafting onto Ti-6Al-4V: physical characterization and interest towards human osteoprogenitor cells adhesion. Biomaterials 2004;25:4837-4846.

98. Puleo DA, Nanci A. Understanding and controlling the bone-implant interface. Biomaterials 1999;20:2311-2321.

99. Puolakka TJ, Pajamaki KJ, Halonen PJ, Pulkkinen PO, Paavolainen P, Nevalainen JK. The Finnish Arthroplasty Register: report of the hip register. Acta Orthop Scand 2001;72:433-441.

100. Qin J, Vinogradova O, Plow EF. Integrin bidirectional signaling: a molecular view. PLoS Biol 2004;2:726-729.

101. Rahbek O, Overgaard S, Jensen TB, Bendix K, Soballe K. Sealing effect of hydroxyapatite coating: a 12-month study in canines. Acta Orthop Scand 2000;71:563-573.

102. Rahbek O, Overgaard S, Lind M, Bendix K, Bunger C, Soballe K. Sealing effect of hydroxyapatite coating on peri-implant migration of particles. An experimental study in dogs. J Bone Joint Surg Br 2001;83:441-447.

103. Reddi AH. Implant-stimulated interface reactions during collagenous bone matrix-induced bone formation. J Biomed Mater Res 1985;19:233-239.

104. Reikeras O, Gunderson RB. Failure of HA coating on a gritblasted acetabular cup: 155 patients followed for 7-10 years. Acta Orthop Scand 2002;73:104-108.

105. Reikeras O, Gunderson RB. Excellent results of HA coating on a grit-blasted stem: 245 patients followed for 8-12 years. Acta Orthop Scand 2003;74:140-145.

106. Rezania A, Healy KE. Biomimetic peptide surfaces that regulate adhesion, spreading, cytoskeletal organization, and mineralization of the matrix deposited by osteoblast-like cells. Biotechnol Prog 1999;15:19-32.

107. Rezania A, Healy KE. Integrin subunits responsible for adhesion of human osteoblast-like cells to biomimetic peptide surfaces. J Orthop Res 1999;17:615-623.

108. Rezania A, Thomas CH, Branger AB, Waters CM, Healy KE. The detachment strength and morphology of bone cells contacting materials modified with a peptide sequence found within bone sialoprotein. J Biomed Mater Res 1997;37:9-19.

109. Robertsson O, Knutson K, Lewold S, Lidgren L. The Swedish Knee Arthroplasty Register 1975-1997: an update with special emphasis on 41,223 knees operated on in 1988-1997. Acta Orthop Scand 2001;72:503-513.

110. Robinson AH, Palmer CR, Villar RN. Is revision as good as primary hip replacement? A comparison of quality of life. J Bone Joint Surg Br 1999;81:42-45.

111. Rokkum M, Brandt M, Bye K, Hetland KR, Waage S, Reigstad A. Polyethylene wear, osteolysis and acetabular loosening with an HA-coated hip prosthesis. A follow-up of 94 consecutive arthroplasties. J Bone Joint Surg Br 1999;81:582-589.

112. Ruoslahti E. RGD and other recognition sequences for integrins. Annu Rev Cell Dev Biol 1996;12:697-715.

113. Ruoslahti E, Pierschbacher MD. New perspectives in cell adhesion: RGD and integrins. Science 1987;238:491-497.

114. Ryd L. Roentgen stereophotogrammetric analysis of prosthetic fixation in the hip and knee joint. Clin Orthop 1992;56-65.

115. Röhrl, S. M. Wear and fixation of the acetabular component. In vivo evaluation of different polyethylenes and modes of fixation in total hip arthroplasty. Thesis, Umeå University, Umeå, Sweden 2004

116. Scarborough RM, Naughton MA, Teng W, Rose JW, Phillips DR, Nannizzi L, Arfsten A, Campbell AM, Charo IF. Design of potent and specific integrin antagonists. Peptide antagonists with high specificity for glycoprotein IIb-IIIa. J Biol Chem 1993;268:1066-1073.

117. Schaffner P, Dard MM. Structure and function of RGD peptides involved in bone biology. Cell Mol Life Sci 2003;60:119-132.

118. Schimmel JW, Huiskes R. Primary fit of the Lord cementless total hip. A geometric study in cadavers. Acta Orthop Scand 1988;59:638-642.

119. Schliephake H, Scharnweber D, Dard M, Rossler S, Sewing A, Meyer J, Hoogestraat D. Effect of RGD peptide coating of titanium implants on periimplant bone formation in the alveolar crest. An experimental pilot study in dogs. Clin Oral Implants Res 2002;13:312-319.

120. Skinner JA, Kroon PO, Todo S, Scott G. A femoral component with proximal HA coating. An analysis of survival and fixation at up to ten years. J Bone Joint Surg Br 2003;85:366-370.

121. Skinner JA, Kroon PO, Todo S, Scott G. A femoral component with proximal HA coating. An analysis of survival and

fixation at up to ten years. J Bone Joint Surg Br 2003;85:366-370.

122. Snorrason FKarrholm J. Primary migration of fully-threaded acetabular prostheses. A roentgen stereophotogrammetric analysis. J Bone Joint Surg Br 1990;72:647-652.

123. Soballe K. Hydroxyapatite ceramic coating for bone implant fixation. Mechanical and histological studies in dogs. Acta Orthop Scand Suppl 1993;255:1-58.

124. Soballe K. Hydroxyapatite ceramic coating for bone implant fixation. Mechanical and histological studies in dogs. Acta Orthop Scand Suppl 1993;255:1-58.

125. Soballe K, Brockstedt-Rasmussen H, Hansen ES, Bunger C. Hydroxyapatite coating modifies implant membrane formation. Controlled micromotion studied in dogs. Acta Orthop Scand 1992;63:128-140.

126. Soballe K, Hansen ES, Brockstedt-Rasmussen H, Bunger C. Hydroxyapatite coating converts fibrous tissue to bone around loaded implants. J Bone Joint Surg Br 1993;75:270-278.

127. Soballe K, Hansen ES, Brockstedt-Rasmussen H, Hjortdal VE, Juhl GI, Pedersen CM, Hvid I, Bunger C. Gap healing enhanced by hydroxyapatite coating in dogs. Clin Orthop 1991;300-307.

128. Soballe K, Hansen ES, Brockstedt-Rasmussen H, Pedersen CM, Bunger C. Hydroxyapatite coating enhances fixation of porous coated implants. A comparison in dogs between press fit and noninterference fit. Acta Orthop Scand 1990;61:299-306.

129. Soballe K, Hansen ES, Rasmussen H, Jorgensen PH, Bunger C. Tissue ingrowth into titanium and hydroxyapatite-coated implants during stable and unstable mechanical conditions. J Orthop Res 1992;10:285-299.

130. Soballe K, Toksvig-Larsen S, Gelineck J, Fruensgaard S, Hansen ES, Ryd L, Lucht U, Bunger C. Migration of hydroxyapatite coated femoral prostheses. A Roentgen Stereophotogrammetric study. J Bone Joint Surg Br 1993;75:681-687.

131. Sodek J, Ganss B, McKee MD. Osteopontin. Crit Rev Oral Biol Med 2000;11:279-303.

132. Spicer DD, Schaper LA, Pomeroy DL, Badenhausen WE, Jr., Curry JI, Suthers KE, Smith MW. Cementless cup fixation in total hip arthroplasty after 5-8 years. Int Orthop 2001;25:286-289.

133. Sumner DR, Turner TM, Galante JO. Symmetry of the canine femur: implications for experimental sample size requirements. J Orthop Res 1988;6:758-765.

134. Sumner DR, Galante JO. Bone ingrowth. In : Surgery of the musculoskeletal system, 2nd ed., (Ed. Evarts C). Churchill-Livingstone, New York 1990: 151-76.

135. Thanner J. The acetabular component in total hip arthroplasty. Evaluation of different fixation principles. Acta Orthop Scand Suppl 1999;286:1-41.

136. Therkelsen, A. J. Medicinsk Statistik, 2. udgave. FADL's Forlag, København 1983

137. Thomas CH, McFarland CD, Jenkins ML, Rezania A, Steele JG, Healy KE. The role of vitronectin in the attachment and spatial distribution of bone-derived cells on materials with patterned surface chemistry. J Biomed Mater Res 1997;37:81-93.

138. Udomkiat P, Dorr LD, Wan Z. Cementless hemispheric porous-coated sockets implanted with press-fit technique without screws: average ten-year follow-

up. J Bone Joint Surg Am 2002;84-A:1195-1200.

139. Ugarova T, Agbanyo FR, Plow EF. Conformational changes in adhesive proteins modulate their adhesive function. Thromb Haemost 1995;74:253-257.

140. Verrier S, Pallu S, Bareille R, Jonczyk A, Meyer J, Dard M, Amedee J. Function of linear and cyclic RGD-containing peptides in osteoprogenitor cells adhesion process. Biomaterials 2002;23:585-596.

141. Won YY, Dorr LD, Wan Z. Comparison of proximal porous-coated and grit-blasted surfaces of hydroxyapatite-coated stems. J Bone Joint Surg Am 2004;86-A:124-128.

142. Zangwill, A. Physics at Surfaces. Cambridge University Press, Cambridge 1988

Appendix

The *in vivo* effects of RGD coated titanium implants inserted in two bone gap models

Accepted Journal of Biomedical Materials Research, Part A, In Press

Brian Elmengaard *#, Joan E. Bechtold^, Kjeld Søballe*#

*Orthopaedic Research Laboratory, Department of Orthopaedic Surgery, Aarhus University Hospital, Aarhus, Denmark

^ Midwest Orthopaedic Research Foundation and Minneapolis Medical Research Foundation at Hennepin County Medical Center, Minneapolis, Minnesota and University of Minnesota Departments of Orthopaedic Surgery, Biomedical Engineering and Mechanical Engineering

Interdisciplinary Nano Science Center (iNANO), University of Aarhus, Denmark

Address of authors:
Brian Elmengaard, MD
Orthopaedic Research Laboratory
Aarhus University Hospital
AKH, Norrebrogade 44, Bygn. 1A
DK-8000 Aarhus C
Denmark
Phone: +45 8949 4162
Fax: +45 8949 4150
Email: brianelm@dadlnet.dk

SUMMARY

RGD (Arg-Gly-Asp) coating has been suggested to enhance implant fixation by facilitating the adhesion of osteogenic cells to implant surfaces. Orthopaedic implants are unavoidably surrounded partly by gaps, and these regions represent a challenging environment for osseointegration. We examined the effects of cyclic RGD coated implants on tissue integration and implant fixation in two cancellous bone gap models. In canines we inserted loaded RGD coated implants with 0.75 mm gap (n=8) and unloaded RGD coated implants with 1.5 mm gap (n=8) into the distal femur and proximal tibia respectively. Control gap implants without RGD were inserted contralaterally. The titanium alloy (Ti-6Al-4V) implants were plasma spayed and cylindrical. The observation period was four weeks and the fixation was evaluated by push-out test and histomorphometry.

Mechanical implant fixation was improved for RGD coated implants. Unloaded RGD coated implants showed a significant increase in bone while both loaded and unloaded implants showed a significant reduction in fibrous tissue anchorage.

The results are encouraging, as RGD had an overall positive effect on the fixation of titanium implants in regions where gaps exist with the surrounding bone. RGD peptide coatings can potentially be used to enhance tissue integration in these challenging environments.

Keywords: RGD peptide, in vivo, implant fixation, bone, gap healing

INTRODUCTION

Up to one million hip replacements are carried out each year worldwide. The majority of hip implants are inserted using cemented techniques. However, the use of uncemented implants is increasing especially for the younger patients. Currently, approximately 30-40% of total hip arthroplasties are partly or completely uncemented[1,2]. The long term fixation of the uncemented implants relies on the biological response from the surrounding tissue.

Coating of orthopedic implants with Arg-Gly-Asp (RGD) peptide is a new technique which recently has been introduced. The purpose of RGD coating is to biofunctionalize the metallic implant surface and thereby facilitate osteoblast adhesion and promote bone growth on and close to the implant [3,4,5].

RGD peptide, first discovered by Pierschbacher et al. [6], is a ligand to integrins, a group of transmembrane cell receptors, whose function is to control cell adhesion to a substrate. *In vivo*, the integrins are believed to control the cell adhesion process via interaction with RGD-containing

extracellular bone matrix proteins which are absorbed to the implant surface. *In vitro* studies have shown that a high concentration of the RGD peptide on the implant surface can enhance osteoblast adhesion and activation[3,7,4,8] .

Although the biological events after implantation are not fully understood, the adsorption of RGD containing extracellular proteins to the implant surface is likely to play a large role in osteoblast spreading and subsequent proliferation. Okamoto et al. have suggested that RGD peptide contributes to the osteoconductive effect of hydroxyapatite more than to titanium. They found that extracellular proteins containing the RGD peptide adsorb more easily to the hydroxyapatite surface than on titanium [9,10].

More than 20 subunits of integrins have been recognized [11]. The integrin affinity and specificity to the RGD peptide may be affected by both steric conformation [12] and the amino acid sequences flanking the RGD peptide[13]. Cyclic RGD peptides are more stable than linear RGD peptides both in conformation and in resistance to enzymatic cleavage[14].

In this study we use a synthetic cyclic RGD developed to enhance the biointegration of metallic implants[15]. The specific cyclic RGD binds to the $\alpha_V\beta_3$ and $\alpha_V\beta_5$ integrin subunits. These subunits are commonly associated with vitronectin, and are known to play an important role in bone biology [16].

The purpose of this study is to investigate whether cyclic RGD coated on a titanium implant inserted with a gap between the implant and the surrounding bone can promote a favorable tissue response across this gap, and thereby improve the implant fixation. The peptide is coated on a plasma sprayed titanium alloy surface, which is commonly used clinically in orthopedic applications.

We hypothesized that RGD peptide coated implants inserted in loaded and unloaded gap models in cancellous bone will result in improved mechanical implant fixation and significantly increased bone ongrowth, and bone volume in the inner gap zone, and reduced fibrous tissue.

MATERIALS AND METHODS

Implants and coating technique

Cylindrical plasma sprayed porous coated implants were made of titanium alloy (Ti-6Al-4V) with a nominal diameter of 6.0 mm and length of 10.0 mm (Biomet® Inc., Warsaw, IN, USA). The plasma spraying technique results in a porous coating with an average pore size of 200 μm at the substrate and 1000 μm at the outer surface of the coating as described elsewhere[17]. The gross

surface roughness of the plasma spray process (Ra) was 47 μm, with profile depth of 496 μm (determined using a roughness meter (Perthen, Hannover, Germany) with a stylus tip radius of 3 μm).

The cyclic RGD peptide (-RGDfK[-beta-mercaptopropionyl]) with a thiol anchor was synthesized as described by Haubner et al [18] according to Jonczyk et al [19]. After cleaning, the implants were suspended in a sterile filtrated 100 μM solution of the RGDfK peptide in PBS-Buffer at pH 8.3. The implants were left in the suspension for 24 hours and subsequently washed 3 times in PBS-Buffer. Implants were dried in a laminar airflow chamber. All implants were sterilized using irradiation (35 kGy of Co-60 for 14 h, Risø National Laboratory, Roskilde, Denmark). The coating procedure was performed by Biomet Merck BioMaterials GmbH (Darmstadt, Germany).

Animals and surgical procedure

A controlled animal study was carried out. The protocol was approved by our institution's Animal Care and Use Committee. NIH guidelines for the care and use of laboratory animals (NIH Publication #85-23 Rev.1985) were observed. Implants were inserted in cancellous bone sites in the distal femur and proximal tibia under general anesthesia, using sterile technique. Loaded implants surrounded by a 0.75 mm gap were inserted bilaterally in the medial condyle of the distal femur and unloaded implants with 1.5 mm gaps were inserted bilaterally in the proximal tibia, Figure 1, in 8 skeletally mature mongrel dogs (21.0 kg ± 1.3). The study design was paired with insertion of RGD coated implants on one side, and identical control implants without RGD on the contralateral side. After 4 weeks observation the animals were sacrificed and the bones removed.

Loaded gap model

In the distal femur, the medial condyle was exposed through a medial approach. A guide wire was inserted, oriented along the weight-bearing axis of the condyle. A 7.5 mm cannulated drill was used to prepare the bone to receive the implant. An anchor screw with a centralized threaded pin and a distal centralizing ring was inserted. The implants were then screwed onto the threaded pin. A polyethylene (PE) plug was screwed on the pin distally and extended into the joint cavity. Through contact between the PE plug and the tibial plateau, the implants were loaded during each gait cycle. The PE plug allowed for full range of motion in the knee joint.

Unloaded gap model

In the proximal tibia, the implantation site was exposed through a medial approach leaving the medial collateral ligament intact. The periosteum was removed only at the site of drilling, 10 mm distal to the joint line. A guide wire was inserted, and then a 9.0 mm cannulated drill prepared the hole to receive the implant. Drilling was performed at 2 rotations per second to prevent thermal trauma to the bone. Bottom and top washers, 9.0 mm diameter, were attached to stabilize the implants and prevent soft tissue ingrowth, and the implants were inserted.

In both models, the implantation site was lavaged using isotonic saline mixed with polymyxin B prior to implant insertion. After insertion, the overlying soft tissue was closed in layers. Postoperative X-rays were taken to verify implant placement. Prophylactic antibiotics were administrated, consisting of Rocephin (1 gram IV) preoperatively, and Rocephin (1 gram IM per day in a minimum of 3 days or until afebrile) postoperatively.

Specimen preparation

At the end of the observation period, the proximal tibia and distal femur were harvested and stored at –20 ° C for two weeks. The bone-implant specimens were cut on a water-cooled diamond band saw (Exact Appartebau, Germany) leaving two transverse sections. The outermost section of 3 mm was used for mechanical testing. The remaining specimen was sectioned for histomorphometric analysis.

Mechanical testing

Implants were tested to failure in shear by a push-out test on an Instron Universal Test Machine (Model 4302, Instron, UK). The specimens were placed on a metal support jig with a 7 mm circular opening. A preload of 2 N was applied, to ensure contact with implant. The displacement rate was 5.0 mm/minute. Ultimate shear strength (MPa), apparent shear stiffness (MPa/mm), and total energy absorption (J/m^2) were determined from the recorded load-displacement data.

Histological evaluation

The specimens were dehydrated in graded ethanol (70-100%) containing 0.4% basic fuchsin, and embedded in methylmethacrylate. After sectioning, the specimens were counterstained with 2% light green [20]. The preparation method allows distinction between mineralized bone, fibrous tissue and bone marrow. The embedded specimens with the implant *in situ* were randomly rotated around

the vertical axis of the implant. In the central part of implants four serial sections of 15-20 μm was produced using a Leiden microtome (Leiden, Holland) [21].
Histomorphometry was performed in a blinded fashion using an image-analysis system (C.A.S.T-Grid; Olympus, Denmark). The quantification of tissue was performed applying stereological principles. This allows the representation of the three-dimensionally structured trabecular bone tissue in the gap to be quantified with a three-dimensional measure (bone volume)[22].

Tissue ongrowth was defined as tissue in direct contact with the implant surface, and was determined using a line intercepting technique. The number of intersections with tissue in contact with the implant surface was counted in successive adjacent fields at the tissue-implant interface.

The gaps were divided into inner and outer zones and tissue volumes in the two zones adjacent to the implant were determined. In the loaded model, tissue volume percentages were estimated in 0-375 μm and 375-750 μm zones, and in the unloaded model in 0-750 μm and 750-1500 μm zones.

Statistics

Statistical analysis was performed using Intercooled STATA 8.0 software (TX,USA). As the difference between pairs did not follow a normal distribution, a paired non-parametric analysis was applied (Wilcoxon Signed Ranks Test). Accordingly, all parameters are presented as medians and interquartile ranges. P-values less than 0.05 were considered significant.

Push-out testing of the implants inserted with a 0.75 mm gap produced two outliers, one in the control group and one in the RGD group. The values for both implants were more the 10 times the median for each group. No relationship to higher percentage of bony fixation could be established for either implant. As malalignment during mechanical testing was the only plausible explanation the implants were excluded. After exclusion the two groups were accordingly compared using an unpaired test (Mann-Whitney two-sample rank sum test).

RESULTS

No postoperative complications were seen. All dogs were fully weight-bearing within two days after surgery. All animals completed the observation period of four weeks. No signs of infection were observed at time of termination, and intraarticular swabs showed no bacterial growth**.**

The results of the push-out test are seen in Table 1. A significant 2-fold increase in apparent shear stiffness was seen for unloaded RGD coated implants. The total energy absorption and

ultimate shear strength were not significantly different according to the statistical tests used. Loaded RGD coated implants demonstrated a 2-3 fold median increase in all push-out test parameters with a significant increase in total energy absorption.

Results from histomorphometrical analysis are seen in Table 2 and showed significantly more bone in the inner gap zone (0-375 μm) surrounding the unloaded RGD coated implants. For both loaded and unloaded groups, RGD coated implants were fixated by significantly less fibrous tissue than the control implants.

Only small percentages of bone ongrowth were observed. Four of eight of the unloaded and loaded RGD coated implants had bone ongrowth versus only two of eight unloaded control implants and one of eight loaded control implants.

DISCUSSION

In this study, two experimental models in cancellous bone have been used to examine the effect of RGD coating on porous coated implants in a taxing gap setting.

Although most orthopedic implants are inserted as press-fit in the clinical setting, as little as 10-20% of a press-fit clinical implant is in direct contact with bone early after implantation[23]. This is mainly due to anatomical variations at the implantation site [24,25]. Hence, the interface between bone and implant can be described as series of gaps with variable gap sizes intersected by focal loaded bone-implant contact points. Experimental studies of the *in vivo* effect of implant coatings in both press-fit and gap settings are therefore relevant and crucial in the prediction of the biological response to an implant in a clinical application. The implantation sites used in the proximal tibia and distal femur of the canine are rich in high quality cancellous bone, and are representative of the bony fixation regions for example, in proximal femoral and acetabular prostheses in humans.

The gap sizes in these two models are selected to be critical gaps in terms of bone ongrowth, this meaning that no bone ongrowth is likely to be observed in the control group. Earlier studies performed at our institutions have demonstrated that such a critical gap surrounding a plasma sprayed porous coated titanium implant in this animal model must be 0.75 mm [26] in a loaded model and at least 1.0 mm in an unloaded model [27,28] at the observation period of four weeks. We have also demonstrated that the application of load during gait increases fibrous tissue formation on plasma sprayed porous coated titanium implants [29].

We had hypothesized that RGD coated implants in these two gap models would increase mechanical implant fixation, stimulate bone ongrowth and bone formation in the inner zone of the

gap closest to the implant and reduce fibrous tissue formation. The results from this study indicates that cyclic RGD had a positive effect on both loaded and unloaded orthopedic implants with gaps separating them from the surrounding bone. Improvement was manifested by a reduction in fibrous tissue formation and moderate increases in bone ongrowth and mechanical resistance to shear loading.

Unloaded gap model

Mechanically, unloaded RGD coated implants were found to have significantly higher shear stiffness compared to the contralateral control implants. The control implants produced load-displacement patterns which were typical for implants fixated by tissue with elastic properties such as fibrous tissue. Control implant had to be displaced further to induce failure in the interface. This resulted in marginally higher median total energy absorption for control implants. The maximum force needed to dislodge the RGD coated implants was higher than for control implants. The difference in total energy absorption and ultimate shear strength was not significant according to the statistical tests used.

The histomorphometric analysis supported the mechanical test results as the tissue response was more favorable for the RGD coated implants. Significantly more bone and significantly less fibrous tissue was found in the inner gap zone surrounding the RGD coated implant, Figure 2. As expected in the challenging gap setting, bone ongrowth at four weeks was limited for all gap implants, Figure 3. Half of the unloaded RGD coated implants (4/8), however, demonstrated a small percentage of bone ongrowth, compared to only one fourth of the control implants (2/8).

Loaded gap model

The mechanical fixation of loaded RGD coated implants was improved for all parameters. This was consistent with the histomorphometrically measured difference in bone and fibrous tissue. A good mechanical fixation was especially seen for implants with bone ongrowth as ultimate shear strength for these implants was 4-8 fold higher than the respective control implants with pure fibrous fixation.

As previously mentioned, in the experimental model we have shown that application of load to the intraarticular implant will promote fibrous tissue ongrowth to porous coated titanium implants. For

both loaded RGD and control implants, fibrous tissue dominated the implant/tissue interface. Half of the RGD coated implants had bone ongrowth(4/8) compared to only one implant in the control group(1/8). All control implants but one had exclusively fibrous tissue ongrowth (7/8). Additionally, the fibrous tissue ongrowth on control implants expanded into a dense fibrous tissue membrane dominating the inner gap zone (0-375 μm), Figure 4. RGD coated implants had significantly less fibrous tissue and more bone marrow in the inner gap zone.

For both models, no difference in tissue distribution was found in the outer gap zones. At the 4 week observation period, this was an expected finding. RGD is expected to facilitate adhesion and proliferation at the interface, and a tissue response in the outer gap would therefore be unlikely.

The tissue response to RGD coated implants is interesting. Although the gap models used were very challenging, we did expect a higher degree of bone tissue on and around the implants. With regards to bone response, the RGD coated implants only resulted in significant increases during unloaded conditions. However, for RGD coated implants we found a significant reduction in fibrous tissue for both unloaded and loaded implants.

Implants fixated by a thick fibrous membrane represent a clinical problem, as the elasticity of the fibrous tissue may result in implant micromotion and subsequent early implant loosening. Also, a dense fibrous membrane may function as a barrier for bony integration of an implant in the long term. The ability to reduce fibrous tissue formation has also been observed for implants with an osteoconductive hydroxyapatite coating[27,29].

One explanation for the reduced fibrous tissue could be that the steric conformation of the cyclic RGD peptide used in this study may create a less suitable environment for fibroblast adhesion and proliferation. However, this particular experimental model is intended to detect the biological response to implants in bone in terms of tissue distribution and its influence on the mechanical fixation. No conclusions regarding the specific interaction between RGD and cells can therefore be drawn from this study. Furthermore, the results have to be interpreted with the limitations of the particular implants and the gap dimensions, observation period and the titanium alloy surface substrate and plasma spray.

Only a few papers have been published on *in vivo* effects of RGD coated implants inserted in bone. Of relevance to implants used in joint replacement therapy, no other studies have explored the effect of RGD on a porous coated titanium alloy surface in a large animal model. Ferris et al. inserted smooth titanium implants intramedullary in the femur of the rat[30] and Schliephake et al. inserted smooth implants in the alveolar crest in the canine[31]. The results in both studies were

mixed. Ferris et al. found increased bone thickness around RGDC coated implants, but no difference in implant bone coverage or mechanical fixation. Schliephake et al. found only weak evidence of increased bone formation between 1 and 3 months of observation requiring further verification of the results.

The results from these *in vivo* studies and this study are not easily compared due to different animal models, implant types/surfaces, RGD characteristics and implantation times.

In conclusion, the results of this study are encouraging. We have shown that RGD coating can improve implant fixation and reduce fibrous tissue formation to both loaded and unloaded implants in a demanding gap setting. RGD peptide coating has a relatively low production cost and is easy to apply to metallic surface. The coating may potentially be used in the future to facilitate a favorable tissue integration of orthopaedic implants. However, further evaluation is needed and is currently underway. Of specific interest is the effect during press-fit condition and in combination with bone allograft.

ACKNOWLEDGEMENTS

We thank Professor Flemming Melsen, Dept. Pathology, Aarhus University Hospital for his assistance in interpretation of histological sections, and laboratory technicians Anette Milton and Jane Pauli at the Orthopaedic Research Laboratory, Dept. Orthopaedics, Aarhus University Hospital for excellent lab work. The staff at the Midwest Orthopaedic Research Foundation for help during surgery.

Financial support was received from The Danish Rheumatism Association, Interdisciplinary Research Group, Nanoscience and Biocompatibility; grant no. 2052-01-0049; Danish Research Agency, The Danish Medical Associations Research Foundation, Helga and Peter Kornings Foundation, Aarhus, Denmark.

Biomet Inc. Warsaw, IN, USA and Biomet Merck Biomaterials GmbH, Darmstadt, Germany provided implants and coatings.

	Loaded 0.75 mm gap			Unloaded 1.5 mm gap		
	Ultimate Shear Strength (MPa)	Apparent Shear Stiffness (MPa/mm)	Total Energy Absorption (J/m^2)	Ultimate Shear Strength (MPa)	Apparent Shear Stiffness (MPa/mm)	Total Energy Absorption (J/m^2)
RGD	0.38 (0.14-0.55)	1.51 (0.47-2.04)	64 (47-81) *	0.19(0.10-0.20)	0.91(0.40-1.49))*	15(7-36)
Control	0.14(0.09-0.30)	0.54 (0.32-0.86)	19 (16-50)	0.15(0.08-0.19)	0.47(0.24-0.64)	23(9-31)

Table 1. Results from the mechanical push-out test. Data presented as median and interquartile ranges. *P<0.05

	Unloaded 1.5 mm gap			Loaded 0.75 mm gap		
	ongrowth	**0-750 µm**	**750-1500µm**	**ongrowth**	**0-375µm**	**375-750µm**
Percentage of bone						
RGD	0.3(0-2)	9*(7-12)	8(6-12)	0.3(0-6)	7(6-14)	7(4-14)
Control	0(0-1)	7(6-10)	6(5-10)	0(0-0)	7(4-10)	10(8-17)
Percentage of fibrous tissue						
RGD	90(77-99)	13(8-36)	0(0-0)	98(94.2-100)	34(27-47)	0.7(0-5)
Control	95(75-100)	21*(13-44)	0(0-0.3)	100(100-100)	59*(32-92)	0.5(0-19)
Percentage of marrow						
RGD	8(0-22)	70(53-78)	90(86-93)	0(0-0)	51*(47-60)	89(82-94)
Control	5(0-23)	68(46-78)	92(90-95)	0(0-0)	28(19-59)	87(60-91)

Table 2. Results from histomorphometrical analysis showing distribution of tissue in relation to the implants. Values presented as percentage of tissue (median and interquartile ranges). * P<0.05

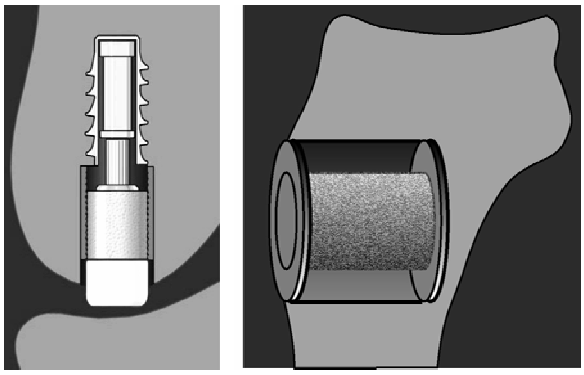

Figure 1: Illustrations of implant gap models. On the left the medial femur condyle with the cylindrical implant surrounded by a 0.75 mm gap. A polyethylene(PE) plug extends into the knee joint. Via the PE plug load is transmitted through contact with the tibial plateau during each gait cycle. On the right the proximal tibia with the non weight-bearing implant surrounded by a 1.5 mm gap.

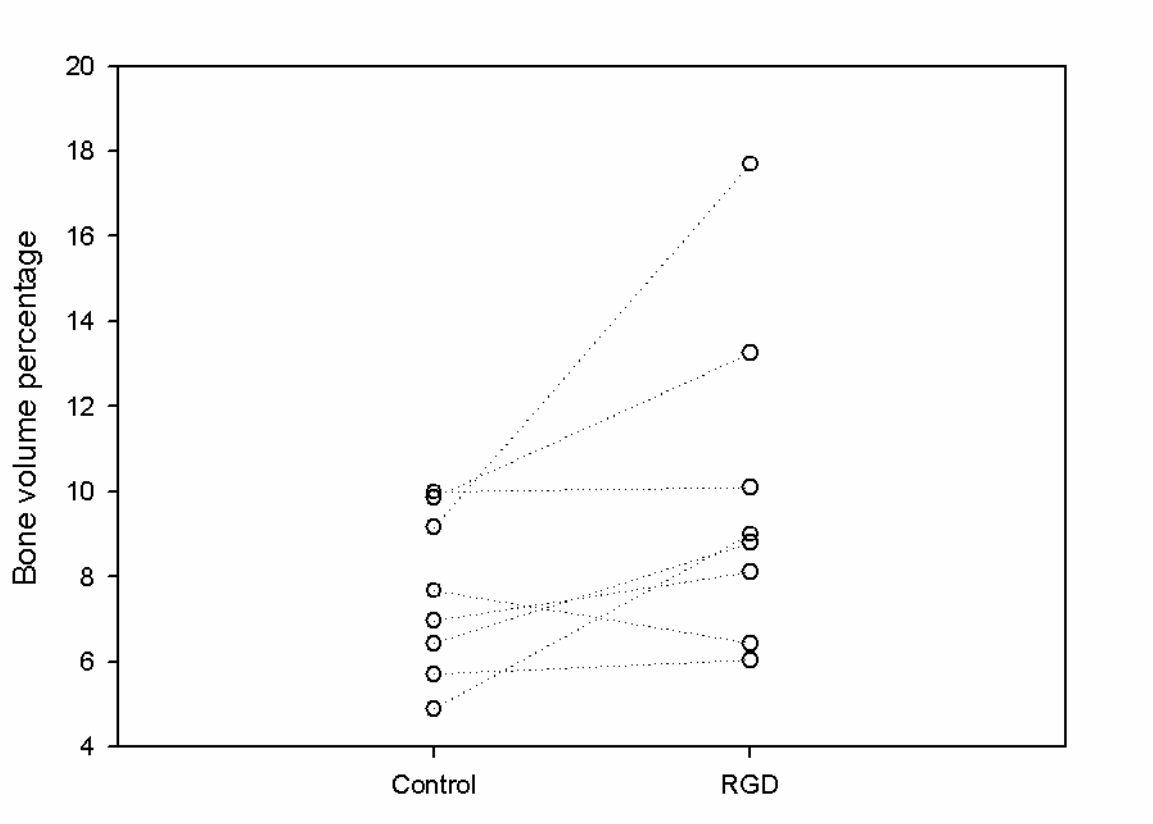

Figure 2. Results from histomorphometry. Line scatter plot showing bone volume percentage in the inner gap (0-750 μm) surrounding unloaded implants. Lines connect the respective implant pairs.

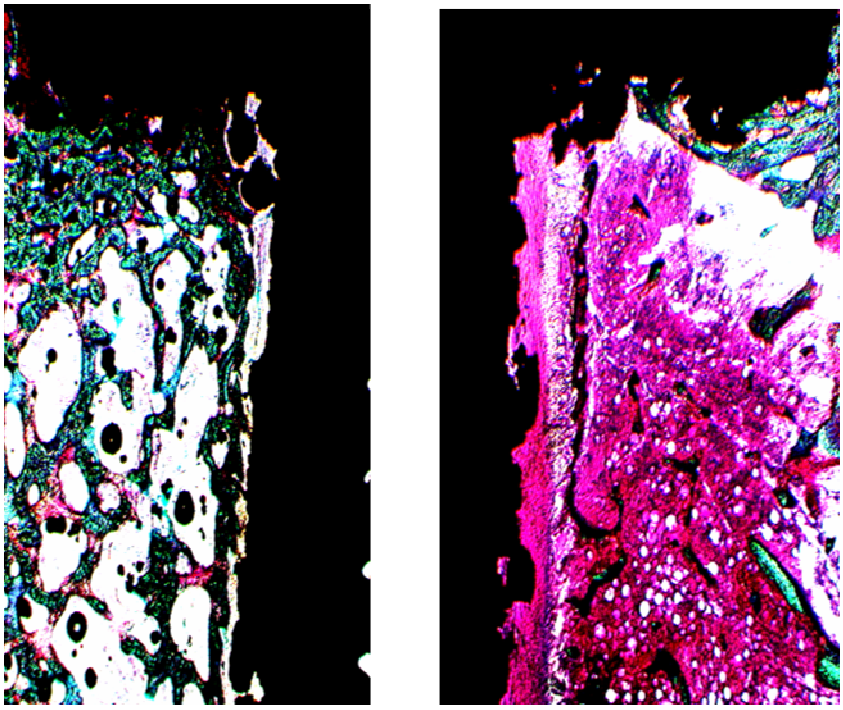

Figure 3. Histological section of unloaded implants (50x magnification, light green and basic fuchsin). Control implant (right) seen with dense fibrous membrane at the interface. RGD coated implant (left) seen with only a thin intersecting fibrous membrane.

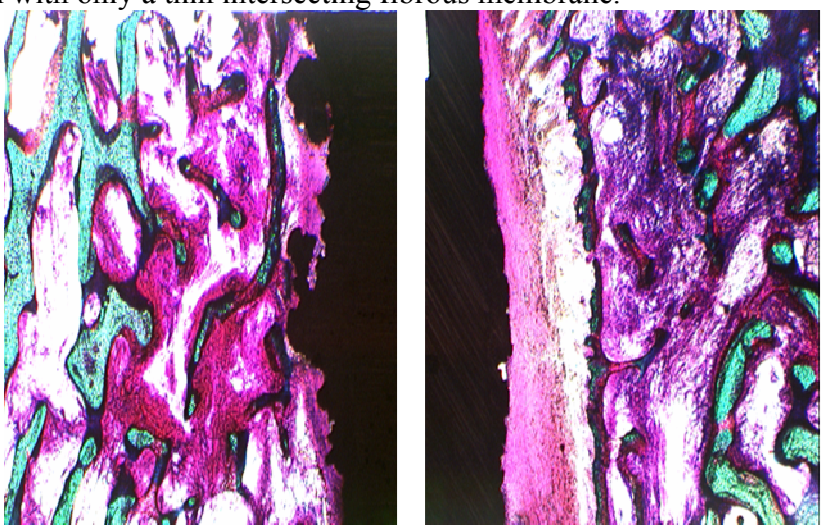

Figure 4: Histological section of loaded implants (50x magnification, light green and basic fuchsin). The interface and inner gap zone of the control implants (right) is dominated by a dense fibrous membrane. On the left a less dominating layer of fibrous tissue is seen at the interface.

REFERENCE LIST

1. Lucht U. The Danish Hip Arthroplasty Register. Acta Orthop Scand 2000;71:433-439.

2. Puolakka TJ, Pajamaki KJ, Halonen PJ, Pulkkinen PO, Paavolainen P, Nevalainen JK. The Finnish Arthroplasty Register: report of the hip register. Acta Orthop Scand 2001;72:433-441.

3. Kantlehner M, Schaffner P, Finsinger D, Meyer J, Jonczyk A, Diefenbach B, Nies B, Holzemann G, Goodman SL, Kessler H. Surface coating with cyclic RGD peptides stimulates osteoblast adhesion and proliferation as well as bone formation. Chembiochem 2000;1:107-114.

4. Rezania A, Healy KE. Integrin subunits responsible for adhesion of human osteoblast-like cells to biomimetic peptide surfaces. J Orthop Res 1999;17:615-623.

5. Ruoslahti E, Pierschbacher MD. New perspectives in cell adhesion: RGD and integrins. Science 1987;238:491-497.

6. Pierschbacher MD, Ruoslahti E. Cell attachment activity of fibronectin can be duplicated by small synthetic fragments of the molecule. Nature 1984;309:30-33.

7. Massia SP, Stark J. Immobilized RGD peptides on surface-grafted dextran promote biospecific cell attachment. J Biomed Mater Res 2001;56:390-399.

8. Verrier S, Pallu S, Bareille R, Jonczyk A, Meyer J, Dard M, Amedee J. Function of linear and cyclic RGD-containing peptides in osteoprogenitor cells adhesion process. Biomaterials 2002;23:585-596.

9. Matsuura T, Hosokawa R, Okamoto K, Kimoto T, Akagawa Y. Diverse mechanisms of osteoblast spreading on hydroxyapatite and titanium. Biomaterials 2000;21:1121-1127.

10. Okamoto K, Matsuura T, Hosokawa R, Akagawa Y. RGD peptides regulate the specific adhesion scheme of osteoblasts to hydroxyapatite but not to titanium. J Dent Res 1998;77:481-487.

11. Ruoslahti E. RGD and other recognition sequences for integrins. Annu Rev Cell Dev Biol 1996;12:697-715.

12. Dechantsreiter MA, Planker E, Matha B, Lohof E, Holzemann G, Jonczyk A, Goodman SL, Kessler H. N-Methylated cyclic RGD peptides as highly active and selective alpha(V)beta(3) integrin antagonists. J Med Chem 1999;42:3033-3040.

13. Howe A, Aplin AE, Alahari SK, Juliano RL. Integrin signaling and cell growth control. Curr Opin Cell Biol 1998;10:220-231.

14. Bogdanowich-Knipp SJ, Chakrabarti S, Williams TD, Dillman RK, Siahaan TJ. Solution stability of linear vs. cyclic RGD peptides. J Pept Res 1999;53:530-541.

15. Aumailley M, Gurrath M, Muller G, Calvete J, Timpl R, Kessler H. Arg-Gly-Asp constrained within cyclic pentapeptides. Strong and selective inhibitors of cell adhesion to vitronectin and laminin fragment P1. FEBS Lett 1991;291:50-54.

16. Schaffner P, Dard MM. Structure and function of RGD peptides involved in bone biology. Cell Mol Life Sci 2003;60:119-132.

17. Soballe K. Hydroxyapatite ceramic coating for bone implant fixation. Mechanical and histological studies in dogs. Acta Orthop Scand Suppl 1993;255:1-58.

18. Haubner R, Gratias R, Diefenbach B, Goodman SL, Jonczyk A, Kessler H. Structural and functional aspects of RGD-containing cyclic pentapeptides as highly potent and selective integrin alpha(v)beta(3) antagonists. Journal of the American Chemical Society 1996;118:7461-7472.

19. Jonczyk A, Goodman S, Diefenbach B, Sutter A, Kessler H. Patent DE 19538741. 97 A.D.;

20. Gotfredsen K, Budtz-Jorgensen E, Jensen LN. A method for preparing and staining histological sections containing titanium implants for light microscopy. Stain Technol 1989;64:121-127.

21. Gundersen HJ, Bendtsen TF, Korbo L, Marcussen N, Moller A, Nielsen K, Nyengaard JR, Pakkenberg B, Sorensen FB, Vesterby A, . Some new, simple and efficient stereological methods and their use in pathological research and diagnosis. APMIS 1988;96:379-394.

22. Overgaard S, Soballe K, Gundersen HJ. Efficiency of systematic sampling in histomorphometric bone research illustrated by hydroxyapatite-coated implants: optimizing the stereological vertical-section design. J Orthop Res 2000;18:313-321.

23. Geesink RG. Osteoconductive coatings for total joint arthroplasty. Clin Orthop 2002;53-65.

24. Noble PC, Alexander JW, Lindahl LJ, Yew DT, Granberry WM, Tullos HS. The anatomic basis of femoral component design. Clin Orthop 1988;148-165.

25. Schimmel JW, Huiskes R. Primary fit of the Lord cementless total hip. A geometric study in cadavers. Acta Orthop Scand 1988;59:638-642.

26. Soballe K, Hansen ES, Rasmussen H, Jorgensen PH, Bunger C. Tissue ingrowth into titanium and hydroxyapatite-coated implants during stable and unstable mechanical conditions. J Orthop Res 1992;10:285-299.

27. Soballe K, Hansen ES, Brockstedt-Rasmussen H, Pedersen CM, Bunger C. Hydroxyapatite coating enhances fixation of porous coated implants. A comparison in dogs between press fit and noninterference fit. Acta Orthop Scand 1990;61:299-306.

28. Soballe K, Hansen ES, Brockstedt-Rasmussen H, Hjortdal VE, Juhl GI, Pedersen CM, Hvid I, Bunger C. Gap healing enhanced by hydroxyapatite coating in dogs. Clin Orthop 1991;300-307.

29. Mouzin O, Soballe K, Bechtold JE. Loading improves anchorage of hydroxyapatite implants more than titanium implants. J Biomed Mater Res 2001;58:61-68.

30. Ferris DM, Moodie GD, Dimond PM, Gioranni CW, Ehrlich MG, Valentini RF. RGD-coated titanium implants stimulate increased bone formation in vivo. Biomaterials 1999;20:2323-2331.

31. Schliephake H, Scharnweber D, Dard M, Rossler S, Sewing A, Meyer J, Hoogestraat D. Effect of RGD peptide coating of titanium implants on periimplant bone formation in the alveolar crest. An experimental pilot study in dogs. Clin Oral Implants Res 2002;13:312-319.

In vivo study of the effect of RGD-treatment on bone ongrowth on press-fit titanium alloy implants

Accepted Biomaterials, In Press 2005

Brian Elmengaard *#, Joan E. Bechtold^, Kjeld Søballe*#

*Orthopaedic Research Laboratory, Department of Orthopaedic Surgery, Aarhus University Hospital, Aarhus, Denmark.

^ Orthopaedic Biomechanics Laboratory, Midwest Orthopaedic Research Foundation and Minneapolis Medical Research Foundation at Hennepin County Medical Center, Minneapolis, Minnesota and University of Minnesota Departments of Orthopaedic Surgery and Biomedical Engineering.

Interdisciplinary Nanoscience Center (iNANO), University of Aarhus, Denmark.

Keywords: Integrins, RGD peptide, Implant fixation, Osteoblasts, In vivo

Address of authors:
Brian Elmengaard, MD
Orthopaedic Research Laboratory
Aarhus University Hospital
AKH, Norrebrogade 44, Bygn. 1A
DK-8000 Aarhus C
Denmark
Phone: +45 8949 4162
Telefax: +45 8949 4150
Email: brianelm@dadlnet.dk

INTRODUCTION

Total hip replacements generally enjoy high rates of success; however the groups of young, physically active patients often outlive prostheses fixated by bone cement. For these patient groups, a non-cemented porous coated titanium prosthesis has become a primary choice. For improved longevity of these implants, studies have shown that early bone ongrowth results in a stronger implant fixation and prevents formation of a fibrous tissue membrane at the interface[1]. A fibrous tissue membrane may in the long term prevent solid bony integration of an implant.

Strategies to improve implant longevity by enhancing early bone ongrowth include the use of different implant coatings to encourage bone growth directly at the implant surface.

Recently the peptide Arg-Gly-Asp (RGD) has been suggested to increase osteoblast adhesion and subsequent proliferation to orthopedic implants[2,3]. The effects of RGD peptide on cell adhesion was first identified by Pierschbacher et al.[4]. The RGD sequence binds to transmembrane proteins in the cell membrane known as integrins. Integrins are mediators of cell adhesion to extracellular matrix. More than 20 subtypes of integrins have been identified and nearly half of them recognize the RGD sequence [5].

Of relevance to bone biology the RGD peptide is found in several extra cellular bone matrix proteins such as vitronectin, fibronectin, osteopontin and bone sialoprotein. Although the biological events after implantation of orthopedic devices is not fully understood, the adsorption of RGD containing extracellular bone matrix proteins to the implant surface is likely to play a large role in osteoblast spreading and proliferation. Okamoto et al. have suggested that RGD peptide contributes to the osteoconductive effect of hydroxyapatite more than titanium. They found that extracellular proteins containing the RGD peptide adsorb more easily to the hydroxyapatite surface than on titanium[6].

Although RGD peptide has been studied extensively *in vitro*[3,7], few *in vivo* studies have been published[8,9]. No other studies have applied RGD peptide on a porous coated titanium implant relevant to orthopaedic joint replacement therapy in a large animal model.

In this study we use a cyclic RGD (Figure 1) which interacts with the $\alpha_V\beta_3$ and $\alpha_V\beta_5$ integrin subunits, commonly associated with vitronectin, and developed to increase biointegration of metal implants [10,11]. Cyclic peptides have been shown to be more stable with regards to three dimensional structure and resistance to enzymatic cleavage[12]. The integrin affinity and specificity to the RGD peptide is affected by both steric conformation and the amino acid sequences flanking the RGD peptide[13,14].

The aim of this study is to investigate whether cyclic RGD coating will enhance the fixation of titanium implants *in vivo*. We examine the application of this cyclic RGD applied to a plasma spray titanium alloy (Ti6Al4V) implant surface inserted in an unloaded cancellous bone site in the canine.

We evaluate the effect of RGD peptide coating with regards to tissue distribution and implant fixation. We hypothesize that RGD peptide coated titanium implants inserted as press-fit will result in an increase in bone ongrowth at the bone-implant interface as measured histomorphometrically, and an increase in mechanical fixation as measured by push-out test.

METHODS

Implants and coating technique

Cylindrical plasma sprayed implants of titanium alloy (Ti6Al4V) with a diameter of 6.0 mm and 10.0 mm of length (Biomet® Inc., Warsaw, IN, USA) were the substrate for application of cyclic RGD coating. Implants had in a pore size of 200-1000 μm at the substrate and the surface of the coating, respectively. The gross surface roughness of the plasma spray process (Ra) was 47 μm, with profile depth of 496 μm (determined using a roughness meter (Perthen, Hannover, Germany) with a stylus tip radius of 3 μm)[1].

The cyclic RGD peptide (-RGDfK[-beta-mercaptopropionyl]) with a thiol anchor was synthesized as described by Haubner et al. [11] according to Jonczyk et al. [15]. The implants were cleaned, autoclaved and thereafter suspended in a sterile filtrated 100 μM solution of the RGDfK peptide in PBS-Buffer at pH 8.3. A 100 μM solution of peptide have in an earlier study shown to promote cell adhesion to RGD coated surfaces [2]. The implants was left in the suspension for 24 hours and subsequently washed 3 times in PBS-Buffer followed by air drying in a laminar airflow chamber. All implants were sterilized using irradiation (35 kGy of Co-60 for 14 h, Risø National Laboratory, Roskilde, Denmark). The peptide coating procedure was performed by Biomet Merck BioMaterials GmbH, Darmstadt, Germany.

Animals and surgical procedure

Approval was obtained from our Institutional Animal Care and Use Committee prior to performing the study.

The 16 implants were inserted in the proximal tibia (Figure 2) bilaterally in 8 skeletally mature mongrel dogs of average weight 21.0 kg +/- 1.3kg. The study design was paired. On the right side,

RGD coated implants were inserted. The contralateral titanium implants without RGD served as controls. The implants were inserted during general anesthesia, using sterile technique.

In the proximal tibia, the implantation site was exposed through a medial approach, leaving the medial collateral ligament intact. The periosteum was removed only at the area of drilling 8 mm distal to the joint line. Initially a guide wire was inserted, followed by a 5.9 mm cannulated drill. Drilling was performed at 2 rotations per second to prevent thermal trauma to the bone. The implantation site was cleaned using isotonic saline with polymyxin B. The implant was incrementally inserted press-fit with repeated hammer blows. The overlying soft tissue was closed in layers. Postoperative x-rays were taken to verify implant placement. Prophylactic antibiotics were administrated, consisting of Rocephin 1 gram IV preoperatively, and postoperatively Rocephin 1 gram IM per day for a minimum of 3 days, or until afebrile.

Specimen preparation

The proximal tibiae were harvested and stored at –20 ° C prior to preparation. Two transverse bone-implant specimens were cut on a water-cooled diamond band saw (Exact Appartebau, Germany). The outermost specimen of 3 mm was used for mechanical testing. The remaining specimen was fixed in 70% ethanol for histological evaluation.

At this point, the sections for histology from two dogs were excluded from all remaining analysis. One section was excluded as 2-3 mm of the implant on one side was protruding from the drill hole, as a result of a piece of bone which broke off during surgery. Following specimen removal, it was determined that the absent bone accounted for too much of the implant surface to allow for histological evaluation. In another dog, the macroscopic examination of one section intended for histological examination suggested it was placed in primarily cortical bone. This was confirmed by histological examination and therefore this section was also excluded. In the mechanical test group implants from one dog had to be excluded due to inadvertent fracture during the cutting procedure. The histological sections from this dog, however, remained intact, and were included in the study.

Histological evaluation

The specimens were dehydrated in graded ethanol (70-100%) containing 0.4% basic fuchsin, counterstained in 2% light green, and embedded in methylmethacrylate [16]. To obtain unbiased histomorphometric estimates the vertical section technique was applied according to stereological principles [17,18]. The embedded specimens were randomly rotated around the vertical axis and

serially sectioned to 20 μm using a Leiden microtome (Leiden, Holland). Histomorphometry was performed blinded using an image-analysis system (C.A.S.T-Grid; Olympus, Denmark). The staining technique allows differentiation between mineralized bone, fibrous tissue and bone marrow like tissue. Tissue ongrowth was defined as tissue in direct contact with the implant surface and was determined using a line intercepting technique. The number of intersections with tissue in contact with the implant surface was counted in successive adjacent fields at the bone-implant interface. Tissue volume fractions in 0-100 μm and 0-750 μm zones adjacent to the implant were determined by point-counting technique.

Mechanical testing

Implants were tested to failure by a push-out test on an Instron Universal Test Machine (Model 4302, Instron, UK). The specimens were placed on a metal support jig with a 7.4 mm circular opening. A preload of 2 N was applied, to define contact position. Displacement rate was 5.0 mm/minute. Ultimate shear strength (MPa), apparent shear stiffness (MPa/mm), and energy absorption (J/m^2) were determined from load-displacement curves.

Statistics

Statistical analysis was performed using STATA Intercooled 8.0 statistical software (STATA,TX). Data was not normal distributed. Therefore a non-parametric paired analysis was performed using Wilcoxon Signed Ranks Test (two-tailed). All data are, unless otherwise stated, presented as medians and interquartile range. P-values less than 0.05 are considered significant.

RESULTS

No postoperative complications were seen. All dogs were fully weight bearing within 2 days after surgery. All animals completed the observation period of 4 weeks. No signs of infection were observed at time of termination and intraarticular swabs showed no bacterial growth. The results of the histomophometric analysis are seen in Table 1. All bone ongrowth to both RGD coated and control implants were newly formed bone (woven bone). Fibrous tissue ongrowth was only observed on two implants in the RGD group compared to five of the control implants. Histological sections with typical patterns of tissue distribution are seen in Figure 3. Results from push-out test are seen in Table 2.

DISCUSSION

The purpose of this study is to identify whether RGD coating has positive effect on the bony fixation of an orthopedic implant, to justify its further evaluation for clinical applications. It is important that biomaterials or surface modifications intended for orthopedic joint replacement therapy are evaluated in clinically relevant models. The model used in this study to evaluate such an implant surface has several advantages.

We inserted the implants in the proximal tibia of the canine as this bone site is rich in high quality cancellous bone, and are representative of the bony fixation regions for example, in proximal femoral and acetabular prostheses in humans. As in clinical practice the implants were inserted as press-fit. The porous coated structure of the implants was produced by plasma spraying technique and the surface is comparable to commercially available orthopedic components used in joint replacement therapy.

Contralateral implants allow a paired study design, allowing RGD coated and control implants to be compared within each animal. Thereby the biological difference between individuals, which can be significant, is essentially eliminated. This allows a reduction in the number of individuals needed to be included in the study. This implant model is unloaded and thereby limited as the effects of weight-bearing conditions are not addressed.

We had hypothesized that we would find a significant increase of bone in direct contact with the implant, and as a result observe an increase in mechanical fixation. Our results did indeed show that after 4 weeks, cyclic RGD had a significant bone stimulating effect directly at the interface. A two-fold median increase in bone ongrowth was observed for RGD coated implants compared to the control implants. Specifically all RGD coated implants did have more bone ongrowth than their respective contralaterally placed control implant (Figure 4). Additionally, RGD coated implants had significantly less fibrous tissue ongrowth than control implants.

In the zone of 0-100 μm from the interface we also found a significantly higher bone volume percentage for RGD coated implants. The difference in bone volume between the two groups gradually diminished as distance to the implant was increased. No difference was seen in bone volume in the 0-750 μm zone adjacent to the implant surface. The effect of RGD in this study was mainly at the interface and we did not see an increase in bone density further away from the implant. The bone density in the area of implantation was measured to be 15-20%.

A moderate increase was seen in the mechanical fixation. Apparent shear stiffness was significantly higher for RGD coated implants, indicating less elasticity in the tissue/implant interface. This is in accordance with the higher percentage of bone on and around the RGD coated implants. Ultimate shear strength and total energy absorption was also generally higher for RGD coated implants. The difference was not as large as for apparent shear stiffness and not all implants with the highest bone percentage yielded higher ultimate shear strength and energy absorption as compared to its respective control. One explanation for this could be the higher percentage of connective tissue fixation and a subsequent increase in elastic properties for control implants. Indeed, control implants generally had to be displaced more than RGD coated implants to induce failure in the interface.

Another explanation is that the mechanical testing provides an overall measure of the fixation of the entire interface between the implant and tissue, whereas histomorphometry quantifies, at extremely high resolution, locations of different tissues. This is particularly the case with plasma sprayed implants, as the irregular texture may affect the test results. Perhaps more importantly, press-fit implants already achieve good fixation because of the mechanical interference between the implant and the slightly underdrilled bone (0.1 mm undersized). Furthermore, the newly formed bone may not have achieved its fully mature material properties, and this may contribute to the modest increase in mechanical fixation at the four week observation period.

A study comparing the osteoconductive hydroxyapatite coating with titanium alloy implants using the same press-fit implant model and observation time found only a significant increase in bone ongrowth and no difference in mechanical fixation[19].

Although this study does not examine the effect of RGD on the cellular level, the positive effect on bone ongrowth and fixation with RGD in the press-fit setting is presumably due to an increase in adhesion and subsequent proliferation of osteoblasts to the cyclic RGD coated surfaces. This effect of the RGD could be assumed to be an osteoconductive effect directly at the interface.

Animal studies examining the effect of RGD coated implants, suggested to be used in joint replacements, should be carefully interpreted since a number of factors play a role for the fixation of implants, e.g. type of metal, surface texture, bone site and test animal. Overgaard et al. have, for example, shown that a plasma sprayed porous coated surface is mechanically superior to a grit blasted surface [20]. The few published studies using RGD coated implants *in vivo* are not easily compared with this study due to different animal models, implant types/surfaces, RGD

characteristics and implantation times. Ferris et al. reported in a study using rats that RGD coating on polished titanium rods inserted in the femur increased total new bone area and bone thickness after 4 weeks. No increase was seen in mechanical pull out force [8]. Schliephake et al. reported mixed results with a significant increase in bone-implant contact after 3 months, but not after 1 month, using a combination of collagen and RGD on smooth dental implants inserted in the alveolar crest in a canine model [9]. Kantlehner et al. inserted RGD coated PMMA implants as press-fit in the patellar groove of rabbits. They observed an increase in direct contact between implant and bone in the RGD treated group, while the uncoated implants were found to have a layer of fibrous tissue between bone and the implant [2].

CONCLUSION

This study show encouraging results as cyclic RGD coating on unloaded press-fit titanium implants significantly increased bone formation on and around the implant. A significant reduction in fibrous tissue fixation was also observed. RGD coating is easily and economically applied and it may be a practical and cost-effective way to enhance the early osseointegration of press-fitted clinical implants. Further information is needed on the integrity of the RGD coating and implant fixation in long-term studies, as well as RGD coated implant performance under loaded and gap conditions.

ACKNOWLEDGEMENTS

Financial support was received from The Danish Rheumatism Association, Interdisciplinary Research Group, Nanoscience and biocompatibility; grant no.2052-01-0049; Danish Research Agency. The Danish Medical Association Research Foundation, Helga and Peter Kornings Foundation, Midwest Orthopaedic Research Foundation, MN, USA.

Biomet Inc.,USA and Biomet BioMaterials GmbH, Darmstadt, Germany provided implants and coating.

REFERENCE LIST

1. Soballe K. Hydroxyapatite ceramic coating for bone implant fixation. Mechanical and histological studies in dogs. Acta Orthop Scand Suppl 1993;255:1-58.

2. Kantlehner M, Schaffner P, Finsinger D, Meyer J, Jonczyk A, Diefenbach B, Nies B, Holzemann G, Goodman SL, Kessler H. Surface coating with cyclic RGD peptides stimulates osteoblast adhesion and proliferation as well as bone formation. Chembiochem 2000;1:107-114.

3. Rezania A, Healy KE. Integrin subunits responsible for adhesion of human osteoblast-like cells to biomimetic peptide surfaces. J Orthop Res 1999;17:615-623.

4. Pierschbacher MD, Ruoslahti E. Cell attachment activity of fibronectin can be duplicated by small synthetic fragments of the molecule. Nature 1984;309:30-33.

5. Ruoslahti E. RGD and other recognition sequences for integrins. Annu Rev Cell Dev Biol 1996;12:697-715.

6. Matsuura T, Hosokawa R, Okamoto K, Kimoto T, Akagawa Y. Diverse mechanisms of osteoblast spreading on hydroxyapatite and titanium. Biomaterials 2000;21:1121-1127.

7. Verrier S, Pallu S, Bareille R, Jonczyk A, Meyer J, Dard M, Amedee J. Function of linear and cyclic RGD-containing peptides in osteoprogenitor cells adhesion process. Biomaterials 2002;23:585-596.

8. Ferris DM, Moodie GD, Dimond PM, Gioranni CW, Ehrlich MG, Valentini RF. RGD-coated titanium implants stimulate increased bone formation in vivo. Biomaterials 1999;20:2323-2331.

9. Schliephake H, Scharnweber D, Dard M, Rossler S, Sewing A, Meyer J, Hoogestraat D. Effect of RGD peptide coating of titanium implants on periimplant bone formation in the alveolar crest. An experimental pilot study in dogs. Clin Oral Implants Res 2002;13:312-319.

10. Aumailley M, Gurrath M, Muller G, Calvete J, Timpl R, Kessler H. Arg-Gly-Asp constrained within cyclic pentapeptides. Strong and selective inhibitors of cell adhesion to vitronectin and laminin fragment P1. FEBS Lett 1991;291:50-54.

11. Haubner R, Gratias R, Diefenbach B, Goodman SL, Jonczyk A, Kessler H. Structural and functional aspects of RGD-containing cyclic pentapeptides as highly potent and selective integrin alpha(v)beta(3) antagonists. Journal of the American Chemical Society 1996;118:7461-7472.

12. Bogdanowich-Knipp SJ, Chakrabarti S, Williams TD, Dillman RK, Siahaan TJ. Solution stability of linear vs. cyclic RGD peptides. J Pept Res 1999;53:530-541.

13. Dechantsreiter MA, Planker E, Matha B, Lohof E, Holzemann G, Jonczyk A, Goodman SL, Kessler H. N-Methylated cyclic RGD peptides as highly active and selective alpha(V)beta(3) integrin antagonists. J Med Chem 1999;42:3033-3040.

14. Howe A, Aplin AE, Alahari SK, Juliano RL. Integrin signaling and cell growth control. Curr Opin Cell Biol 1998;10:220-231.

15. Jonczyk A, Goodman S, Diefenbach B, Sutter A, Kessler H. Patent DE 19538741. 1997

16. Gotfredsen K, Budtz-Jorgensen E, Jensen LN. A method for preparing and staining histological sections containing titanium implants for light microscopy. Stain Technol 1989;64:121-127.

17. Gundersen HJ, Bendtsen TF, Korbo L, Marcussen N, Moller A, Nielsen K, Nyengaard JR, Pakkenberg B, Sorensen FB, Vesterby A, . Some new, simple and efficient stereological methods and their use in pathological research and diagnosis. APMIS 1988;96:379-394.

18. Overgaard S, Soballe K, Gundersen HJ. Efficiency of systematic sampling in histomorphometric bone research illustrated by hydroxyapatite-coated implants: optimizing the stereological vertical-section design. J Orthop Res 2000;18:313-321.

19. Soballe K, Hansen ES, Brockstedt-Rasmussen H, Pedersen CM, Bunger C. Hydroxyapatite coating enhances fixation of porous coated implants. A comparison in dogs between press fit and noninterference fit. Acta Orthop Scand 1990;61:299-306.

20. Overgaard S, Lind M, Rahbek O, Bunger C, Soballe K. Improved fixation of porous-coated versus grit-blasted surface texture of hydroxyapatite-coated implants in dogs. Acta Orthop Scand 1997;68:337-343.

N=6	**Ongrowth**	**0-100 µm**	**0-750 µm**
	Bone (%)		
RGD	18* (10-23)	26*(23-32)	17(11-21)
Control	9(6-11)	19(18-24)	16(14-20)
	Fibrous tissue (%)		
RGD	0(0-33)	0(0-1)	0(0-0)
Control	5* (2-50)	0(0-0)	0(0-0)
	Bone marrow (%)		
RGD	67(54-85)	71(68-76)	83(77-89)
Control	88(45-89)	81*(76-82)	83(80-86)

Table 1. Results from histomorphometry. Values (median and interquartile ranges) presented as percentage of tissue ongrowth and volume percentage in the 0-100 and 0-750µm zones. *p<0.05

N=7	Maximum shear strength (MPa)	Apparent Shear Stiffness (MPa/mm)	Total Energy Absorption (kJ/m2)
RGD	4.47(2.48-8.34)	16.44*(12.56-23.64)	1.49(0.64-2.66)
Control	3.23(2.92-3.97)	9.06(7.92-13.40)	1.25(0.94-1.46)

Table 2. . Results from push-out test*. Values presented as median and interquartile ranges, *p<0.05

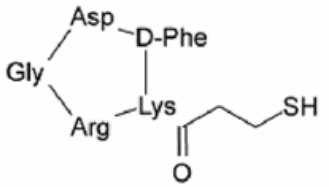

Figure 1. Structure of cyclic RGD pentapeptide with spacer and thiol (-SH) anchor.

Figure 2. Model of a press-fit porous coated Ti6A4V implant (6x10mm) inserted in the cancellous bone region of the canine tibia.

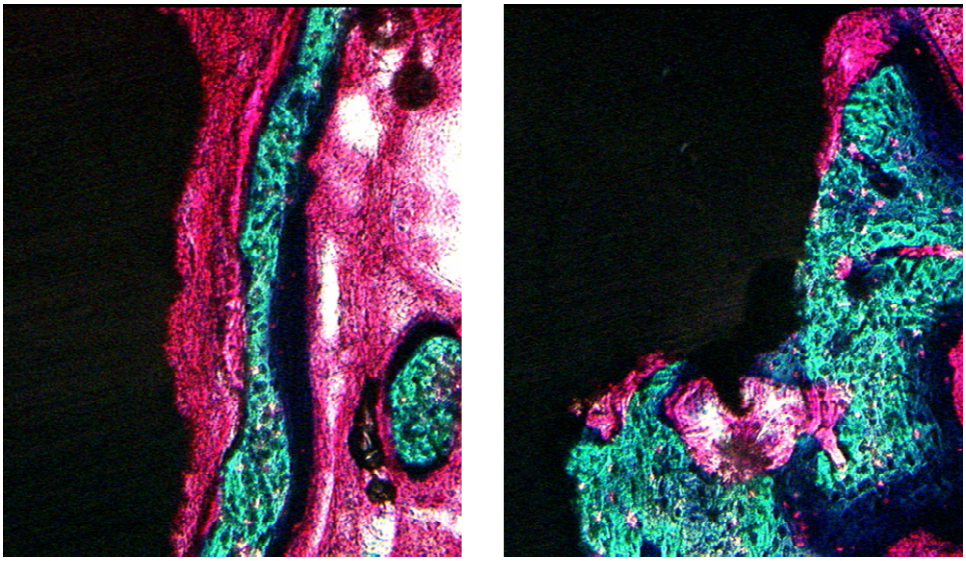

Figure 3. Histological samples (magnification x 430, basic fuchsin and light green). A membrane of fibrous tissue is seen intersecting the bone from the implant on the left (control). On the right an example of bone ongrowth to an RGD coated implant.

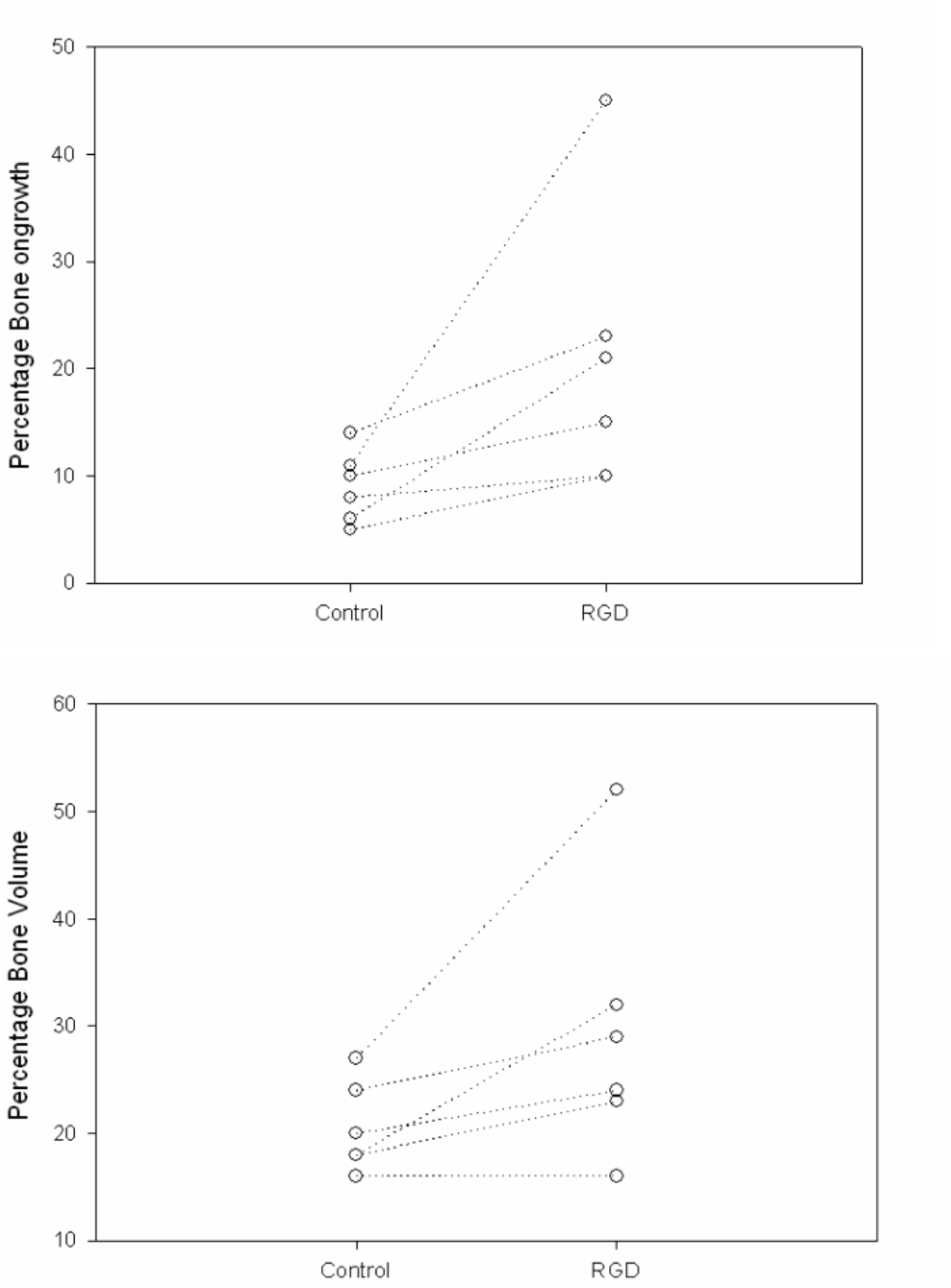

Figure 4. Results from histomorphometry. The lines connect the RGD coated implants with the respective control implant. Bone ongrowth (top) and bone volume in the concentric zone of 0-100 μm (bottom).

RGD coating stimulates bone ongrowth to weight-bearing press-fit orthopaedic implants

Submitted

Brian Elmengaard[1,3], Joan E. Bechtold[2], Morten Foss[4], Mogens Duch[5], Finn Skou Pedersen[5], Flemming Besenbacher[4], Kjeld Søballe[1,3]

(1) Orthopaedic Research Laboratory, Department of Orthopaedic Surgery, Aarhus University Hospital, Denmark
(2) Midwest Orthopaedic and Minneapolis Medical Research Foundation, Orthopaedic Biomechanics Laboratory, Minneapolis, MN, USA
(3) Interdisciplinary Nanoscience Center (iNANO), University of Aarhus, Denmark
(4) Interdisciplinary Nanoscience Center (iNANO), Department of Physics and Astronomy, University of Aarhus, Denmark
(5) Interdisciplinary Nanoscience Center (iNANO), Department of Molecular Biology, University of Aarhus, Denmark

Corresponding author:
Brian Elmengaard, MD
Orthopaedic Research Laboratory
Dept. of Orthopaedic Surgery
Aarhus University Hospital
Norrebrogade 44, bygn 1A
DK-8000 Aarhus C
Denmark
Ph: +45 8949 4162
Fax: +45 8949 4150
Email: brianelm@dadlnet.dk

Abstract

The number of total joint replacements is increasing. To improve the survival rate of cementless prostheses new surface modifications consisting of short peptide sequences have been developed. The Arg-Gly-Asp (RGD) peptide is known to promote cell adhesion through interaction with integrin receptors. This study examines a biofunctionalization of titanium alloy implants by an immobilized cyclic RGD. In a paired and controlled study using canines (n=8), 16 cylindrical porous coated Ti-6Al-4V implants with and without cyclic RGD coating were inserted as press-fit bilaterally in the medial femoral condyles. The observation period was 4 weeks. Analysis consisted of histomorphometry and mechanical push-out test. The RGD coating process was separately examined using X-ray Photoelectron Spectroscopy (XPS). A significant increase in bone ongrowth and bone volume percent in a concentric zone 0-100 μm from the implant surface was seen for the RGD treated group. Although more bone was found around RGD treated implants, only a marginal increase in mechanical fixation was seen. XPS analysis showed that the RGD-spacer-phosphonate molecules had a preferential orientation and the estimated average height of the molecules above the phosphonate anchors was 0.4 nm. In conclusion this study shows that RGD coating can increase bone formation at the interface and therefore could be of importance in both primary and revision total joint replacement therapy.

Keywords: RGD peptide, implant fixation, press-fit, weight-bearing, bone ongrowth, X-ray photoelectron spectroscopy.

Introduction

It is estimated that approximately one million total hip replacements are performed worldwide each year. The overall number of revisions is about 15-20% of the number of primary operations [9,19]. By 2030 in the US, it is estimated that the number of adults with arthritis and chronic joint pain has doubled.

Although implants inserted in joint replacement therapy have excellent survival rates in the older age groups, the implant survival rate is lower for the group of younger patients. Clinically, revision joint replacement implants have shorter longevity, poorer functional outcome, poorer fixation, higher costs and longer rehabilitation times than primary implants [1,2,5,12,14,21].

Therefore efforts have been made to improve the fixation of implant components used in total joint replacement therapy. A new approach in improving orthopaedic implants is

biofunctionalization by transferring or mimicking biological receptor ligands onto the metallic surfaces. The aim is to control the biological response to the orthopaedic implants and thereby potentially improve the bony fixation of the implant.

The Arg-Gly-Asp (RGD) peptide is of special interest since several *in vitro* studies have documented RGD's ability to facilitate cell adhesion and proliferation via interaction with integrin receptors [11,15,20]. The RGD peptide first discovered by Piesenbacher et al. is a ligand to integrins, a group of transmembrane cell receptors, whose function is to control the cell adhesion to a substrate [18]. *In vivo*, the integrins are believed to control the cell adhesion process via interaction with RGD-containing extracellular bone matrix proteins which are absorbed to the implant surface.

The RGD sequence can be attached to a spacer molecule and then covalently bound to the metallic surface via an anchor molecule for example a thiol or phosphonate. In this study we use a specific cyclic RGD which interacts with the $\alpha_v\beta_3$ and $\alpha_v\beta_5$ integrin subunits. These subunits have been identified as playing an important role in bone biology[22,26]. Earlier studies of this specific cyclic RGD have demonstrated that optimal binding of osteoblasts to the RGD coated surface is ensured when the spacer between anchor and constrained RGD sequence is more than 3.5 nm [11].

Recognizing that the three dimensional orientation of molecules plays an important role in the cell adhesion process we analyze the RGD coated surface *in vitro* using X-ray Photoelectron Spectroscopy. We will analyze whether the RGD molecules are preferentially oriented and estimate the average distance from implant surface to the constrained RGD sequence.

The aim of the *in vivo* section of this study is to analyse whether this phosphonate anchored cyclic RGD peptide coating can facilitate new bone formation at the interface of orthopaedic implants, during weight-bearing, press-fit conditions. We hypothesize that this RGD peptide coating on press-fit porous coated titanium alloy implants will increase bone ongrowth and bone volume in an inner zone surrounding the implant. We also hypothesize that an increase in bone ongrowth will result in only a moderate increase in mechanical fixation measured by push-out test, because the implant is initially well fixed.

METHODS

Implants and coating technique

Titanium alloy (Ti-6Al-4V) implants were fabricated with a threaded anchoring tail and a plasma spray surface (Fig. 1). The anchor tail functioned to prevent axial tilting of the implant

when loaded (diameter 3.8 mm, length 10 mm). The plasma spray surface was cylindrical (diameter 5.8 mm and length of 10.0 mm), and was prepared with the same process as for human clinical implants (Biomet® Inc., Warsaw, IN, USA). Earlier studies have shown that this plasma spraying process results in a pore size of 200-1000 μm at the substrate and the surface of the coating, respectively [24]. For XPS analysis polished Ti-6Al-4V discs Ø 10 mm and 1 mm thickness (Biomet Merck Biomaterials GmbH, Darmstadt, Germany) were used.

The cyclic RGD peptide (-RGDfK[-beta-mercaptopropionyl]) with phosphonate anchor was synthesized as described by Haubner et al. [8] according to Jonczyk et al. [10]. The implants were first sterilized by autoclave and thereafter suspended in a sterile filtrated 100 μM solution of the RGDfK peptide in PBS-Buffer at pH 8.3. This concentration has been shown to be optimal for cell adhesion [11]. The implants were left in the suspension for 24 hours and subsequently washed 3 times in PBS-Buffer followed by air drying in a laminar airflow chamber. Following this coating procedure, all implants were sterilized using irradiation (35 kGy of Co-60 for 14 h, Risø National Laboratory, Roskilde, Denmark). The coating procedure for all implants was performed by Biomet Merck BioMaterials GmbH, Darmstadt, Germany.

X-ray Photoelectron Spectroscopy

The X-ray Photoelectron Spectroscopy (XPS) experiments were carried out on beamline 5 at the ASTRID synchrotron-radiation storage ring (University of Aarhus, Denmark), equipped with a Zeiss SX700 plane grating monochromator to select the desired photon energy. P-polarized photons hit the sample surface with an angle of 45° and the data presented were collected with a VG CLAM analyzer at 30 eV pass energy and 2 mm slit. The polar angles (the acquisition angle measured with respect to the surface) were either normal emission or 60° off normal. The base pressure in the chamber was approximately 10^{-10} Torr.

To examine the orientation of the cyclic RGD peptide with phosphonate anchor molecules bound on the titanium alloy surface, the intensity ratio of the 2p phosphor (P2p) and the 1s carbon (C1s) peak was measured for the two different polar angles. The change of emission angle changes the mean path of penetration of the emitted photoelectrons. The primary photon energies were 190 eV and 350 eV for the P2p and the C1s, respectively.

Animals and surgical procedure

Approval was obtained from the Minneapolis Medical Research Foundation Institutional Animal Care and Use Committee prior to performing the study.

Sixteen implants were inserted bilaterally in the distal femur (Fig. 1) in 8 skeletally mature mongrel dogs of average weight 21.8 +/- 1.4 kg. The study design was paired. On the right side, RGD coated titanium alloy implants were inserted. The contralateral titanium alloy implants without RGD served as controls.

Surgery was performed under general anaesthesia, and sterile technique was observed. The animals were given antibiotics (Rocephalin: one gram IV pre-operatively, and one gram daily IM for 3 days or until afebrile). The operative procedure was as follows. Following a medial parapatellar approach, the weight-bearing area of the medial femoral condyle was identified during flexion through a range of motion. A 2.1 mm guide wire was inserted through the weight-bearing articulating surface and remaining within the central portion of the condyle. Using a 3.5 mm cannulated drill, a 2.5 cm deep hole is created. This is followed by a 5.5 mm cannulated drill to a depth of 1.5 cm. Then a 6.1 mm cannulated drill is used for the proximal 0.5 cm portion. This creates press-fit with the proximal threaded tail, and with the plasma spray implant surface. Drilling was performed at 1-2 rotations per second to prevent osteonecrosis by thermal trauma. The implant was inserted axially with tight press-fit by repeated hammer blows. A polyethylene (PE) plug was then screwed onto the threaded distal portion of the implant. Before closure it was assured that the protruding PE plug was loaded, yet did not interfere with full range motion of the knee. Soft tissues were closed routinely, and radiographs were obtained to verify implant placement. After a post-operative recuperation period of approximately two days, the dogs were housed two per cage, and allowed unlimited cage activity in twenty-four square-foot runs. Their hind-limb function was assessed and noted daily, to ensure they were regularly loading their implants. The dogs were allowed two hours per day of free exercise. Postoperative pain management consisted of IM injections of Bupronex (buprenophine hydrocloride) 0.0075 mg/kg/day, until the animal was considered free of pain. Signs of pain and discomfort were evaluated daily. The animals were sacrificed after a four-week observation period. Cultures were taken from joint fluid of the knees. Intact bilateral distal femurs (approximately 12 cm length) were dissected and stored at -20 ^{o}C until specimen preparation and testing.

Specimen preparation

Two transverse bone-implant specimens were cut on a water-cooled diamond band saw (Exact Appartebau, Germany). The outermost specimen of 3 mm was used for mechanical testing. The remaining specimens were fixed and dehydrated in graded ethanol (70-100%) containing 0.4% basic fuchsin, and embedded in methylmethacrylate. According to stereological principles the vertical section technique was applied to obtain unbiased histomorphometric estimates [7,17]. The embedded specimens were randomly rotated around the vertical axis and serially sectioned to 20 μm using a Leiden microtome (Leiden, Holland). The specimens were counterstained during sectioning with light green 2% [6].

Histological evaluation

Histomorphometry was performed on blinded specimens using an image-analysis system (C.A.S.T-Grid; Olympus, Denmark). Mineralized tissue (woven and lamellar), bone marrow and fibrous tissue were quantified. Newly formed bone (woven bone) is distinguished from existing bone (lamellar bone) by the lack of lamellar structure. Tissue ongrowth was defined as tissue in direct contact with the implant surface and was determined using a line intercepting technique. The number of intersections with tissue in contact with the implant surface was counted in successive adjacent fields at the tissue-implant interface. Tissue volume was defined as the percentage of tissue in relation to total tissue volume. Tissue volume in two concentric regions 0-100 μm and 0-500 μm adjacent to the implant was determined by point-counting technique. As the quantification of tissue ongrowth necessarily requires that the implant not be removed, the method used to prepare histological sections with metal implant *in situ*, only allows quantification of mineralized bony tissue. As a consequence, details of osteoid, or of specific bone cell types are not included.

Mechanical testing

Implants were tested to failure by a push-out test on an Instron Universal Test Machine (Model 4302, Instron, UK). The specimens were placed on a metal support jig with a 7.4 mm circular opening. A preload of 2 N was applied, to define contact position. Displacement rate was 5.0 mm/minute. Force/displacement data was recorded and ultimate shear strength (MPa), apparent shear strength (MPa/mm), and energy to failure (J/m^2) were calculated.

Statistics

STATA Intercooled 8.0 statistical software (STATA Inc., TX, USA) was used to test differences between pairs. The Wilcoxon Signed Ranks Test was applied, as differences between the paired values were not normally distributed. Results are given as median and interquartile range unless otherwise stated. Significance is considered for two-tailed $p<0.05$ (*).

Results

X-ray Photoelectron Spectroscopy

By X-ray Photoelectron Spectroscopy (XPS) it is seen that a distinct phosphor signal is detected from the titanium surface coated with the cyclic RGD peptide (Fig. 2). Since this signal is absent in the case of the non-coated titanium samples (not shown) it is concluded that the phosphor signal arises from the phosphonate anchor in the coating. The peak area ratio between normal and 60° off normal emission for the P2p and the C1s differs by a factor of two (0.19 vs. 0.37, respectively) even though the kinetic energy of the emitted photoelectrons are nearly the same, leading to approximately the same mean free path [27]. This indicates that the carbon and phosphor atom distributions in the coated layer are not the same and that the mean distance from the titanium surface to the phosphor atoms is smaller than the mean distance from the titanium to the carbon atoms.

A rough estimate using an electron mean free path of 6 Angstrom gives a mean layer of 0.4 nm material on top of the phosphor atoms. The thickness of 0.4 nm is significantly smaller than the length of the entire RGD molecule, which is approximate 4 nm.

However, the electron density in the self-assembled layer is expected to be low, as compared to a dense carbon layer as e.g. graphite, due to the spatially large anchor molecule consisting of four phosphonate molecules and only one spacer. Therefore, the real value of the thickness of the immobilized layer is probably significantly larger due to the increase in the electron mean free path. Furthermore, although the cyclic RGD-structure is rigid, the linker unit is rather flexible and there is no reason to assume that all linkers will take maximum length. Therefore, there may be areas where the molecules are lying down exposing the phosphonate anchor.

It can therefore be concluded, that the cyclic RGD peptide with phosphonate anchor molecules are not randomly ordered and that in mean the phosphonate anchor is situated closer to the titanium surface than the average carbon atom. Overall, the result supports that there is an average preferred

orientation of the cyclic RGD molecules with the phosphonate anchor directed towards the titanium surface.

Animal study

The distal thread of one implant fractured during implantation. The implant could not be replaced without compromising the standardized surgical conditions, and this individual had to be excluded from the study.

No postoperative complications were seen. All dogs were fully weight bearing within 2 days after surgery. All animals completed the observation period of 4 weeks. No signs of infection were observed at time of termination and intraarticular swabs showed no bacterial growth.

Histomorphometry

Total bone ongrowth and bone volume in a concentric 0-100 μm zone was significantly increased ($p=0.02$) for RGD coated implants (Fig. 3). At the interface, the bone ongrowth consisted almost exclusively of woven bone (newly formed bone). Woven bone as percentage of total bone was 96%(94-98) and 97%(92-99) for the RGD and control groups respectively.

Significantly more woven bone ongrowth ($p=0.02$) and woven bone volume in the concentric 0-100 μm zone ($p=0.02$) was seen in the RGD group (Table 1). The remaining tissue consisted of tissue with bone marrow characteristics. No fibrous tissue ongrowth was seen in either group. The amount of lamellar bone in the 0-100 μm zone was similar between the two groups.

As a means to compare the consistency of cancellous bone density in all the implantation sites, lamellar bone was compared in the zone of 0-500 μm from the implant surface. No differences in lamellar bone were found in this zone.

It should be noted that for each individual animal, RGD coated implants displayed higher bone ongrowth and bone volume in the inner zone surrounding the implant than the respective controls (Fig. 4).

Push-out test

Only marginal differences were detected in any of the three measured parameters: Ultimate shear strength, apparent shear stiffness, and energy to failure (Table 2).

Discussion

The purpose of this study was to identify whether a biofunctionalization of an orthopaedic implant with an RGD-peptide coating can have a positive effect on the bony fixation of an orthopaedic implant, to justify its further evaluation for clinical applications. It is important that biomaterials or surface modifications intended for orthopaedic joint replacement therapy are evaluated in clinically relevant models. The animal model used in this study to evaluate such an implant surface has several advantages. The implant is placed in an intraarticular site in the distal femur. As for clinical implants joint fluid can flow along the implant interface. In the canine, the medial femoral condyle is rich in cancellous bone, and is representative of the bony fixation regions for example, in proximal femoral and acetabular prostheses in humans. Furthermore, the implant is loaded via a polyethylene plug extending into the knee cavity. During each gait cycle the PE plug transfers load developed through contact with the tibial plateau. The implant itself has a plasma sprayed surface that is a commonly used porous coating on orthopaedic implants. Contralateral implants allow a paired study design, meaning that RGD coated and control implants are compared within each animal. Thereby the effect of a biological difference between individuals, which can be significant, is reduced. This allows a reduction in the number of individuals needed to be included in the study. Additionally, the use of a symmetric implant, a serial sectioning technique, and application of stereological principals with point-counting technique allow an unbiased quantification of bone [17]. The three-dimensionally structured trabecular bone is quantified with a three-dimensional measure (bone volume) and not a two dimensional measure (bone area).

There are also limitations of this model. For example, its controlled axial (shear) loading condition does not include the more complex combined loading patterns of a femoral stem and acetabular components under activities of daily living. We have chosen shear loading since it is felt to be detrimental to establishing secure implant-bone fixation [3]. Since the bone turnover rate is 3-4 faster in canines compared to humans, this allows shorter observation times to be used. Additionally, the canine is known to heal more rapidly than human patients [13]. Due to the need to preserve the bone-implant interface, the histological analysis is limited to evaluation of mineralized bone tissue. Hence, this study cannot address detailed aspects of interaction between cells and the RGD molecules on the implant surface.

We had hypothesized that RGD coating on the weight-bearing, press-fitted implants would stimulate bone ongrowth and result in an increase in bone volume in the immediate space surrounding the implant. Due to the expected high fixation in the press-fit location, we had also

hypothesized that a difference in mechanical fixation between the two implants would not be detected.

We did indeed find significant increases in both bone ongrowth and bone volume in a 0-100 μm perimplant zone. The significant difference between total bone percent for RGD coated and Ti controls was accounted for by the increase in newly formed woven bone. It should be noted that for each individual pair the RGD coated implants had higher percentage of bone tissue compared to the control (Fig. 4).

The mechanism by which the RGD coated implants had increased bone ongrowth and percent bone volume could not be determined. Potential mechanisms are due to (a) spreading of cells from the bone contact points along the implant surface after implantation, (b) through adhesion of single cells, subsequent proliferation, differentiation and chemotactical recruitment or a combination of the two.

As the zone of bone counting was expanded, the differences between the two groups diminished. This was an expected finding, as the theoretical effect of RGD is mainly in adhesion of cells to the implant. Since the RGD, then, would be a local effect directly at the implant surface, we did not expect it to cause greater than a normal bone density within the larger 500 μm concentric zone. In fact, the finding of similar bone volume percent corroborated our assumption that the bony beds in the implantation sites in the paired implants were indeed similar.

The increases in bone ongrowth and bone volume did not result in similar increases in the mechanical fixation. The RGD group had marginally higher median values than the control group; however the variance was also increased. When looking at the individual pairs, we found no association between the mechanical output and the amount of bone ongrowth or the bone volume fractions in the two zones.

However, on the basis of these results, we cannot conclude that histomorphometrically measured bone stimulating effect of RGD will not eventually affect the mechanical fixation. In our experience, in contrast to histomorphetric parameters for similar implants, mechanical parameters have required substantial increases to yield significant results, due to larger variations. This could, in part be due to the fact that mechanical testing provides an overall measure of the fixation of the entire interface between the implant and bone, whereas histomorphometry quantifies, at extremely high resolution, locations of different tissues. This is particularly the case with plasma sprayed implants, as the irregular texture may affect the test results. Perhaps more importantly, press-fit implants already achieve good fixation because of the mechanical interference between the implant

and the slightly underdrilled bone (0.3 mm undersized). In light of the positive effect seen in the histological evaluation, it is possible that mechanical fixation will be improved in the long term. Similar results have been reported in studies using the osteoconductive hydroxyapatite (HA) coating. When inserted press fit, HA coated implants stimulated bone ongrowth, but had no positive effect on the implant fixation [25].

The few published studies using RGD coated implants *in vivo* are not easily compared due to different animal models, implant types/surfaces, RGD characteristics and implantation times. Ferris et al. inserted smooth K-wires coated with RGDC (H-Arg-Gly-Asp-Cys-OH) in the femur of the rat. The RGDC peptide is recognized by $\alpha_5\beta_1$ integrins. They found a significantly higher bone thickness of the bone surrounding the implant in the RGD coated group but no difference in bone coverage or mechanical fixation [4]. .

Schliephake et al. inserted square smooth implants in the mandibula of the canine [23]. A comparison was made between uncoated implants, collagen + cyclic RGD peptide coated implants and collagen coated implants in an unloaded setting. They found no difference in bone ongrowth between the three implant types after one or three months. RGD coated implants had significant more bone ongrowth after three months compared to RGD coated implants after one month. The authors concluded that the study only provided weak evidence of a positive effect of RGD.

Kantlehner et al. implanted cyclic RGD coated PMMA implants in the patellar groove of the rabbit [11]. They reported that RGD coated implants had extensive bone ongrowth while uncoated control implants were covered in fibrous tissue.

As with other coatings such as hydroxyapatite the clinician may be concerned about the stability of the coating and the risk of delamination when exposed to mechanical stimuli during implantation. It is unknown whether the RGD peptide coating is resistant to mechanical stimuli exerted on the surface during press-fit insertion. The RGD peptide complexes form individual covalent bonds with the surface and do not represent a layer that can delaminate. Considering that the maximum height of individual molecules is 4 nm, the majority of the RGD peptide complexes will be protected by the macrostructure of the rough plasma sprayed implant. Furthermore the implant is this study was subjected to substantial mechanical stimulus under insertion as the drill hole was undersized relative to the implant diameter. Hence it is expected that these conditions would simulate worst case implantation. The positive results for bone ongrowth and bone volume percent under these conditions indicate that a potential abrasion of the RGD coating bond does not present a limiting factor in the application of RGD.

In conclusion, this study has demonstrated that RGD coating on plasma spray titanium alloy implants stimulates bone ongrowth and bone volume. The XPS results indicate that, as desired, the RGD orientation was organized with the phosphonate anchor facing the metal surface. The encouraging results provide motivation for further evaluations of RGD. Results from additional large animal *in vivo* studies using RGD in a gap model and with bone allograft are currently being evaluated.

Acknowledgements

Financial support was received from NIH (AR4205), Interdisciplinary Research Group, Nanoscience and Biocompatibility; Grant no. 2052-01-0049; Danish Research Agency. Biomet Merck Biomaterials GmbH, Darmstadt, Germany provided cyclic RGD coating, Biomet Inc., Warsaw, IN, USA provided plasma sprayed implants.

Reference List

[1] Dohmae Y, Bechtold JE, Sherman RE, Puno RM, Gustilo RB. Reduction in cement-bone interface shear strength between primary and revision arthroplasty. Clin Orthop 1988:214-20.

[2] Dreghorn CR, Hamblen DL. Revision arthroplasty: a high price to pay. BMJ 1989;298:648-9.

[3] Duda GN, Eckert-Hubner K, Sokiranski R, Kreutner A, Miller R, Claes L. Analysis of inter-fragmentary movement as a function of musculoskeletal loading conditions in sheep. J Biomech 1998;31:201-10.

[4] Ferris DM, Moodie GD, Dimond PM, Gioranni CW, Ehrlich MG, Valentini RF. RGD-coated titanium implants stimulate increased bone formation in vivo. Biomaterials 1999;20:2323-31.

[5] Furnes A, Lie SA, Havelin LI, Engesaeter LB, Vollset SE. The economic impact of failures in total hip replacement surgery: 28,997 cases from the Norwegian Arthroplasty Register, 1987-1993. Acta Orthop Scand 1996;67:115-21.

[6] Gotfredsen K, Budtz-Jorgensen E, Jensen LN. A method for preparing and staining histological sections containing titanium implants for light microscopy. Stain Technol 1989;64:121-7.

[7] Gundersen HJ, Bendtsen TF, Korbo L, Marcussen N, Moller A, Nielsen K, Nyengaard JR, Pakkenberg B, Sorensen FB, Vesterby A, . Some new, simple and efficient stereological methods and their use in pathological research and diagnosis. APMIS 1988;96:379-94.

[8] Haubner R, Gratias R, Diefenbach B, Goodman SL, Jonczyk A, Kessler H. Structural and functional aspects of RGD-containing cyclic pentapeptides as highly potent and selective

integrin alpha(v)beta(3) antagonists. Journal of the American Chemical Society 1996;118:7461-72.

[9] Havelin LI, Engesaeter LB, Espehaug B, Furnes O, Lie SA, Vollset SE. The Norwegian Arthroplasty Register: 11 years and 73,000 arthroplasties. Acta Orthop Scand 2000;71:337-53.

[10] Jonczyk A, Goodman S, Diefenbach B, Sutter A, Kessler H. Patent DE 19538741. 1997

[11] Kantlehner M, Schaffner P, Finsinger D, Meyer J, Jonczyk A, Diefenbach B, Nies B, Holzemann G, Goodman SL, Kessler H. Surface coating with cyclic RGD peptides stimulates osteoblast adhesion and proliferation as well as bone formation. Chembiochem 2000;1:107-14.

[12] Katz RP, Callaghan JJ, Sullivan PM, Johnston RC. Results of cemented femoral revision total hip arthroplasty using improved cementing techniques. Clin Orthop 1995:178-83.

[13] Kimmel DB, Jee WS. A quantitative histologic study of bone turnover in young adult beagles. Anat Rec 1982;203:31-45.

[14] Lavernia CJ, Drakeford MK, Tsao AK, Gittelsohn A, Krackow KA, Hungerford DS. Revision and primary hip and knee arthroplasty. A cost analysis. Clin Orthop 1995:136-41.

[15] Massia SP, Stark J. Immobilized RGD peptides on surface-grafted dextran promote biospecific cell attachment. J Biomed Mater Res 2001;56:390-9.

[16] Overgaard S, Lind M, Rahbek O, Bunger C, Soballe K. Improved fixation of porous-coated versus grit-blasted surface texture of hydroxyapatite-coated implants in dogs. Acta Orthop Scand 1997;68:337-43.

[17] Overgaard S, Soballe K, Gundersen HJ. Efficiency of systematic sampling in histomorphometric bone research illustrated by hydroxyapatite-coated implants: optimizing the stereological vertical-section design. J Orthop Res 2000;18:313-21.

[18] Pierschbacher MD, Ruoslahti E. Cell attachment activity of fibronectin can be duplicated by small synthetic fragments of the molecule. Nature 1984;309:30-3.

[19] Puolakka TJ, Pajamaki KJ, Halonen PJ, Pulkkinen PO, Paavolainen P, Nevalainen JK. The Finnish Arthroplasty Register: report of the hip register. Acta Orthop Scand 2001;72:433-41.

[20] Rezania A, Healy KE. Integrin subunits responsible for adhesion of human osteoblast-like cells to biomimetic peptide surfaces. J Orthop Res 1999;17:615-23.

[21] Robinson AH, Palmer CR, Villar RN. Is revision as good as primary hip replacement? A comparison of quality of life. J Bone Joint Surg Br 1999;81:42-5.

[22] Schaffner P, Dard MM. Structure and function of RGD peptides involved in bone biology. Cell Mol Life Sci 2003;60:119-32.

[23] Schliephake H, Scharnweber D, Dard M, Rossler S, Sewing A, Meyer J, Hoogestraat D. Effect of RGD peptide coating of titanium implants on periimplant bone formation in the alveolar crest. An experimental pilot study in dogs. Clin Oral Implants Res 2002;13:312-9.

[24] Soballe K. Hydroxyapatite ceramic coating for bone implant fixation. Mechanical and histological studies in dogs. Acta Orthop Scand Suppl 1993;255:1-58.

[25] Soballe K, Hansen ES, Brockstedt-Rasmussen H, Pedersen CM, Bunger C. Hydroxyapatite coating enhances fixation of porous coated implants. A comparison in dogs between press fit and noninterference fit. Acta Orthop Scand 1990;61:299-306.

[26] Verrier S, Pallu S, Bareille R, Jonczyk A, Meyer J, Dard M, Amedee J. Function of linear and cyclic RGD-containing peptides in osteoprogenitor cells adhesion process. Biomaterials 2002;23:585-96.

[27] Zangwill A. Physics at Surfaces. Cambridge: Cambridge University Press 1988

	Total bone		Woven bone		Lamellar bone	
	RGD	Control	RGD	Control	RGD	Control
Ongrowth	48* (41-52)	34(27-37)	46*(40-50)	32(27-35)	2(1-3)	1(0-3)
0-100 μm zone	59* (57-64)	48(42-55)	40*(37-46)	33(21-36)	19(13-21)	15(11-19)
0-500 μm zone	51(48-54)	50(46-51)	7(6-8)	6(5-7)	43(42-44)	44(40-49)

Table 1. Histomorphometrical results presented as percentage of total tissue (ongrowth) and total tissue volume(concentric zones). Values presented as median and interquartile ranges. *P< 0.05.

	Ultimate shear strength (MPa)	Apparent shear stiffness (MPa/mm)	Energy to failure (kJ/m^2)
RGD	6.9(4.9-8.4)	29(23-37)	1.3(0.8-1.6)
Control	6.7(5.7-7.9)	25(21-33)	1.2(1.0-1.4)

Table 2 . Mechanical properties derived from push-out test, presented as median and interquartile ranges.

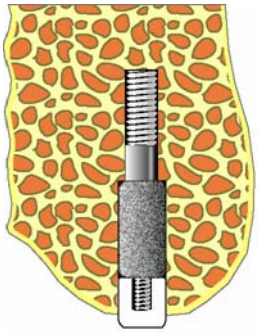

Fig. 1. Model of the press-fit implant placed intraarticularly in the distal femur. Implant is inserted into 0.3 mm undersized predrilled cavity by hammer blows. Implant is loaded during each gait cycle as the polyethylene plug is pushed against the tibial plateau. Proximally, the threaded tail prevents axial tilting of the implant.

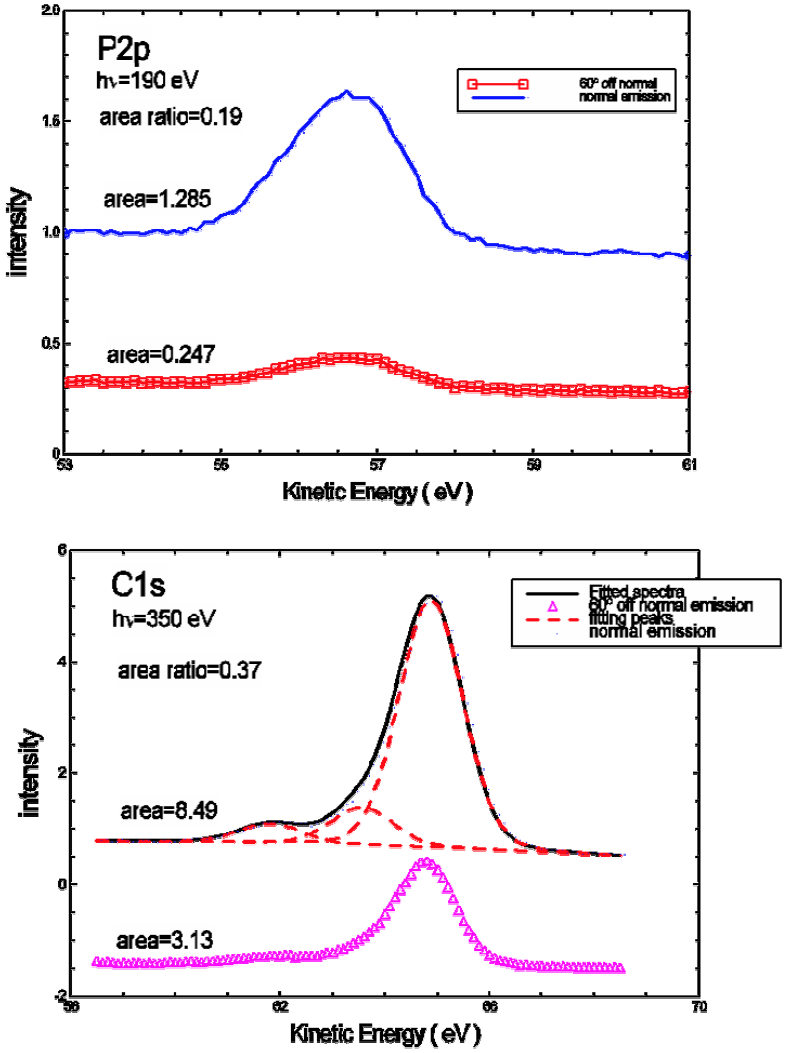

Fig. 2. Results from Xray Photoelecton Spectroscopy. The 2p phosphor (P2p) peak (top) and the 1s carbon (C1s) peaks (bottom) measured for normal emission and 60° off normal emission. The photon energy was h□=190 eV and 350 eV, respectively.

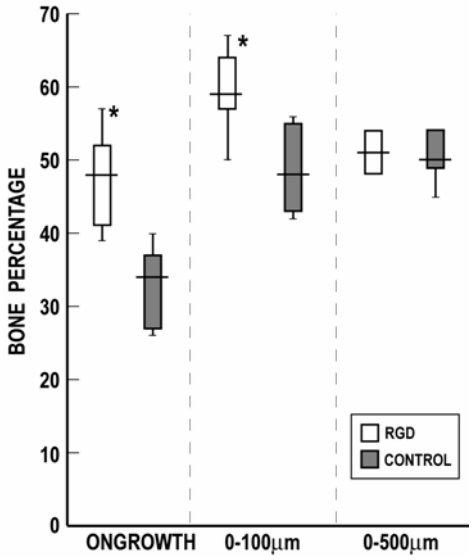

Fig. 3. Results from histomorphometry. Box plot showing median, interquartile range, and total range. Values are shown for bone ongrowth, and bone in two concentric zones 0-100 microns and 0-500 microns from the implant surface. * $p<0.05$

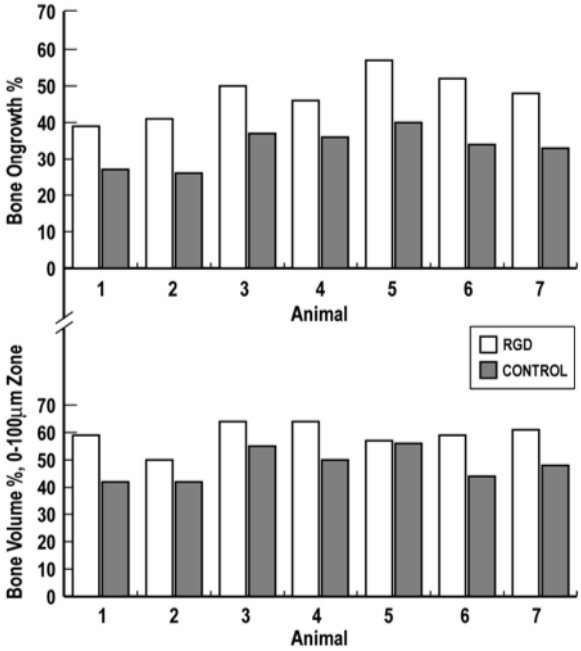

Fig. 4. Histomorphometrical results shown for the bilateral paired implants in each individual animal. Percentage of total bone is seen for bone ongrowth and bone volume in a concentric 0-100 μm zone.